THE EFFECTS OF PERINATAL IRON DEFICIENCY ON BROWN ADIPOSE TISSUE AND WHOLE-BODY ENERGY METABOLISM

by

Stephana Julia Cherak

A thesis submitted in partial fulfillment of the requirements for the degree of

Master of Science

Department of Pharmacology

University of Alberta

Abstract

Developmental exposure to an adverse environment can lead to altered growth and developmental trajectories, thereby increasing susceptibility to chronic disease in later life. Iron deficiency (ID) is the most common nutritional disorder in the world, and pregnant women are the most susceptible subgroup. Perinatal ID (PID) has been shown to program offspring metabolic function, characterized by an increased propensity for fat accumulation in later life; however, the mechanisms underlying this metabolic dysfunction are unknown. Brown adipose tissue (BAT) is a highly active metabolic tissue that has the capacity to generate large quantities of heat. The capacity of BAT to burn calories as heat makes it an attractive therapeutic target for obesity. Conversely, dysfunctional or reduced thermogenic capacity of BAT may represent a factor that predisposes individuals to obesity. The purpose of these studies was to determine whether PID predisposes offspring to obesity by chronically altering the thermogenic capacity of BAT, and thus whole-body metabolism.

Female Sprague Dawley rats were fed either an iron-restricted (3-10 mg/kg iron) or control diet (35 mg/kg iron) prior to and throughout gestation. At birth, dams were fed a normal rat chow, and offspring were fed a high-fat/high-sucrose diet at weaning (postnatal day [PD]21). At 4 wk of age, one male and female offspring from each litter were subjected to a chronic cold exposure protocol (4˚C, 12 h/day, 5 wk) to stimulate BAT, and one male and female littermate were maintained at room temperature (22˚C). Body composition was assessed using a whole-body composition analyzer. Metabolic parameters were analyzed *in vivo* via open-circuit indirect calorimetry, and maximal thermogenic capacity from BAT was assessed following pharmacological stimulation with the β3-adrenoceptor agonist, CL316,243. The expression levels

of the thermogenic regulatory proteins were assessed in BAT. Adipose tissue morphology was assessed by light microscopy.

Maternal iron restriction throughout pregnancy caused anemia and growth restriction in male and female offspring at birth. All offspring subsequently recovered in the neonatal period, such that hemoglobin (Hb) levels and body weight (BW) were no longer different between groups at PD21. Cold exposure increased intrascapular BAT (IBAT) mass, uncoupling protein-1 expression, and thermogenic capacity in all offspring, albeit these effects were diminished in the PID offspring. Whereas cold exposure had minimal effects on control offspring BW and body composition, cold exposure prevented BW and fat mass gain in male PID offspring, but not in female PID offspring.

In summary, PID affects the quantity and thermogenic capacity of BAT in the offspring, albeit these differences are qualitatively different between males and females. Alterations in BAT physiology did not impair cold-induced loss of fat in offspring, suggesting alternative mechanisms may be implicated in chronic cold-stimulated weight loss. Nonetheless, the immense caloric burning capacity of BAT makes it an attractive target for therapeutic intervention to prevent obesity and metabolic dysfunction; however, albeit the extent to which such therapeutics are effective may depend on numerous factors, including perinatal health.

Preface

This thesis is an original work by Stephana Julia Cherak. The research project, of which this thesis is a part, received research ethics approval from the Canadian Council on Animal Care and the University of Alberta Animal Care and Use Committee.

Dedication

This work is dedicated to my family.

The Unknown Holds Promise.

Acknowledgements

I am immensely grateful to those individuals who have molded and encouraged my passion for science.

First and foremost, I would like to thank my supervisor Dr. Stephane L. Bourque. Your mentorship, enthusiasm, and encouragement have been remarkable. I feel exceptionally fortunate to have had the opportunity to work with you. Our many captivating conversations have been instrumental in shaping my capacity for research.

I have also been remarkably privileged to have worked with, and been mentored by, Dr. Raymond J. Turner. I applaud your continual interest in my career as a young scientist. I am exceedingly thankful.

I am also tremendously appreciative of the support of my talented co-workers. Your assistance, insight and advice, of both academic and personal regard, have been immensely helpful. This degree is an accumulation of your efforts.

Finally, I gratefully acknowledge the Women and Children's Health Research Institute, Alberta Health Services, the Stollery Children's Hospital Foundation, the Lois Hole Hospital for Women, the Faculty of Graduate Studies and Research, the Faculty of Medicine and Dentistry, and the Department of Pharmacology for financial support.

Table of Contents

List of Figures

List of Tables

List of Abbreviations

ANOVA	Analysis of variance
ATP	Adenosine triphosphate
BAT	Brown adipose tissue
BCA	Bicinchoninic acid
BMI	Body mass index
BSA	Bovine serum albumin
BW	Body weight
CCE	Chronic cold exposure
CR	Crown rump
CTL	Control
CVD	Cardiovascular disease
ddH_2O	Distilled and deionized water
DOHaD	Developmental origins of health and disease
EDTA	Ethylenediaminetetraacetic acid
EchoMRI	Echo magnetic resonance imaging
Fe	Iron
GD	Gestational date
H&E	Hematoxylin and eosin
HF	High fat
HS	High sucrose
IBAT	Intrascapular brown adipose tissue
i.p.	Intraperitoneal
ID	Iron deficiency
IDA	Iron deficiency anemia
Hb	Hemoglobin
mRNA	Messenger ribonucleic acid
PD	Postnatal date
PGC-1α	Peroxisome proliferator-activated receptor gamma coactivator 1-alpha
PID	Perinatal iron deficiency
PPARγ	Peroxisome proliferator-activated receptor gamma
RER	Respiratory exchange ratio
RMR	Resting metabolic rate
RT	Room temperature
SDS-PAGE	Sodium dodecyl sulfate polyacrylamide gel electrophoresis
SEM	Standard error of the mean
UCP-1	Uncoupling protein-1
VAT	Visceral adipose tissue
VCO_2	Carbon dioxide production
VG	Visceral girth
VO_2	Oxygen consumption
WAT	White adipose tissue
WHO	World health organization

Chapter 1

Introduction

1.1 Fetal Programming

1.1.1 The Developmental Origins of Health and Disease

The Developmental Origins of Health and Disease (DOHaD) hypothesis posits that the quality of fetal development plays a significant role in establishing vulnerabilities for chronic disease later in life (Figure 1) [1–3]. In 1990 David Barker coined the term 'fetal programming' to describe a conceptual framework based on his epidemiological studies, such that adverse perinatal environments can affect the function of various fetal tissue and organ systems, and consequently, the way they develop [4]. Since then, numerous studies have revealed that various mechanisms for disease susceptibilities can be traced back to fetal life and early infancy. The importance of development during these early periods of life is well-established, and is considered a strong predictor for non-communicable disease in adult-life [2].

The DOHaD hypothesis states that there are specific windows during development whereby the fetus is particularly vulnerable to stressors. Insults during pregnancy can therefore alter the developmental trajectory, resulting in structural and functional changes

in cells, tissues, and organ systems [5–8]. Although these changes are not necessarily evident at birth [9] they can increase susceptibility to the development of chronic disease in adult-life [4,10–12]. To date, a large literature of studies, consisting of basic research, clinical and epidemiological studies describe the intrauterine programming of chronic disease by impaired fetal growth and development.

Suboptimal fetal nutrition *in utero* and in early infancy can permanently change the body's structure, physiology, and metabolism, thereby programming chronic diseases [13]. There is a myriad of perinatal insults that have been shown to cause long-term programming of cardiovascular, metabolic and neurological function [14]. It is now evident that many of these insults share common mechanisms [15].

Birth weight is commonly used as a surrogate of an individual's exposure to developmental stress. In general, the lower the birth weight, the higher the risk of infant morbidity and mortality [16–18]. Altered birth weight has been associated with numerous health outcomes in later life [2,17,19]. Anthropometric indicators of impaired fetal growth, for example, thinness, shortness, low abdominal circumference, and a high placental ratio, have as well been linked with chronic disease. Among the many variables that impact these indicators, nutritional status is believed to be the most important [20].

Under-nutrition and micronutrient deficiencies continue to affect mothers and children of developing countries. Maternal under-nutrition impacts offspring birth size, and low birth weight associated with retarded fetal growth is at least twice as common in developing countries [21]. Concurrently, obesity and related chronic disease are rapidly increasing in most developing countries and in countries undergoing economic transition. Compelling evidence from epidemiological studies indicates that low birth weight babies have an increased propensity for childhood and adulthood obesity [20,22]; small size at birth is a risk factor for several adulthood metabolic complications, including high body mass index (BMI), insulin resistance, increased visceral adiposity, and impaired glucose tolerance [23]. Importantly, a smaller size at birth appears to be more closely related to chronic disease when due to intrauterine growth impairment rather than premature birth [24]. Inadequate maternal nutrition, and consequentially suboptimal fetal growth, may therefore contribute substantially to increased risk of chronic disease [25,26].

Fetal programming may represent an additional source of environmental risk that interacts with, and modulates, other determinants throughout the life course. While perinatal insults can have important organizational effects to alter the physiology of the offspring, these effects may not necessarily lead to disease until additional risk factors are imposed. These disruptions, such as a high-fat or high-salt diet, age, and stress, may have activational effects that can impact the progression and and severity of disease [15]. Because the perinatal period represents an important window for the programming of later-life

chronic disease risk, intervention strategies adopted before or during gestation, or early in the postnatal period, are likely to prevent the transmission of these traits to the offspring.

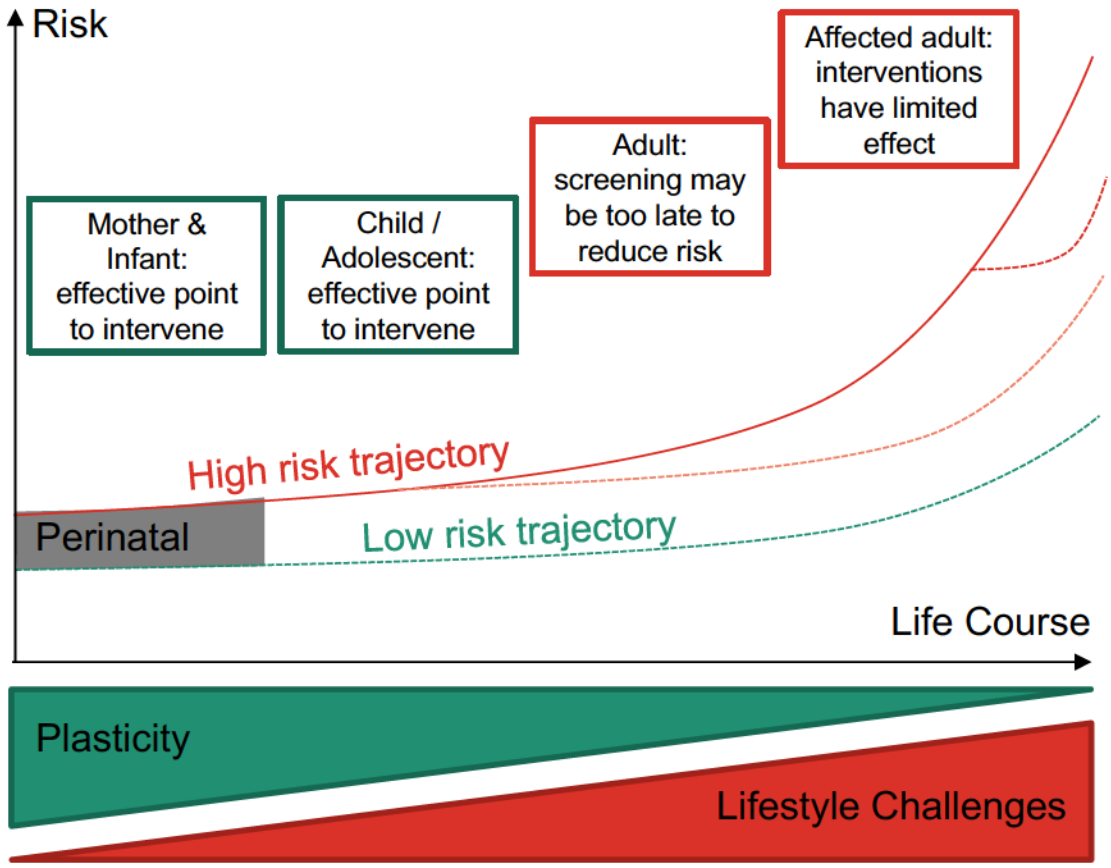

Figure 1 Fetal programming of non-communicable disease (NCD)

The risk of NCD through the lifetime increases in a non-linear fashion. Interventions in adulthood may be too late to lessen risk substantially, whereas interventions in adolescents are likely to be more effective in lessening the risk of NCDs in future generations. Importantly, the perinatal period is important in dictating the risk of non-communicable diseases throughout the lifespan. Adapted from Gluckman and Hanson [27].

1.2 Iron Deficiency

1.2.1 Overview

Iron deficiency (ID) is the most common nutritional disorder in the world [28], affecting 66-80% of the global population to some degree [29,30]. The populations most at risk for ID include pregnant women, women of childbearing ages, neonates, and young children [31–34]. As a functional component of both hemoglobin and myoglobin, iron is essential for oxygen transport and utilization [35].

In general, ID is a consequence of a chronic state of negative iron balance, wherein the net amount of iron lost from the body exceeds the amount of iron absorbed. This can result from insufficient dietary iron consumption, iron loss (e.g. blood loss) or due to inadequate iron uptake, either due to impaired absorption or increased iron demands (such as with blood volume expansion during pregnancy) [36,37]. Though continuous, the progression of iron deficiency occurs in stages that are characterized by changes in storage and functional/transport iron. The first stage is characterized by the reduction in tissue iron stores and a parallel decrease in ferritin, an intracellular iron storage protein [38]. Tissue iron stores are thought to be depleted first in the body's attempt to maintain circulating levels of Hb and the production of red blood cells (erythropoiesis), in order to preserve tissue oxygenation [39]. Depletion of iron stores in stage 1 can occur without causing symptoms.

Beyond stage 1 (depletion of iron stores), a sustained negative iron balance begins to diminish iron supply to the bone marrow, which impacts erythropoiesis [40]. In stage 2, Hb levels begin to fall to impact functional iron, but may remain within a range considered normal; 13.75-17.5 g/dL for men and 12.0-15.5 g/dL for women [32]. The term 'latent iron deficiency' (or iron-deficiency non-anemic) is sometimes used to refer to stage 2, due to the depletion of iron stores in the absence of anemia. In stage 3, total body iron is insufficient to maintain a normal Hb concentration and erythropoiesis, resulting in ID anemia (IDA) [32].

Anemia is a medical condition that is diagnosed from a deficient count of red blood cells, which results in a reduced oxygen carrying capacity within the blood. Currently, IDA is defined by the World Health Organization (WHO) as a reduction in hemoglobin concentrations to < 13 g/dL in men and < 12 g/dL in women, and is often associated with symptoms such as fatigue, pallor, dyspnea, headache, and concentration disorders [36,41]. The severity of ID and IDA is now recognized, and various health organizations are implementing measures to prevent future development. For example, Canadian Blood Services recently increased the time required to wait between donations for both men and women.

Although anemia can be caused by numerous factors (e.g. vitamin deficiencies, chronic inflammation, hemolysis, genetic deficiencies, bone marrow disorders), ID is the

most common cause of anemia worldwide [42]. The WHO estimates that half of the 1.6 billion cases of anemia worldwide are due to ID [42]. As noted above, , the most susceptible subpopulations are pregnant women and young children. Importantly, within the context of the DOHaD hypothesis, these are the populations in which ID has the potential to do the most harm.

1.2.2 Iron Requirements During Pregnancy

Pregnant women experience blood volume expansion and increased iron demands from the fetal placental unit throughout gestation [34] (Figure 2). In Canada it is estimated that 50% of pregnant women are ID at some point during pregnancy. Globally, approximately 42% of pregnant women suffer from anemia, of which half are attributed to ID [42]. Even in the absence of anemia, maternal ID during pregnancy impacts fetal iron stores [43] which may impact fetal growth and development. In the most severe of cases, maternal ID can lead to pre-term birth, and even maternal and fetal death [44].

The severity of ID in pregnancy increases throughout gestation. An increase of more than 4-fold from the first trimester to the third [45] is intimately associated with physiological changes in Hb concentrations [46]. The level of Hb declines throughout the first and second trimesters, reaches the lowest point late in the second to early in the third trimester, and then rises again nearer to term [47]. Clinically, pregnant women with Hb levels

less than 11.0 g/dL in the first and third trimester, and less than 10.5 g/dL in the second trimester, are considered anemic [48].

Iron delivery to the fetus is particularly important for growth and development [49]. Rapid fetal growth occurs in the first half of pregnancy, resulting in depletion of fetal iron stores. Furthermore, 60% of fetal iron stores are acquired during the third trimester of gestation, making this a critical period for iron accretion for use in the neonatal period. Immediately following birth, all newborns experience a decrease in Hb levels that results in varying degrees of anemia [50]. As the offspring oxygen supply transitions from the placenta to the lung, there is a progressive switch from high-oxygen affinity Hb to low oxygen-affinity Hb. An immediate increase in oxygen tension occurs as arterial Hb becomes fully saturated with oxygen. Oxygen delivery to the tissues increases as normal cardiac function matures, and at 5-7 days of age an abrupt decline in plasma erythropoietin followed by a decline in reticulocyte and nucleated red blood cell counts occurs [40]. As such, early infancy is characterized by a 30-50% decrease in Hb due to cessation of erythropoiesis, degradation of red blood cells, and blood volume expansion with growth [51]. Normally, newborn Hb can reach levels as low as 10-11 g/dL between 6 to 8 weeks of age, and 11-15 g/dL during fetal life [40]. Inadequate iron delivery to the fetus during the early or late stages of pregnancy can therefore have long-lasting effects on offspring health.

Early symptoms of ID can be so mild that it often goes unnoticed until IDA has progressed. A definitive diagnosis requires laboratory tests [52]. Regulation of iron uptake is through a series of coordinated protein interactions [53] that is controlled by the systemic level of iron [54] and is decreased during anemia and pregnancy [55]. Thus, iron replenishment must be slow and over a long period of time to prevent undesirable side effects such as gastric upset, constipation, nausea, abdominal pain.

As IDA in pregnancy stems primarily from inadequate iron intake or uptake during pregnancy, treatments may seem simple at first glance; however, there are many problems associated with treating ID and IDA during pregnancy. The body innately prevents excessive iron uptake in an effort to reduce iron toxicity, thereby preventing quick replenishment of iron stores. Even prolonged iron supplementation can be deleterious, as excess iron accumulation and free-radical damage can occur [56]. A high Hb concentration (> 135 g/dL) during pregnancy has been associated with gestational hypertension, preeclampsia, low birth weight, and low Apgar scores [57], and a marker of oxidative damage of DNA in the placental unit increases by over 2-fold with high concentrations of Hb [47]. Furthermore, severe cases of iron overload (> 60 mg/day) during pregnancy can lead to organ failure, coma, convulsion, and maternal and fetal death [58]. Unfortunately approximately 10-15 cases of reported iron overdose per year are in pregnant women [59]. Thus, while iron supplementation during pregnancy has still proven successful – 40 mg/day has been shown to reduce ID during pregnancy in > 90% of women in developed countries

[60] – there is still potential for adverse effects, especially as pregnancy itself is a condition characterized by susceptibility to oxidative stress [61]. Indiscriminate iron supplementation to pregnant women has and continues to be a contentious issue.

Given its prevalence, its tendency to affect pregnant women, and the difficulty in treatment, ID and IDA may be among the most widespread and important fetal 'stressors'. As described above, the DOHaD paradigm posits that susceptibility to long-term metabolic dysfunction may be influenced by exposure to stressor *in utero* [62,63]. As such, PID may be an important contributor to the global burden of obesity and metabolic dysfunction [34].

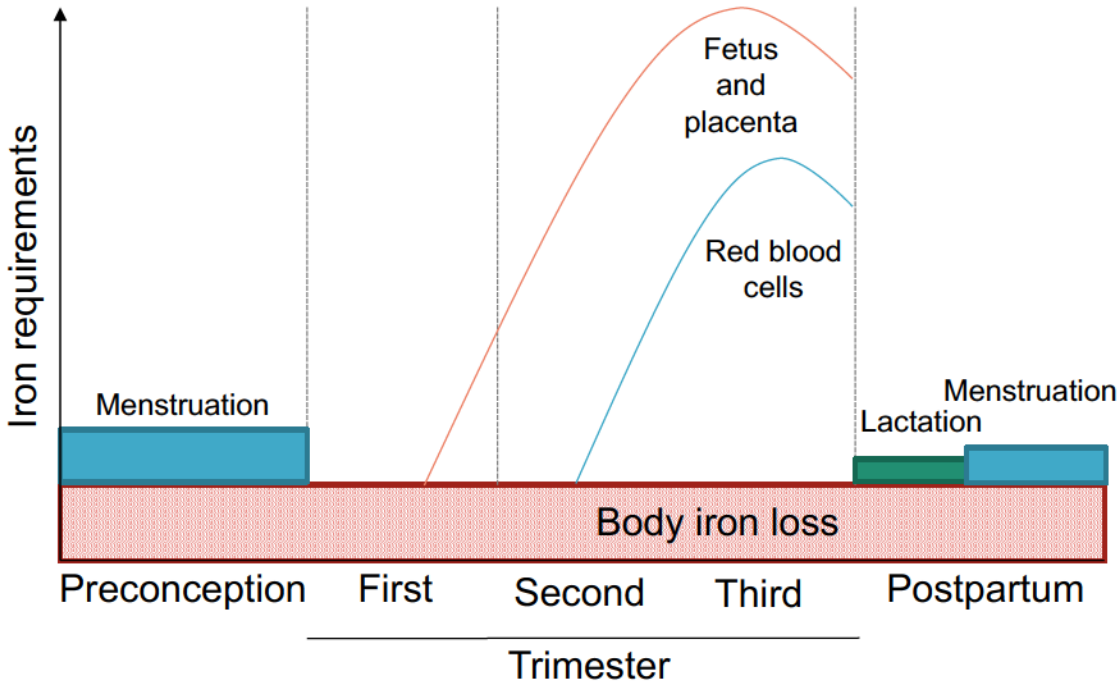

Figure 2 Iron requirements during pregnancy

The estimated iron requirements prior to, throughout and after pregnancy are shown. Although reduced during the first trimester, iron requirements rise to between 4 and 6 mg/day in the second and third trimesters, respectively, and to as much as 10 mg/day during the last 6-8 wk of pregnancy. This heightened demand is a consequence of major changes in red blood cell mass that begin only in the middle of the second trimester. Adapted from Bothwell et. al [41]

1.2.3 Perinatal Iron Deficiency and the Programming of Obesity

Obesity is a risk factor for several metabolic diseases and cancers, contributing to morbidity and mortality throughout Canada and the developed world [64]. In the last decade alone, the incidence and prevalence of obesity has risen dramatically, presenting itself as a substantial health challenge [14]. Among Canadian adults, 40% of men and 28% of women are overweight (BMI 25 to < 30 kg/m^2; body fat percentage 25 to 31%), while 20% of Canadian adults overall are classified as obese (> 30 kg/m^2; body fat percentage > 32%). Furthermore, 33% of children are overweight or obese, and are thus at an increased risk of adult obesity [64]. The WHO estimates that 2.8 million people worldwide die every year due to obesity and its complications [65], with 2.1 billion people classified as obese or overweight in 2014 [14]. Moreover, abdominal obesity – a disproportionate gain of fat within the abdomen, relative to other parts of the body – is as well an important risk factor for morbidity and mortality [66,67]. The two distinct fat compartments within the abdomen are the subcutaneous and visceral adipose tissue depots; the subcutaneous depot is located directly below the dermis and the visceral depot surrounds the internal organs [67]. Importantly, visceral adipose tissue (VAT) has shown several deleterious effects, such as increased levels of triglycerides [67], hyperglycemia [68], metabolic syndrome [69], endothelial dysfunction [70], and hepatic steatosis [71]. Recent studies have suggested that those with excess abdominal fat (> 120 cm for men and > 110 cm for women) while maintaining a normal BMI are at a greater risk of dying than those with overt obesity [72], thus defining the

accumulation of visceral adipose tissue as a major risk factor for metabolic and cardiovascular (CVD) [71]. As the physiological, psychological, and economic costs of obesity span all cultural and ethnic backgrounds [73,74], there is an increasing global need for novel treatment and prevention options for obesity [75].

At the biological level, obesity results when energy intake consistently exceeds energy expenditure (Figure 3). Although the increasing incidence of obesity is often attributed to poor eating habits and inadequate physical activity, the mechanisms dictating energy uptake and storage, as well as energy utilization, are far more complex. It is becoming increasingly recognized that insults during the prenatal and early postnatal periods life can have long-term consequences on cardiometabolic health. As such, there are a number of insults during early life that appear to influence the later development of metabolic dysfunction, such as maternal undernutrition [11], gestational hypertension and diabetes [76], maternal obesity [77], excessive weight gain during pregnancy [24], maternal alcohol consumption [78], and maternal stress [79].

Maternal ID has been implicated in the fetal programming of obesity. Specifically, maternal ID during pregnancy (i.e. PID) has been shown to alter fetal growth trajectories associated with an increased propensity for body weight gain and the accumulation of visceral fat [80–83]. Although a complete mechanistic basis for the effect of PID on offspring obesity has not been elucidated, there are several mechanisms that have been proposed.

These include (i) increased appetite in response to stimulatory factors [84] and a reduced satiety following feeding [85]; (ii) alteration in offspring stress response thereby stimulating a heightened caloric intake [86]; (iii) changes in energy homeostasis and metabolism with the most important pathways being the hypothalamic-pituitary-adrenal axis, which is intimately involved in digestion, energy storage, and energy expenditure [62]; and (iv) programming of adipose tissue growth and function [87]. The focus of the present studies was on the role of brown adipose tissue in the programming of obesity by perinatal iron deficiency.

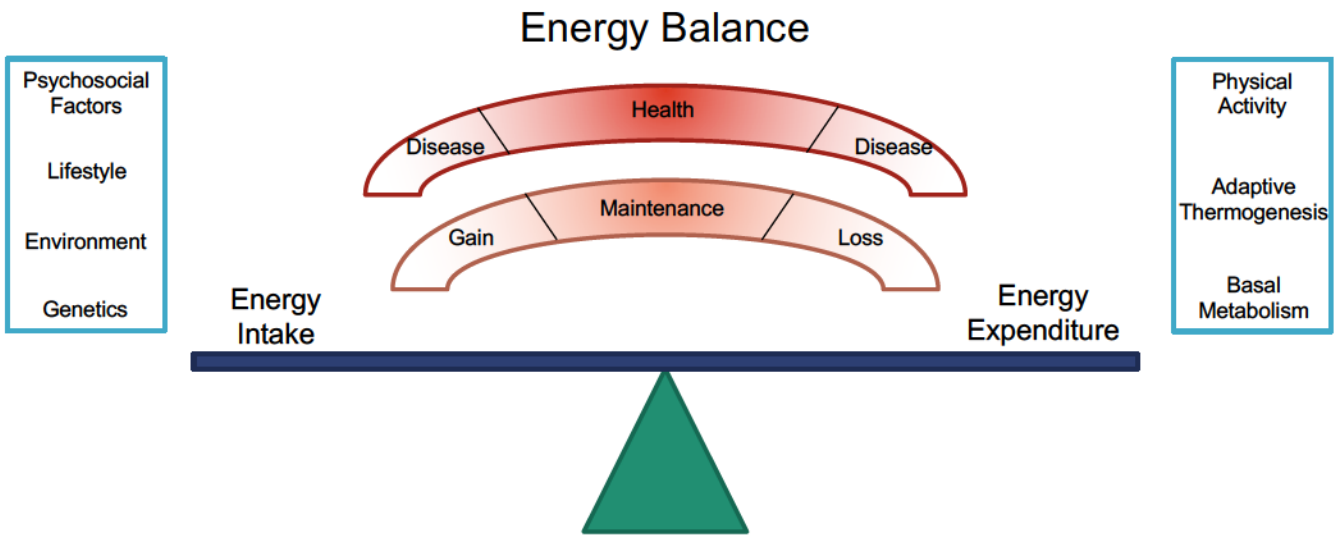

Figure 3 Fundamental contributors to energy balance

A positive energy balance occurs when energy intake exceeds energy expenditure. A consistent positive balance promotes weight gain and obesity. Conversely, a consistent negative balance promotes weight loss. Adapted from Prieto-Hontoria et. al [88].

1.3 Brown Adipose Tissue

1.3.1 Overview

Brown adipose tissue (BAT) is a highly metabolically active tissue capable of producing large quantities of heat. The metabolic capacity of BAT allows mammals to maintain core body temperature without shivering when exposed to cold [89,90]. This response has appropriately been coined 'non-shivering thermogenesis' [91]. BAT possesses a markedly different morphology and physiology in comparison to white adipose tissue (WAT) [92–94]. BAT is easily distinguished from WAT by its brownish color – a consequence of the large number of mitochondria found within [95–97]. In addition to the quantity, the mitochondria are qualitatively different between WAT and BAT, in that mitochondria found in BAT uniquely express uncoupling protein 1 (UCP-1), a protein that acts to decouple substrate oxidation with adenosine-5'-triphosphate (ATP) production to release large amounts of energy as heat [98–101].

1.3.2 Brown Adipose Tissue in Human Adults

Unlike human adults, infants are incapable of shivering due to the immaturity of their skeletal muscles [102] and require an alternative means to maintain core body

temperature [103]. Neonates achieve this additional heat generation to prevent hypothermia via upregulation of the quantity and activity of BAT [93]. In fact, a deficiency in BAT has been linked to increased infant mortality due to inadequate prevention against hypothermia [91].

Interestingly, the activation of BAT in young children is related to changes in weight and adiposity [104]. On average, BW was three times greater, and VAT six times greater, in children aged 4-8 years who did not demonstrate any BAT activity when compared to children with metabolically active BAT [105]. However, BAT mass and activity is rapidly lost within the first years of life as children develop the ability to generate heat via shivering thermogenesis; < 20% of prepubertal girls or boys have metabolically active BAT [104]. For these reasons, it was previously thought that the role of BAT in the metabolic function in adults was negligible.

In 2009, several independent research groups demonstrated that adult humans possess physiologically relevant quantities of BAT in the cervical and subscapular regions with a demonstrated role in energy metabolism [106–110]. Previously, the metabolic activity, and hence the importance, of BAT in human adults was overlooked as studies did not assess the activation of BAT. Thus, the prevalence of BAT was thought to be low (approximately 5%-10%) [91,106]. Subsequent studies using an experimental protocol of a mild cold exposure (16˚C, 2 hr/day, 5 days) demonstrated that only 50 g of maximally stimulated BAT could

account for 20% of total resting expenditure, which amounts to an expenditure of an additional 400 to 500 calories per day [106,107,110].

1.3.3 Activation and Regulation of Brown Adipose Tissue

BAT converts chemical energy into heat during cool ambient temperatures through a complex signaling pathway; a simplified overview is provided in Figure 4. Cold receptors in the skin relay the signal to temperature regulating hypothalamic centers in the brain [111], which subsequently activates the sympathetic nervous system as the predominant governing pathway for thermogenesis [111]. Upon stimulation, sympathetic nerves release the neurotransmitter norepinephrine [112] that binds to all three types of adrenergic receptors in the membrane of brown adipocytes: α1, α2, and β [113]. The most studied pathway for stimulation of thermogenesis is the β-adrenergic pathway; the

β3-adrenergic receptor is the most highly expressed subtype of adrenergic receptors in brown adipocytes [114,115]. Binding of norepinephrine to β3-adrenergic receptors leads to marked increases in triglyceride breakdown (lipolysis) and energy expenditure through the up-regulation of UCP-1 [116], which acts to uncouple oxidative phosphorylation from ATP production [99]. More specifically, the lipolytic pathway stimulates thermogenesis in the brown adipocyte [113] as fatty acids are involved in the activation of UCP-1 activity [98,100]. Typically in mitochondria, accumulation of a proton gradient via substrate oxidation is coupled to ATP production via ATP synthase. In the case of BAT mitochondria, activated

UCP-1 uncouples the proton gradient from ATP generation by allowing protons to flow back into the mitochondrial matrix [117]. The energy generated by dissipation of the membrane potential is released as heat [118].

Several transcription factors are implicated in the molecular regulation of BAT. Attention focuses on the master regulators of mitochondrial function, peroxisome proliferator-activated receptor gamma (PPARγ) and peroxisome proliferator-activated receptor gamma coactivator-1α (PGC-1α), whose regulation is intimately associated with BAT thermogenesis. The PPARs (PPARα, PPARδ, and PPARγ) [119] are part of a relatively large family of nuclear receptors [120]. Adipose tissue development and differentiation are primarily controlled by PPARγ [121], whereas PPARα and PPARδ are essential in the control of fatty acid oxidation [122]. While it is known that the transcription factor PPARγ is an important regulator of adipogenesis, it is unable to induce brown fat differentiation alone [119] and is subject to transcriptional coactivation by PGC-1α [123]. Specifically, PGC-1α binds to PPARγ to stimulate the transcription of genes involved in the brown adipocyte differentiation process [119]. The expression of PGC-1α is strongly induced by cold exposure, intimately linking this environmental stimulus to non-shivering thermogenesis [124,125]. PGC-1α is crucial for BAT adaptations to cold exposure via stimulation of mitochondrial biogenesis and oxidative metabolism [112,119]. More precisely, PGC-1α promotes muscle tissue remodeling to a fiber-type composition that is metabolically more oxidative and less

glyclolytic in nature [112,126], thereby allowing participation in both carbohydrate and lipid metabolism [127].

Not surprisingly, PPARγ and PGC-1α have important implications for metabolic dysfunction. Functional impairment or dysregulation of PPARγ and/or PGC-1α are shown to lead to obesity, lipodystrophy, fatty liver, insulin resistance, type 2 diabetes, or cardiomyopathy. For example, PPARγ is a molecular target for the type 2 diabetes drug thiazolidinedione as this receptor can greatly impact insulin sensitivity and glucose homeostasis. Taken together, PPARγ and PGC-1α play a simultaneous crucial role in linking stimuli such as cold exposure, to an internal metabolic response like mitochondrial biogenesis, to better understand the molecular mechanisms of metabolic disease.

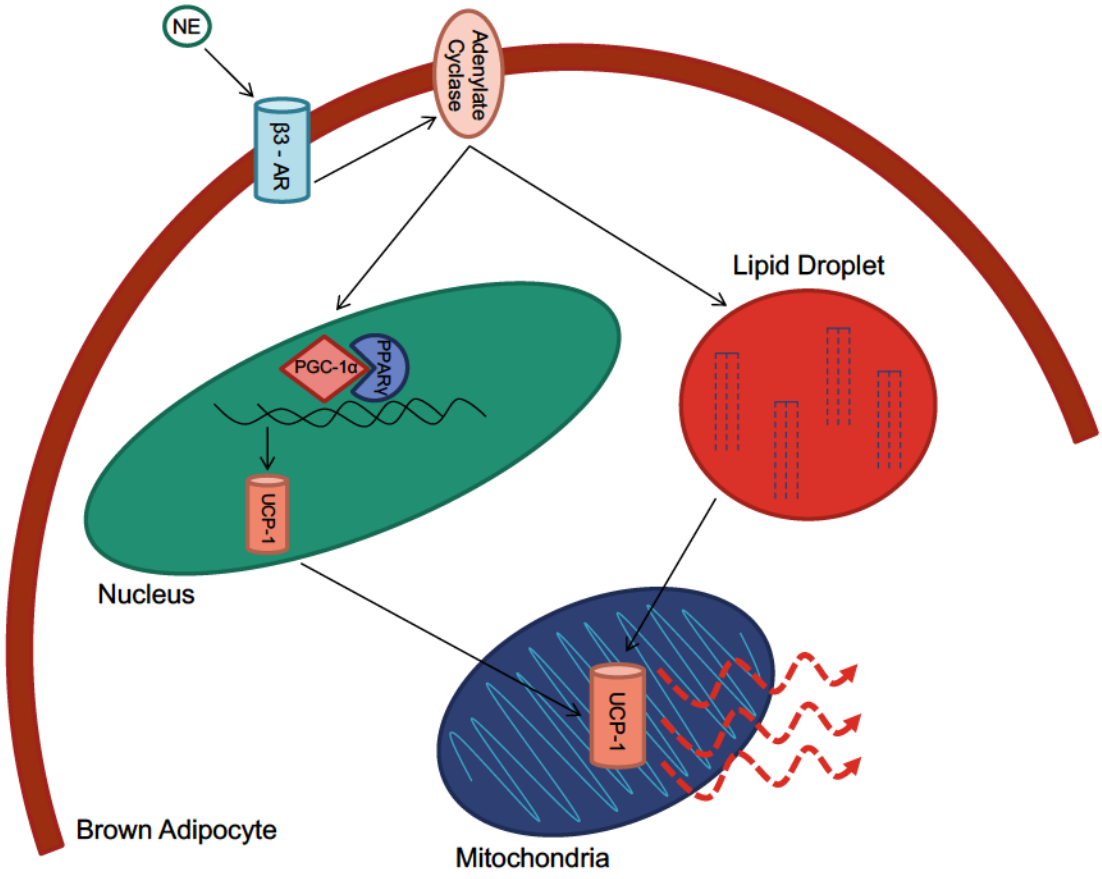

Figure 4 Adrenergic control of thermogenesis in brown adipose tissue

A simplified schematic of the activation of non-shivering thermogenesis as we understand it currently. Adapted from Valle et. al [128].

1.3.4 Implications of Brown Adipose Tissue for Obesity

Numerous studies have demonstrated an inverse relationship between the amount of BAT with BMI [106–108,110], central obesity parameters (visceral adipose tissue, visceral/total adipose tissue, waist circumference) [129], and subcutaneous adipose tissue [96]. In humans, several studies have confirmed that the quantity and activity of BAT was decreased in obesity [105–107,110], diabetes [130], insulin resistance [108], and fasting [105]. These findings suggest an intimate role for BAT in the regulation of energy metabolism and body composition [91,131,132]. By virtue of its intense metabolic capacity, low quantity or activity of BAT may result in a 'slow' metabolic phenotype characterized by fat accumulation and obesity.

Numerous animal models are of use to study human disease and many are currently utilized in effort to understand the mechanisms that underpin BAT thermogenesis. Although a rodent should not be considered a claim of identity with a human, there are several analogies between the two that make a rodent model ideal in the study of human obesity. In rats, the same inverse relationship between BAT and BMI is seen as in humans. Indeed, BAT is thought to play a central role in the protection against diet-induced obesity in rats [133]; ablation of the BAT causes a reduced energy expenditure and increased prevalence of obesity, especially in response to a high-fat/high sucrose Western diet [120].

Stimulation of adult human BAT represents an innovative pharmacological principle and physiological candidate for the treatment of obesity and metabolic dysfunction. As active BAT can take up ~50% of nutrient lipids [134], resulting in a significantly increased resting energy expenditure [135,136], BAT is a promising candidate for the treatment of obesity. For example, β3-andrenergic receptor agonists increase rodent BAT activity to successfully prevent obesity and insulin resistance [137]. In adult human males, β3-andrenergic receptor agonist administration can increase fatty acid oxidation and insulin sensitivity [85]. Another physiological approach involves a mild cold exposure to stimulate BAT. Amazingly, an increase in resting energy expenditure was seen after a single 5 hr cold exposure (CE) (16˚C). Assuming that this increase could be maintained over days and weeks, it could result in the energy expenditure equivalent to approximately 0.9 kg of fat per month! This equates to the loss of 1 lb per week and approximately 17 lbs per year [106,138]. Morevoer, repeated intermittent exposure (17˚C for 2 hr/day, 6 wks) of healthy Japanese men without detectable BAT activity at baseline, resulted in recruitment and expansion of BAT to lead to a decreased body fat mass [131]. Furthermore, even reduction of the ambient thermostat temperature from 24˚C to 19˚C consequentially increased energy expenditure by 5% and BAT activity by 10% in lean adult males [131]. Thus, on a population-based level, even slightly reducing indoor temperatures could potentially aid in the prevention of obesity.

BAT may be an important contributor to basal metabolism and therefore represents a potential therapeutic target for sustained weight loss. Although the molecular mechanisms that contribute to whole-body thermogenesis are not fully understood, BAT nevertheless is an important consideration for the efficacy of future weight loss therapeutics.

1.4 Statement of Hypotheses and Objectives

Alterations in mechanisms regulating adipose tissue development and function, energy expenditure, and food intake can be programmed by exposure to stressors *in utero* [84,122,139]. Maternal ID during pregnancy programs an altered metabolic phenotype in the offspring, which increases their propensity for fat accumulation and subsequent obesity in adult life [80,82,140]. By virtue of its prevalence and tendency to afflict pregnant women, PID may be an important contributor to the global health burden of obesity and related health complications. Currently, there is a paucity of data on the effects of PID on the immediate and long-term health of the offspring.

BAT is a highly metabolically active type of adipose tissue found in physiologically relevant quantities in adult humans, with a demonstrated role in metabolic function [106–110]. As little as 60 g of BAT contributes up to 20% of daily heat production in adult humans [91]. By virtue of its metabolic capacity, low quantity and/or activity of BAT may result in a 'slow' metabolic phenotype characterized by fat accumulation and obesity. As such, the overarching hypothesis of the present study is: *PID offspring exhibit reduced quantity and activity of BAT, thereby influencing basal metabolic rate and increasing susceptibility to obesity in later life.*

To test this hypothesis, experiments were conducted to accomplish the following specific objectives:

1. To assess the impact of perinatal ID on IBAT quantity and thermogenesis.

2. To assess the impact of perinatal ID on chronic cold exposure-induced changes in thermogenesis and whole-body metabolism.

3. To assess the impact of perinatal ID on chronic cold exposure-induced alterations in body composition.

Chapter 2

Materials and Methods

2.1 Experimental Animals

The experimental protocols described herein conform to the guidelines of the Canadian Council on Animal Care and the University of Alberta Animal Care and Use Committee. A total of 243 Sprague Dawley rats were used for experiments; 24 female rats were bred with 8 age-matched Sprague Dawley males; 2 females did not become pregnant. Dams were maintained on a 12:12 hr light-dark cycle (0500:1700) at an ambient temperature of 23˚C with 35-35% relative humidity, and with *ad libitum* access to food and water. A 1 wk acclimatization period occurred before breeding. Breeding produced 211 viable offspring, 160 were used for data acquisition and 51 were culled at PD1 (< 24 hr after birth.Litters were reduced to 5 male and 5 female offspring on PD1 to standardize postnatal conditions. Although there were isolated incidents of still-birth (5 of 12 litters) and infanticide (3 of 12 litters) in the PID group, no litters were excluded from the study. No offspring died unexpectedly after PD21.

2.1.1 Model of Perinatal Iron Deficiency

We employed a well-characterized model of PID [80,81]. Twenty-four female Sprague Dawley rats, approximately 6 wk of age, were obtained from Charles River Laboratories (Saint-Constant, QC, Canada). Dams were randomized (by the flipping of a coin) to ether the control (CTL) or iron-restricted (PID) group. All purified diets used prior to and throughout gestation were based on the AIN-93G rodent diet (Research Diets Inc., New Brunswick, NJ) (Reeves, Nielsen, AIN-93 purified, 1993). The CTL and PID diets were identical in composition, with the exception of the amount of added ferric citrate. During the 2 wk pre-pregnancy phase, 12 of 24 dams were fed a control diet (35 mg/kg Fe, in the form of ferric citrate) (D10012G) while the other 12 were fed an iron restricted diet (3 mg/kg Fe, no added ferric citrate) (D03072501). After 2 wks, dams were naturally bred (i.e. without synchronization of estrus) with age-matched male Sprague Dawley rats fed a standard grain-based rodent chow (185 mg/kg Fe) (LabDiet, St. Louis, MO). Daily vaginal smears determined pregnancy success. Upon confirmation of pregnancy, PID dams were fed a moderately iron-restricted diet (10 mg/kg Fe, in the form of ferric citrate) (D15092501) until parturition; CTL dams were fed the control diets until parturition. All dams were individually housed and BW, food intake, and Hb were monitored weekly. Hb was measured in blood (~10 μL) obtained via saphenous venipuncture with the HemoCue® B-Hemoglobin system (Hemocue AB, Ängelholm, Sweden) which uses a modified azide-

methemoglobin reaction. At birth, all dams were fed the standard grain-based rodent chow (185 mg/kg Fe).

2.1.2 The High-Fat/High-Sucrose Western Diet

To exacerbate the metabolic phenotype of obesity, all offspring were fed a purified high-fat/high-sucrose Western diet starting at the time of weaning, PD21. The diet contains 45% energy from fat (40% derived from lard and 5% from soybean oil) and 35% energy from sucrose (Research Diets Inc., D12451). Offspring BW, food intake and Hb were monitored weekly from PD21 onwards.

2.1.3 Chronic Cold Exposure

A chronic cold exposure (CCE) protocol was used to study the effects of PID on the ability of offspring to induce and activate BAT [141]. Starting at 4 wk of age (PD28), 1 male and 1 female from each litter were subjected to a CCE protocol (4˚C, 12 hr/day [17:00-05:00], 5 wk) by placing these rats in a cold-room. A 5 wk protocol was chosen as full morphological and molecular adaptations, and maximal capacity for non-shivering thermogenesis, requires 3-5 wks of cold exposure [142]. Littermates in each group remained at room temperature (22˚C). Offspring BW, food intake, and Hb were measured weekly. Core body temperature was measured in conscious animals before and after daily cold

exposure using rectal probe thermometry (RET-3, MLT1404, ADINSTRUMENTS, Colorado Springs, CO, USA).

After completion of the CCE protocol, 1 cold-exposed male and female from both the CTL and PID groups, in addition to their room temperature (RT) littermates, underwent a 3-day metabolic testing (as described below), and were subsequently euthanized and tissues were collected; these offspring outcomes reflect the immediate effects of CCE (i.e. after 3 days). The remaining offspring, such being 1 cold-exposed and RT male and female from the CTL and PID groups, were placed at RT for an additional 4 wks, and then underwent a similar 3-day metabolic testing regiment and were subsequently euthanized; these offspring outcomes reflect the residual effects of CCE (i.e. after 4 weeks + 3 days).

2.2 Analysis of Metabolic Parameters *in vivo*

2.2.1 Lean Mass and Fat Mass

Body composition was analyzed in conscious animals by EchoMRI-100TM (Echo Medical Systems, Houston, TX, USA); parameters assessed included fat mass, lean mass, free water, and total body water.

2.2.2 Fasted Blood Glucose

Animals were fasted overnight in clean cages. Blood samples were obtained by saphenous venipuncture and glucose levels were assessed using a glucometer (Accu-check® Aviva, Roche Diagnostics, Laval, QC, Canada).

2.2.3 Whole-Body Energy Metabolism

Metabolic parameters were assessed using an open circuit indirect calorimeter (Oxymax/CLAMS, Columbus Instruments, Columbus, OH, USA) consisting of a sealed Perspex chamber connected to an infrared CO_2 analyzer and an electrochemical O_2 sensor. Following an initial 24 hr acclimatization period, rats were monitored every 13 min for 48 hr maintained on a 12:12 hr light/dark cycle (6:00-18:00). The respiratory exchange ratio ($RER=VCO_2/O_2$) was used to estimate fat and carbohydrate utilization *in vivo*. Basal heat production was derived from the exchange of oxygen for carbon dioxide that occurred during foodstuff combustion (heat[kg/kcal/hr]=[3.815+(1.233*RER)]* VO_2). Physical activity was monitored by dual-axis detection (X, Z) using infrared photocell technology. Total physical activity was calculated by adding Z count (rearing) to total counts associated with ambulatory movement and typical behavior (grooming). The consumption and heat production data are presented as mL/kg/hr and kcal/hr, and are normalized to 25˚C and 760 mmHg.

2.2.4 Activation of the β3-Adrenergic Receptor in Brown Adipose Tissue

On the final day of metabolic testing (day 3), the maximal thermogenic capacity of BAT was assessed using a selective β3-adrenergic receptor agonist. Prior to administration, baseline metabolic parameters were recorded for 60 min. A single supramaximal dose (2 mg/kg, i.p.) of CL316,243 (Tocris Bioscience, Ellisville, MO, USA) was then administered. Offspring were returned to their individual metabolic cages and were monitored for 60 min thereafter.

2.3 Euthanasia and Tissue Collection

All rats were anesthesized with isoflurane prior to euthanasia. BW was measured prior to administration of anesthetic. Crown-rump (CR) length, visceral girth (VG) and Hb were measured in anesthetized offspring. Rats were subsequently euthanized by cardiac puncture and exsanguination. Tissues (i.e. brown and white adipose and skeletal muscle [gastrocnemius]) and organs (i.e. brain [including cerebellum], heart, liver, pancreas and kidneys) were collected, rinsed in phosphate-buffered saline (PBS) (0.1M, pH 7.4), blotted dry, and weighed. Samples were immediately frozen in liquid nitrogen or fixed in 4% paraformaldehyde (pH 7.4) at 4˚C overnight, rinsed with PBS (pH 7.4) and stored in 70% EtOH at 4˚C. BAT was assessed from the interscapular depot using a standardized

postmortem dissection. WAT was assessed from the post mortem dissection of visceral fat depots (omental, mesenteric, epididymal, and retroperitoneal) [143].

2.4 Analysis of Molecular and Morphological Parameters *in vitro*

2.4.1 Western Blotting in Brown Adipose Tissue

The protein content of UCP-1, PGC-1α, PPARγ, and β-actin was determined in BAT samples by Western blot analysis. Frozen tissue samples were homogenized in NP40 lysis buffer (20mM Tris-HCl [pH 7.4], 5mM EDTA, 10mM $Na_4P_2O_7$, 100mM sodium fluoride, 1% NP40) using a Minilys Personal Tissue Homogenizer (Precellys #10435, Michigan, USA). Sodium orthovanadate (Sigma, S6508, 2 mM final), protease inhibitor cocktail (Sigma, P8340, 10% (v/v) final) and phosphatase inhibitor (Calbio, 524628, 20 µg/mL final) were added directly prior to homogenization. Protein concentrations were determined via BCA protein assay (Pierce Biotechnology, Rockford, IL, USA) according to manufacturer's instructions. Lysates were resolved by SDS-PAGE, transferred to nitrocellulose membrane, and incubated for 1 hr at RT with blocking solution (2% BSA in Tris-buffered saline [TBS] buffer containing 0.1% Tween 20). The blocked membranes were incubated with rabbit anti-UCP-1 (Abcam, ab10983, 1.38 µg/mL), anti-PGC-1α (Abcam, ab54481, 1.33 µg/mL), and anti-PPARγ (Abcam, ab209350, 1.86 µg/mL) as primary antibodies. A mouse monoclonal anti-β-actin (Abcam, ab6276, 0.2 µg/mL) was

used as a primary antibody for loading control. Several studies have demonstrated that cold exposure does not affect the level of β-actin mRNA or protein expression [144]. Membranes were probed with primary antibodies overnight at 4˚C. Membranes were washed with TBS buffer containing 0.1% Tween 20, and probed with secondary antibody conjugated with AlexaFluor® fluorophore for 1 hr at room temperature. UCP-1 and associated metabolites were labeled with donkey anti-rabbit AlexaFluor® 680 (Abcam, ab175772, 0.2 µg/mL) and β-actin with donkey anti-mouse AlexaFluor® 790 (Abcam, ab175782, 0.2 µg/mL). Membranes were washed and imaged with an Odyssey Infrared Imaging System (LI-COR Biosciences, Lincoln, NE, USA). Expression was quantified by densitometry using Image Studio™ Software (LI-COR Odyssey Software version 5; LI-COR Biosciences, Lincoln, NE, USA).

2.4.2 Adipose Tissue Cell Morphology

BAT and WAT morphology was visualized by microscopy after hematoxylin & eosin (H&E) staining. Paraformaldehyde fixed adipose tissue samples were embedded in paraffin, sections cut at 5 µm, and then subsequently de-paraffinized and re-hydrated. The slides were incubated in Mayer's hematoxylin for 15 min at RT, washed in tap water for 20 min, and counterstained in eosin for 1 min. The slides were dehydrated and mounted with Organo/Limolene Mount (Sigma, O8015) and visualized on a light microscope (Olympus LX81, Melville, NY, USA); images were captured at a magnification of 10X

using a CoolSNAP HQ camera. At least 200 adipocytes per tissue sample were randomly analyzed from 4 microscopic fields of view of confluent adipocyte sections. Mean adipocyte area were determined using ImageJ software (Schneider, Rasband, NIH Image, 2012).

2.5 Statistical Analysis

In all data sets, n values reflect experimental units (i.e. dam or litter). Where multiple values were derived from a single litter (i.e. analyses of pups from the same litter), values were pooled and a single mean value was used; male and female offspring data were analyzed separately. Maternal BW, food intake, and Hb were analyzed by repeated measures, two-way ANOVA for the effects of iron-restriction and time. Litter outcomes were analyzed by unpaired Student's *t*-test. Postnatal offspring BW, Hb, and CR:VG were analyzed by repeated measures two-way ANOVA (for the effects of perinatal iron-restriction and time) or by unpaired Student's *t*-test as appropriate. All other data were analyzed by two-way ANOVA (for the effects of perinatal iron-restriction and offspring temperature exposure) and Bonferonni *post hoc* where statistical significance was found. The fold change (Δ) by CCE was calculated by subtracting values of the CCE littermate from the RT littermate in each group; thus, the comparison of Δ values between CTL and PID groups (by unpaired Student's *t*-test) reflects the interaction parameter in the two-way ANOVA. Grubb's test was conducted on all data sets to determine statistical outliers

($P<0.05$). The only outlier identified was in the male CTL group in the comparison of BAT mass and maximal heat production and was subsequently excluded. All data are presented as mean ± SEM. $P<0.05$ was considered significant. Histology and Western blotting data were analyzed by two independent investigators, one of whom was blinded to the experimental conditions. All statistical analyses were conducted using Prism 7.0 (GraphPad Software, Inc.).

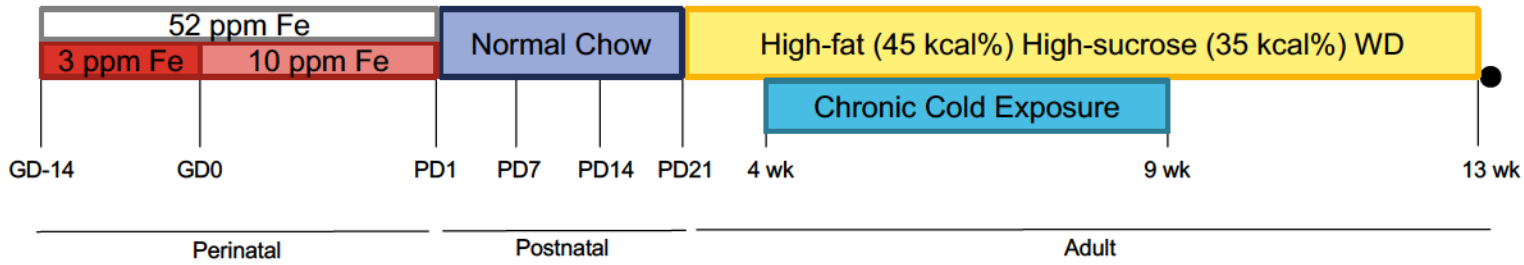

Figure 5 Schematic timeline of the experimental design

The process is divided into four main segments including perinatal iron deficiency (GD-14 to GD22), postnatal growth (PD1 to PD 20), adult growth on a high-fat/high-sucrose Western diet (PD21 to 13 wk), and chronic cold exposure on a high-fat/high-sucrose Western diet (4 wk to 9 wk).

Chapter 3

Results

3.1 Model of Perinatal Iron Deficiency

3.1.1 Maternal Outcomes

Maternal iron restriction (3 mg/kg Fe) for two wks prior to pregnancy caused an 18% reduction in maternal Hb by GD 0, and continued moderate iron restriction (10 mg/kg Fe) resulted in a 32% reduction in maternal Hb by the time of parturition (Figure 6C). Maternal dietary iron restriction did not affect food intake (Figure 6A) or BW gain (Figure 6B) throughout gestation.

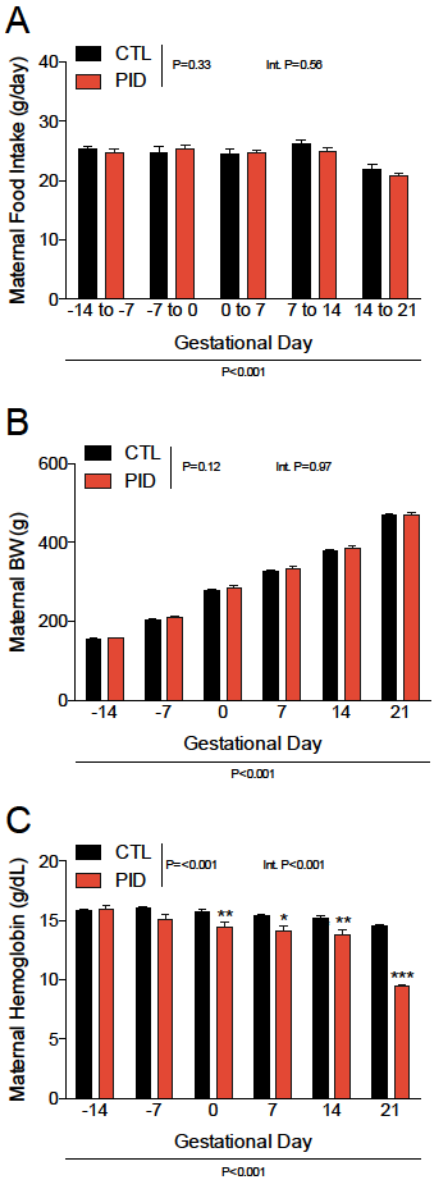

Figure 6 The effect of PID on maternal gestational outcomes

Maternal food intake (A); body weight (B); and hemoglobin (C) were measured weekly. Data are presented as means ± SEM, n=8 per group. CTL, control; PID, perinatal iron deficiency; GD, gestational day. *, P<0.05; **, P<0.01; ***, P<0.001 compared with control at same time interval.

Table 1 The effect of PID on pregnancy outcomes

	Control (n=12)	Perinatal ID (n=12)	P Value
Pups per litter (n)	13.0 ± 0.8	10.5 ± 1.6	0.19
Male offspring (%)	63.8 ± 6.8	58.8 ± 5.5	0.58
Non-viable pups per litter (n)	0.5 ± 0.3	1.1 ± 0.6	0.38

Data are mean ± SEM, n=12 per group.

3.1.2 Offspring Outcomes

Maternal iron restriction throughout pregnancy resulted in a 42% reduction in Hb and a 10% lower BW in both male and female offspring at birth. The lower BW (Figures 7A and 7D) and Hb (Figures 7B and 7E) in the male and female PID offspring recovered by the time of weaning (PD21). No trend was observed in the CR:VG ratio of PID and CTL male offspring; however, differences were observed at PD1 (PID greater, $P<0.001$) and PD21 (PID lesser, $P<0.001$) (Figure 7C). Conversely, the CR:VG ratio of female PID offspring was increased at PD7 ($P<0.01$), PD21 ($P<0.01$), and PD28 ($P<0.05$), when compared to CTL offspring (Figure 7F).

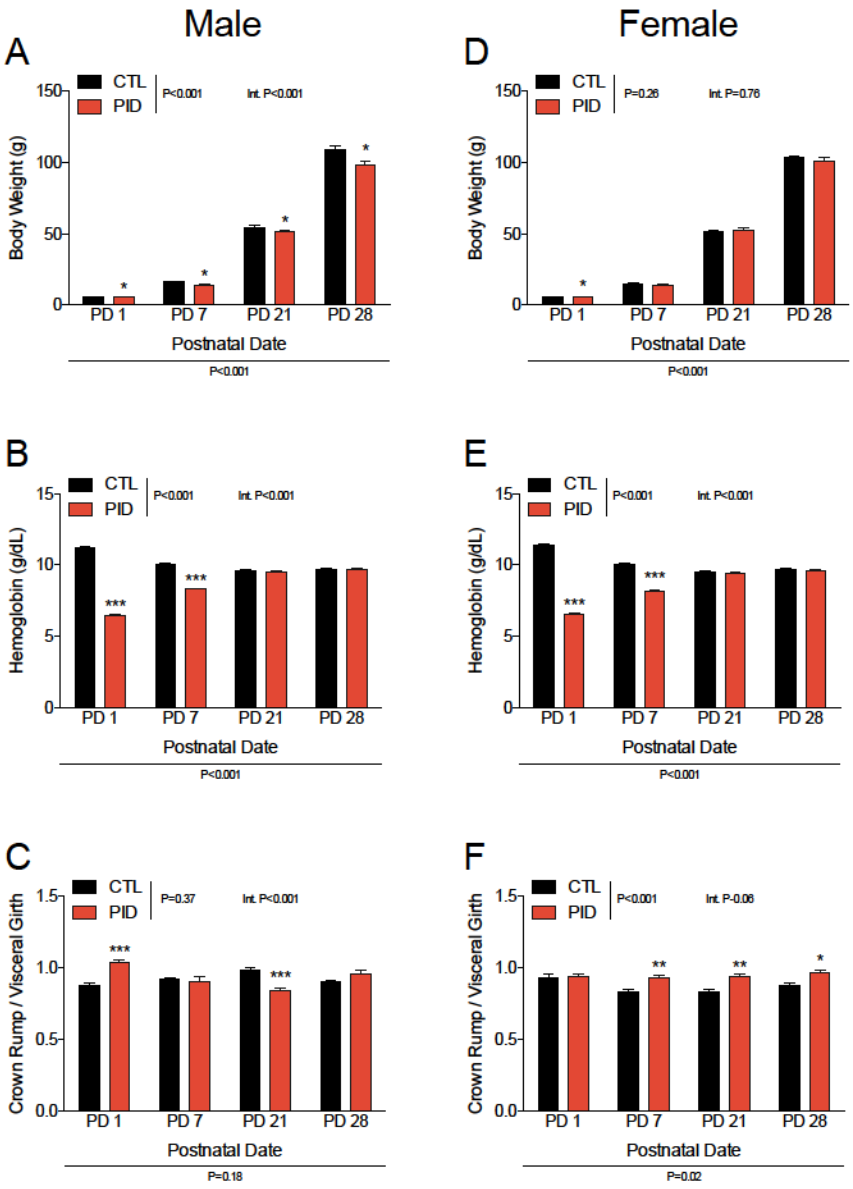

Figure 7 The effect of PID on offspring birth outcomes

Growth measurements: body weight (A and D); hemoglobin (B and E); and crown rump:visceral girth (C and F) were taken <24 hr following birth. PD1 – PD21 all offspring were fed the normal rodent chow; PD21 – PD28 all offspring were fed the high-fat/high-sucrose diet. Data are presented as means ± SEM, n=12 per group. CTL, control; PID, perinatal iron deficiency; PD, postnatal date. *, P<0.05; **, P<0.01; ***, P<0.001 compared with control at same time interval.

The proportion of lean mass in male PID offspring was lower than CTL throughout the postnatal period, and the greatest difference between CTL and PID was seen at PD14 ($P<0.01$ PD14 to PD1, $P<0.01$ PD14 to PD7) (Figure 8A). The proportional fat mass of male offspring continuously increased with age (Figure 8B).

Female PID offspring had lower lean mass (Figure 8C) and greater fat mass (Figure 8D) throughout the postnatal period; the largest differences between PID and CTL were observed at PD7 ($P<0.01$ to PD1) and PD28 ($P<0.01$ to PD1, $P<0.05$ to PD21) for lean mass and fat mass, respectively.

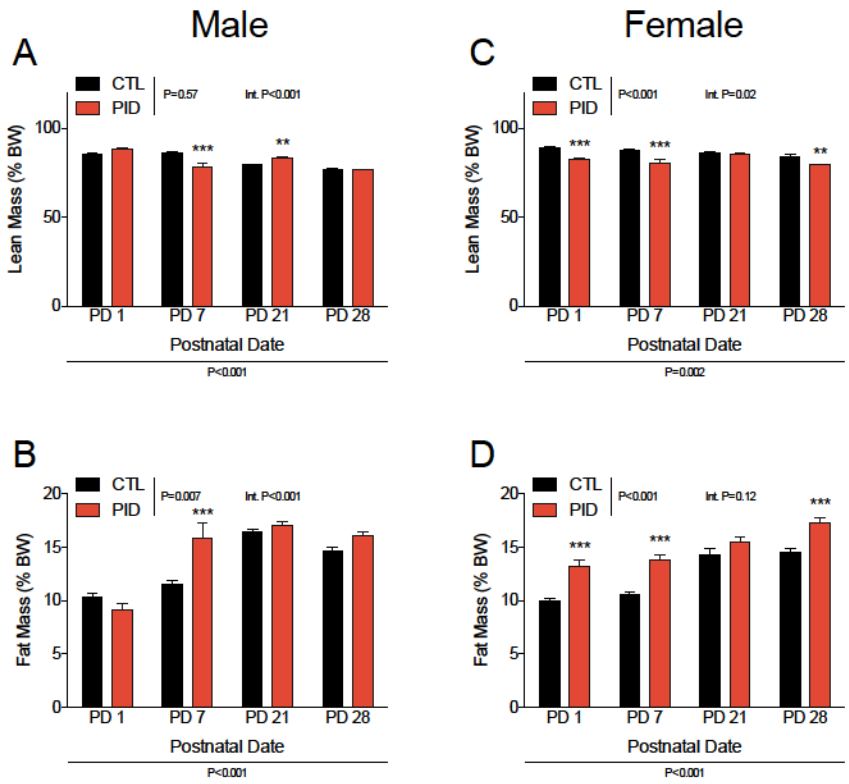

Figure 8 The effect of PID on neonatal offspring body composition

Lean mass (A) and fat mass (B) proportionate to body weight was determined by whole-body composition analysis. PD1 – PD21 all offspring fed normal chow; PD21 – PD28 all offspring fed high-fat/high-sucrose diet. Data are presented as means ± SEM, n=12 per group. CTL, control; PID, perinatal iron deficiency; PD, postnatal date. **, P<0.01; ***, P<0.001 compared with control at same time interval.

3.2 The Immediate Effects of Chronic Cold Exposure

3.2.1 Male Offspring

A 5 wk CCE protocol successfully increased the expression of the primary thermogenic protein, UCP-1 ($P<0.001$), and the increase was larger in PID offspring ($P<0.001$) (Figure 9A). An interaction between the effects of PID and CCE was also found ($P<0.001$). The net difference (Δ) in UCP-1 expression between CCE offspring and their RT littermates was greater in the PID group; this is shown in the scatter plots in Figure 9A. The expression of key thermogenic regulatory proteins, PGC-1α and PPARγ, were also increased by CCE ($P<0.001$ for both parameters); however, the mean expression in PID offspring did not differ from CTL (Figures 9B and 9C).

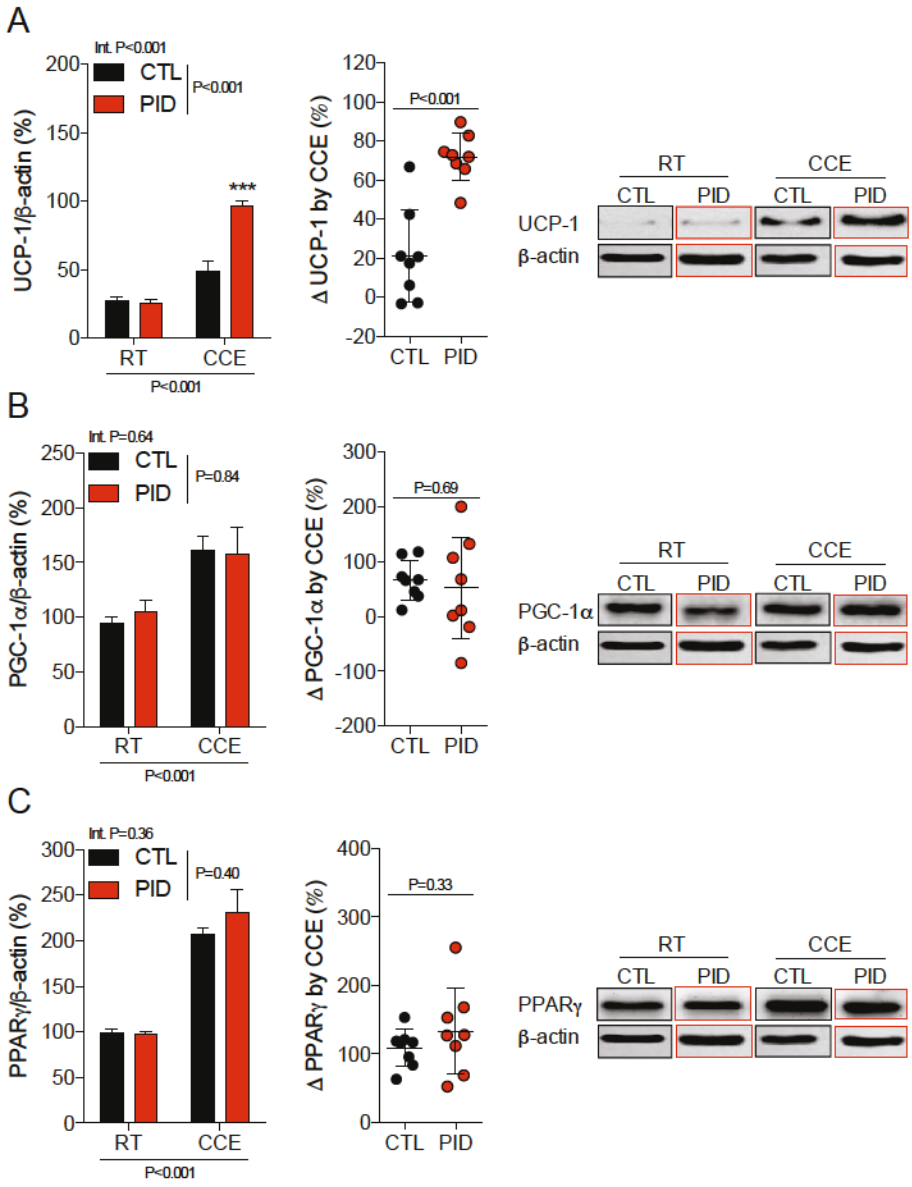

Figure 9 The immediate effect of PID and CCE on male thermogenic protein expression

Expression of UCP-1 (A), PGC-1α (B), and PPARγ (C) was determined by Western blot analysis directly following cold exposure. CTL, control; PID, perinatal iron deficiency; RT, room temperature; CCE, chronic cold exposure. Data are presented as means ± SEM, n=8 per group. ***, P<0.001 compared to control.

The effect of CCE caused marked alterations in BAT and WAT. IBAT mass (normalized to body weight) was increased ($P<0.001$) (Figure 10A) and the area of IBAT adipocytes was decreased ($P<0.001$) (Figure 10B) by CCE, and the difference in IBAT mass and IBAT area between CCE and RT littermates was lesser in PID offspring ($P<0.001$). The degree of change by CCE was altered in PID offspring, such that normalized IBAT mass was lesser ($P<0.001$) and IBAT adipocyte area was greater ($P=0.02$) when compared to CTL. CCE effectively decreased the relative mass of VAT ($P<0.001$) (Figure 10C), but the area of WAT adipocytes was unaffected (Figure 10D). Interestingly, both RT and CCE PID offspring exhibited a smaller WAT adipocyte area ($P<0.001$, for both parameters). Nonetheless, the Δ by CCE in the PID offspring did not differ from CTL.

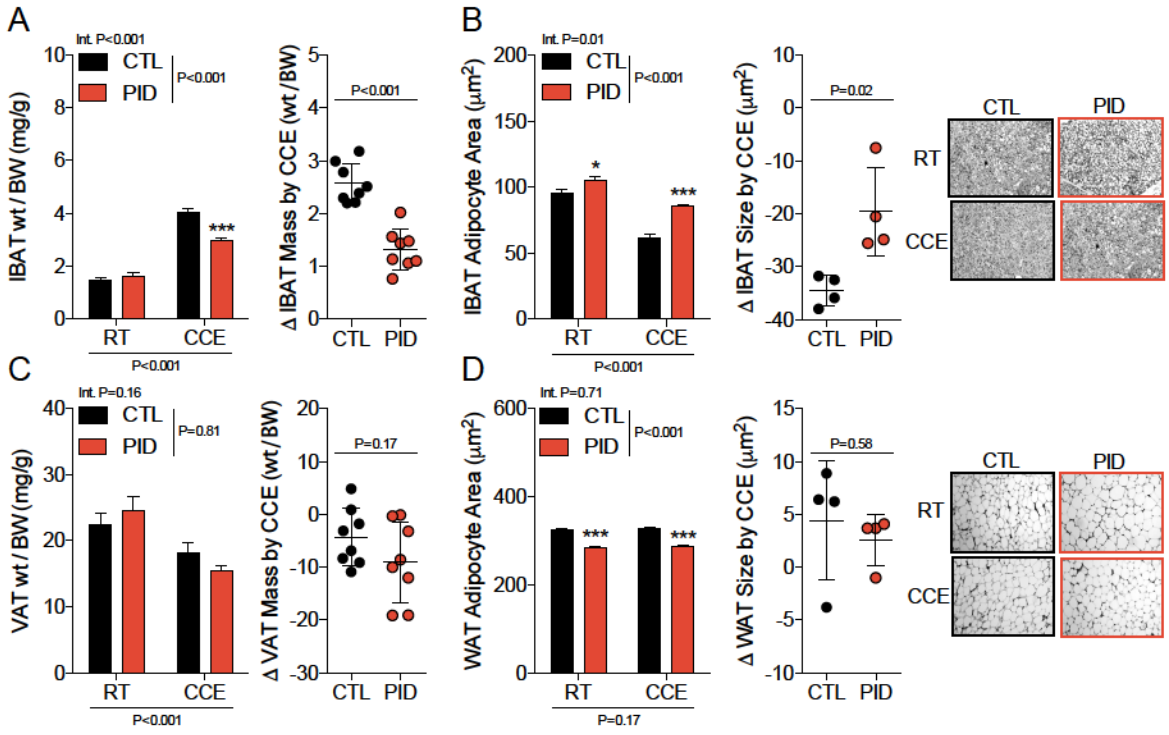

Figure 10 The immediate effect of PID and CCE on male offspring WAT and BAT

IBAT mass (A) and VAT mass (C) was determined from adipose tissue samples directly following euthanization. IBAT size (B) and WAT size (D) was determined by routine H&E staining. CTL, control; PID, perinatal iron deficiency; RT, room temperature; CCE, chronic cold exposure. Data are presented as means ± SEM, n=8 per group. *, P<0.05; ***, P<0.001 compared to control.

Heat production is proportionate to the quantity of IBAT and the expression of UCP-1 in IBAT. Accordingly, an increase in both basal ($P<0.001$) (Figure 11A) and maximal heat production ($P<0.001$) (Figure 11B) was found in CCE offspring. In both measurements, an effect of PID was also found ($P=0.02$ basal and $P=0.007$ maximal). Whereas the increase in basal heat production did not differ between CTL and PID offspring, the increase in maximal heat production due to CCE was mitigated in PID offspring compared to CTL ($P<0.001$).

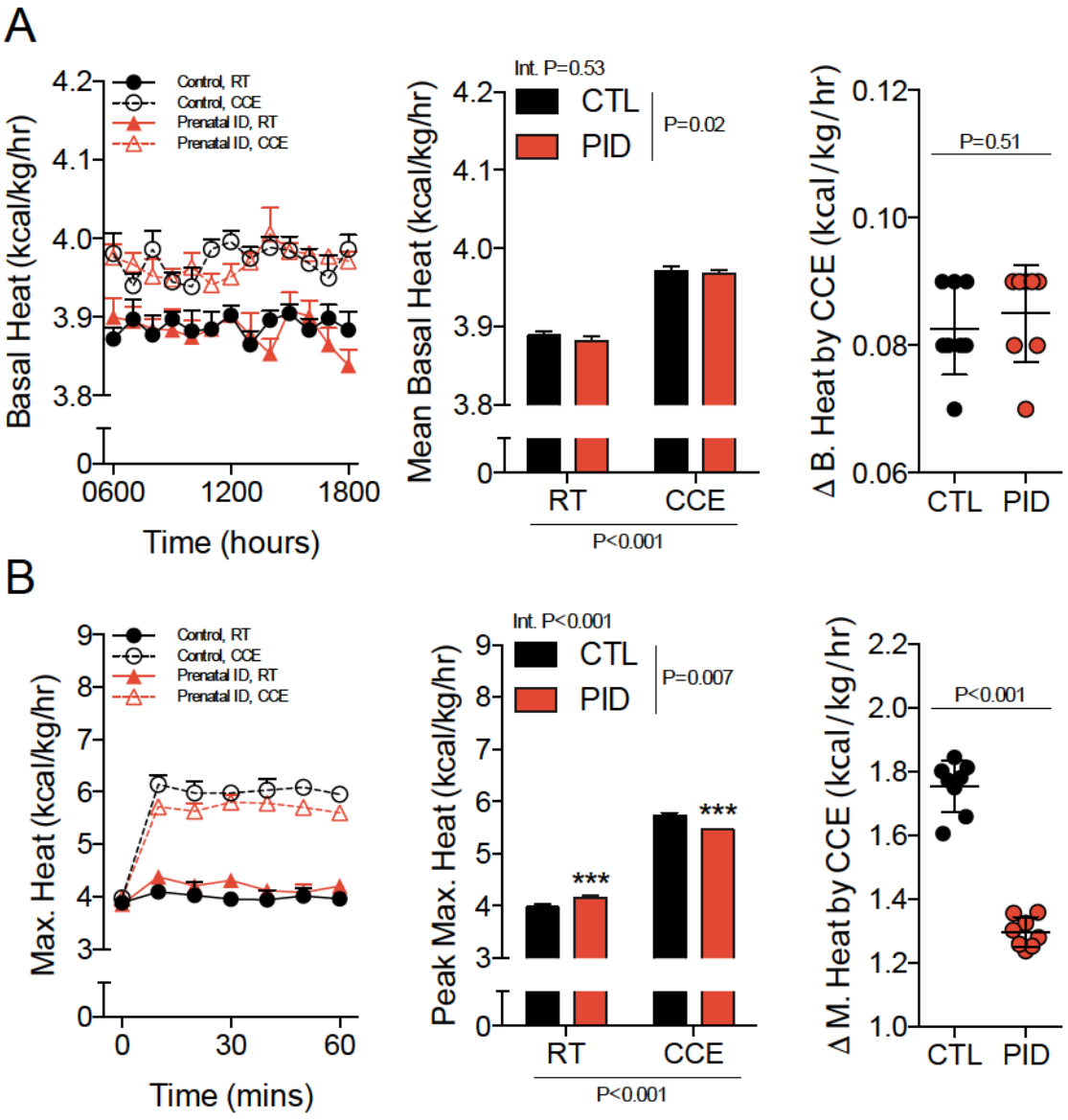

Figure 11 The immediate effect of PID and CCE on male heat production

Basal heat production (A) was collected for 12 hr uninterrupted in the light phase and maximal heat production (B) was calculated from the peak maximum following a single supramaximal dose (2 mg/kg, i.p.) of the β3 agonist CL216,243 directly following cold exposure. CTL, control; PID, perinatal iron deficiency; RT, room temperature; CCE, chronic cold exposure. Data are presented as means ± SEM, n=8 per group. ***, P<0.001 compared to control.

All cold-exposed male offspring demonstrated a lower VCO_2 ($P<0.001$) (Figure 12B) and a lower VO_2 ($P<0.001$) (Figure 12C) when compared to RT, and all PID offspring exhibited lower values when compared to CTL ($P<0.001$ for both parameters). The change in VO_2 by CCE was lower in PID offspring ($P<0.001$) but no difference between CTL and PID offspring was observed when VO_2 was assessed. These changes by CCE led to an increased RER ($P<0.001$) that was larger in PID offspring ($P<0.001$) (Figure 12A).

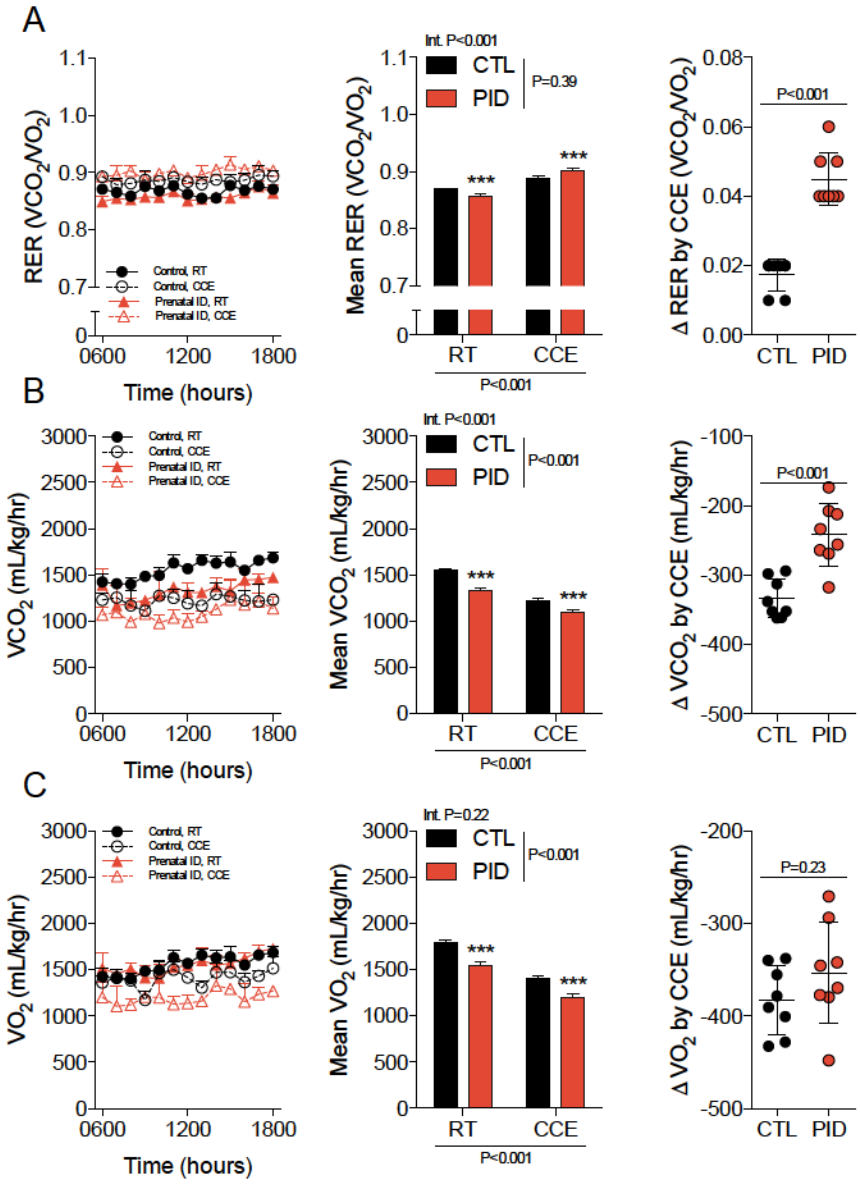

Figure 12 The immediate effect of PID and CCE on male offspring energy metabolism

Open-circuit indirect calorimetry was used to assess RER (A), VCO_2 (B), and VO_2 (C) for 12 hr uninterrupted in the light phase directly following cold exposure. CTL, control; PID, perinatal iron deficiency; RT, room temperature; CCE, chronic cold exposure. Data are presented as means ± SEM, n=8 per group. ***, P<0.001 compared to control.

Alterations in the lean mass and the fat mass were then evidenced *in vivo* by whole-body composition analysis. Cold-exposed offspring had a higher proportional lean mass ($P<0.001$) (Figure 13A) and a lower proportional fat mass ($P<0.001$) (Figure 13B) compared to their RT littermates. The Δ in both the lean and fat mass by CCE was to a larger extent in the PID offspring, although an effect of PID was only evidenced in the fat mass ($P=0.03$).

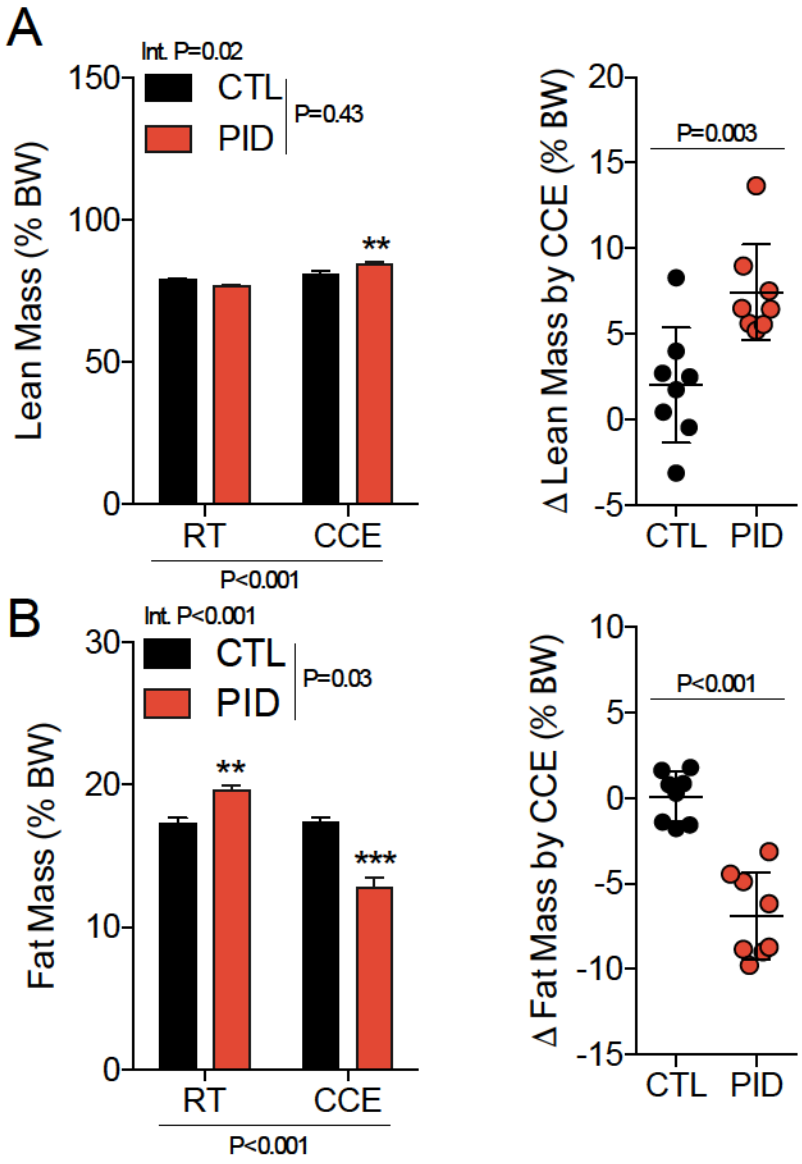

Figure 13 The immediate effect of PID and CCE on male offspring body composition

Lean mass (A) and fat mass (B) proportionate to body weight was determined by whole-body composition analysis. Data was assessed directly following cold exposure. CTL, control; PID, perinatal iron deficiency; RT, room temperature; CCE, chronic cold exposure. Data are presented as means ± SEM, n=8 per group. **, P<0.01; ***, P<0.001 compared to control.

While the effect of CCE on body composition was further exemplified by a lower BW in the cold exposed offspring (P=0.009) (Figure 14A), the Δ of BW was not different between CTL and PID offspring when RT and CCE littermates in each group were paired. Interestingly, the decrease in the BW of CCE offspring was observed despite an increase in caloric intake (P<0.001) (Figure 14B). An interaction between the effects of CCE and PID on caloric intake (P=0.02) was observed (P=0.002).

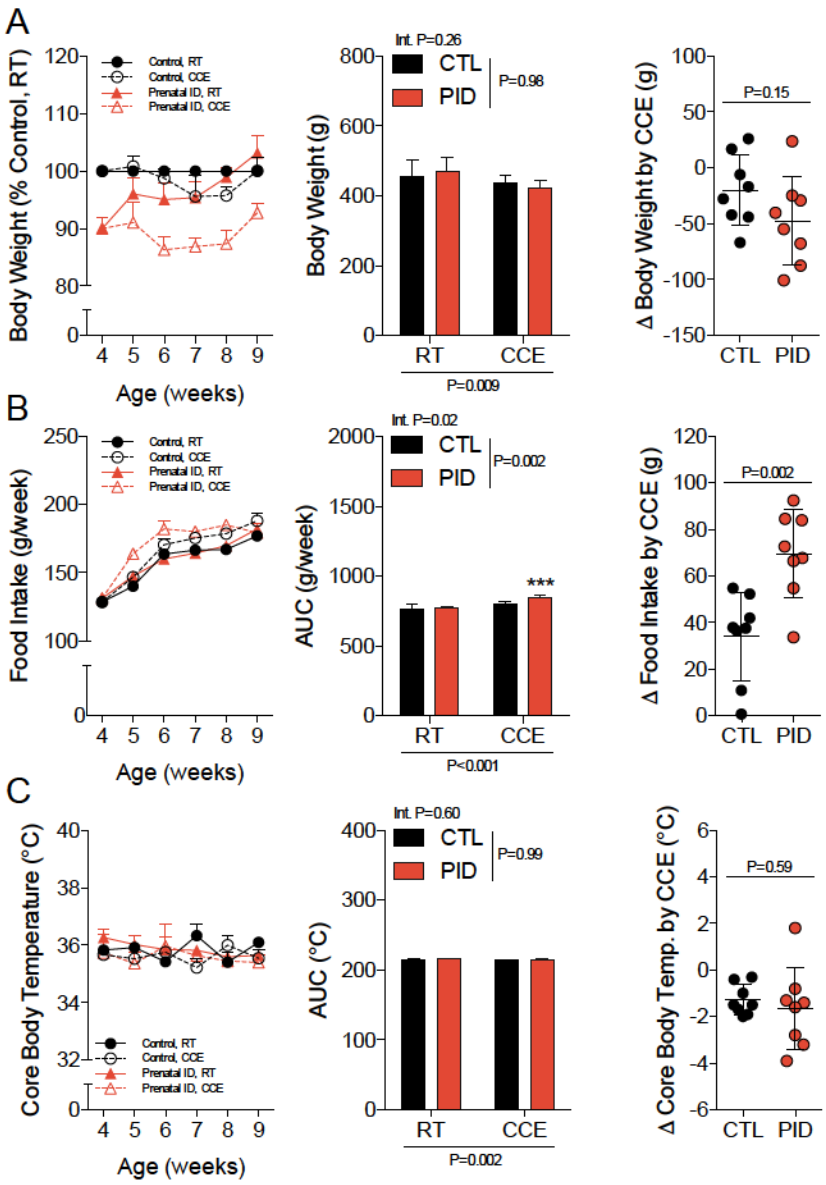

Figure 14 The immediate effect of PID and CCE on male body weight, food intake, and core body temperature

Body weight (A) was assessed at 9 wk of age; food intake (B), and core body temperature (C) was assessed throughout cold exposure. CTL, control; PID, perinatal iron deficiency; RT, room temperature; CCE, chronic cold exposure. Data are presented as means ± SEM, n=8 per group. ***, P<0.001 compared to control.

3.2.2 Female Offspring

In female CCE offspring, the expression of UCP-1 (Figure 15A), PGC-1α (Figure 15B), and PPARγ (Figure 15C) were increased ($P<0.001$, for all parameters). An effect of PID was observed in all proteins ($P<0.001$, for all parameters). An interaction between the effects of CCE and PID was seen for UCP-1 and PGC-1α; accordingly, the Δ in expression of UCP-1 and PGC-1α due to cold exposure in paired offspring was lower in the PID offspring ($P=0.001$ and $P=0.05$, respectively).

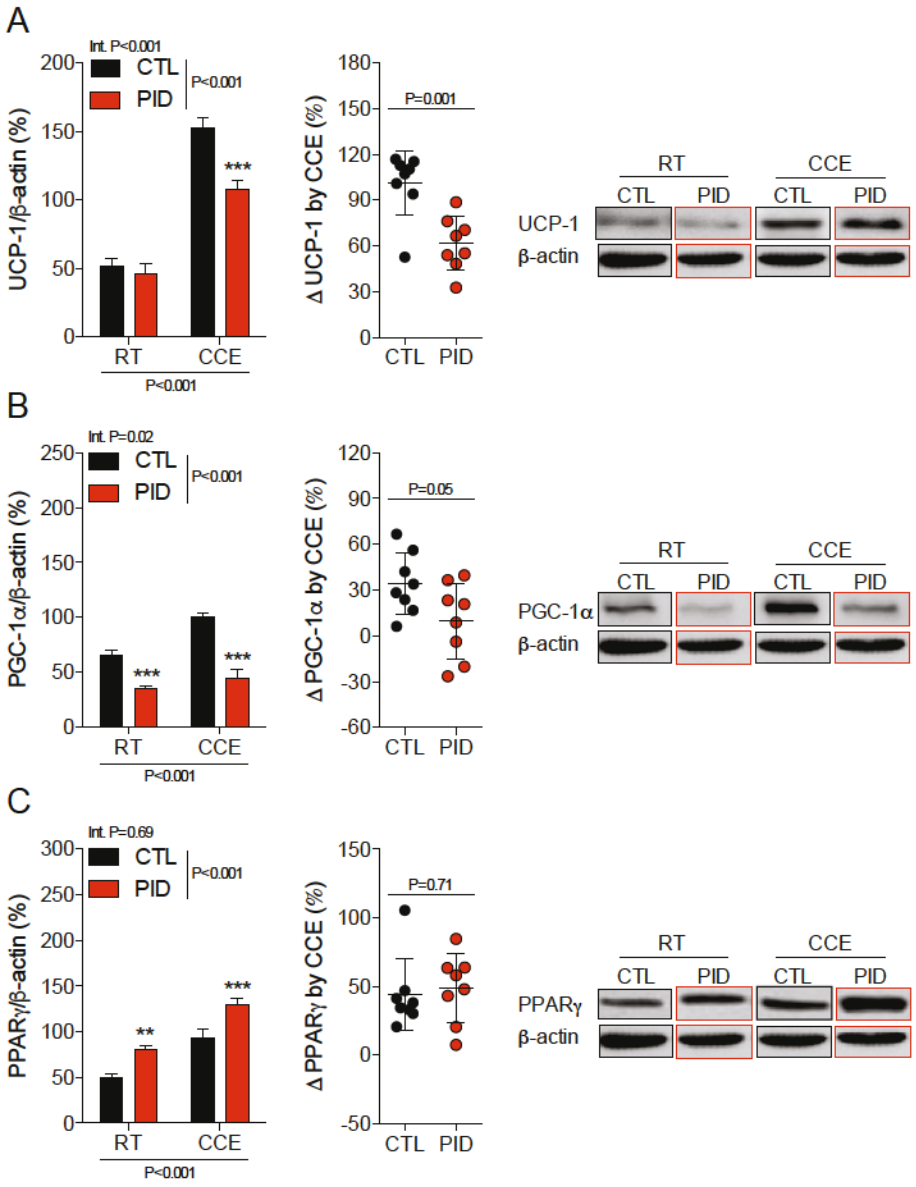

Figure 15 The immediate effect of PID and CCE on female thermogenic protein expression

Expression of UCP-1 (A), PGC-1α (B), and PPARγ (C) was determined by Western blot analysis directly following cold exposure. CTL, control; PID, perinatal iron deficiency; RT, room temperature; CCE, chronic cold exposure. Data are presented as means ± SEM, n=8 per group. **, P<0.01; ***, P<0.001 compared to control.

An increase in the thermogenic regulatory proteins by CCE substantiated an effect of CCE on IBAT mass and adipocyte area. All female offspring had an increased IBAT mass ($P<0.001$) (Figure 16A) and a decreased IBAT adipocyte area ($P<0.001$) (Figure 16B) as a result of CCE. Although PID offspring showed a greater increase in IBAT mass when compared to CTL ($P<0.001$), the decrease in IBAT adipocyte area was less, such that PID offspring demonstrated a larger IBAT adipocyte area than CTL ($P<0.001$). The primary difference between PID and CTL female offspring IBAT was seen in the lesser reduction on IBAT adipocyte area. The mass of VAT did not differ due to effects of either PID or CCE, and nor did the change in VAT mass by way of CCE when littermates were paired (Figure 16C). Conversely, the adipocyte area of WAT (Figure 16D) was larger in CCE offspring ($P<0.001$). Interestingly, all PID offspring had a smaller WAT adipocyte area ($P<0.001$), but there was no interaction in WAT adipocyte area between CCE and PID.

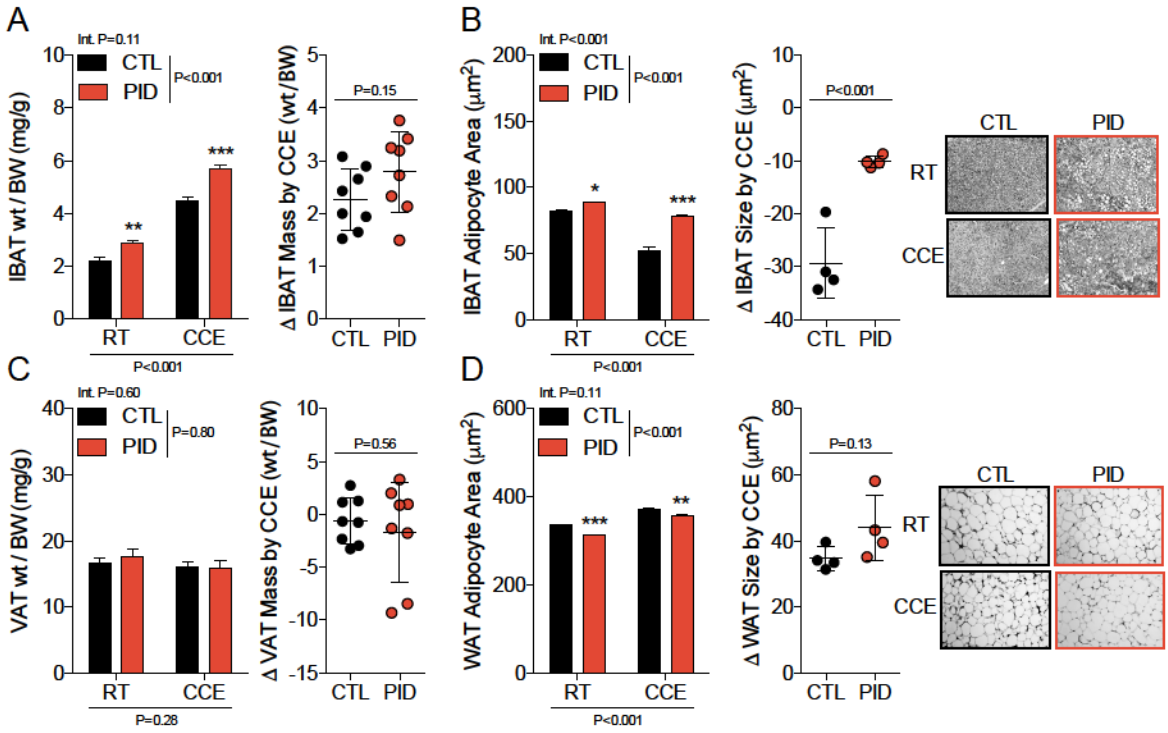

Figure 16 The immediate effect of PID and CCE on female offspring BAT and WAT

IBAT mass (A) and VAT mass (C) was determined from adipose tissue samples directly following euthanasia. IBAT size (B) and WAT size (D) was determined by routine H&E staining. CTL, control; PID, perinatal iron deficiency; RT, room temperature; CCE, chronic cold exposure. Data are presented as means ± SEM, n=8 per group. *, P<0.05; **, P<0.01; ***, P<0.001 compared to control.

An increase in IBAT quantity due to CCE was accompanied with an increase in both basal ($P<0.001$) (Figure 17A) and maximal heat production ($P<0.001$) (Figure 17B). Basal heat production was also affected by PID ($P<0.001$), and an interaction between CCE and PID ($P<0.001$) was observed. Interestingly, the results of maximal heat production paralleled those seen in IBAT mass, such that PID offspring demonstrated a higher peak maximum compared to CTL offspring; the effect of CCE was similar in both CTL and PID.

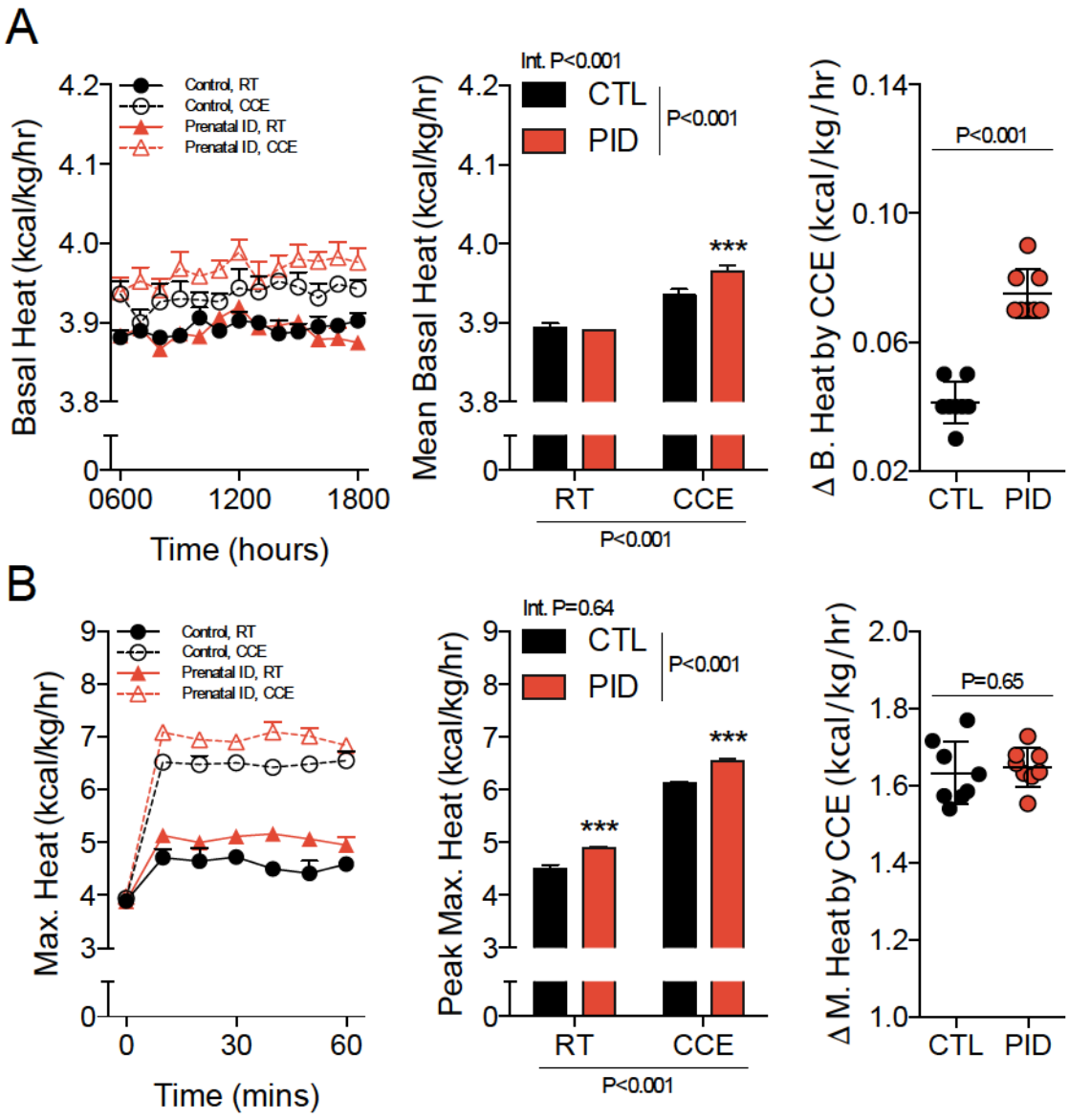

Figure 17 The immediate effect of PID and CCE on female offspring heat production

Basal heat production (A) was collected for 12 hr uninterrupted in the light phase and maximal heat production (B) was calculated from the peak maximum following a single supramaximal dose (2 mg/kg, i.p.) of CL216,243 directly following cold exposure. CTL, control; PID, perinatal iron deficiency; RT, room temperature; CCE, chronic cold exposure. Data are presented as means ± SEM, n=8 per group. ***, P<0.001 compared to control.

All female offspring exposed to chronic cold exhibited a lower VCO_2 ($P<0.001$) (Figure 18B) and a lower VO_2 ($P<0.001$) (Figure 18C). PID also affected both parameters ($P<0.006$, for both parameters), but no interaction was observed. These results led to an increased RER ($P<0.001$) (Figure 18A) due to CCE. The increase in RER caused by CCE was lower in PID offspring when compared to CTL ($P<0.001$).

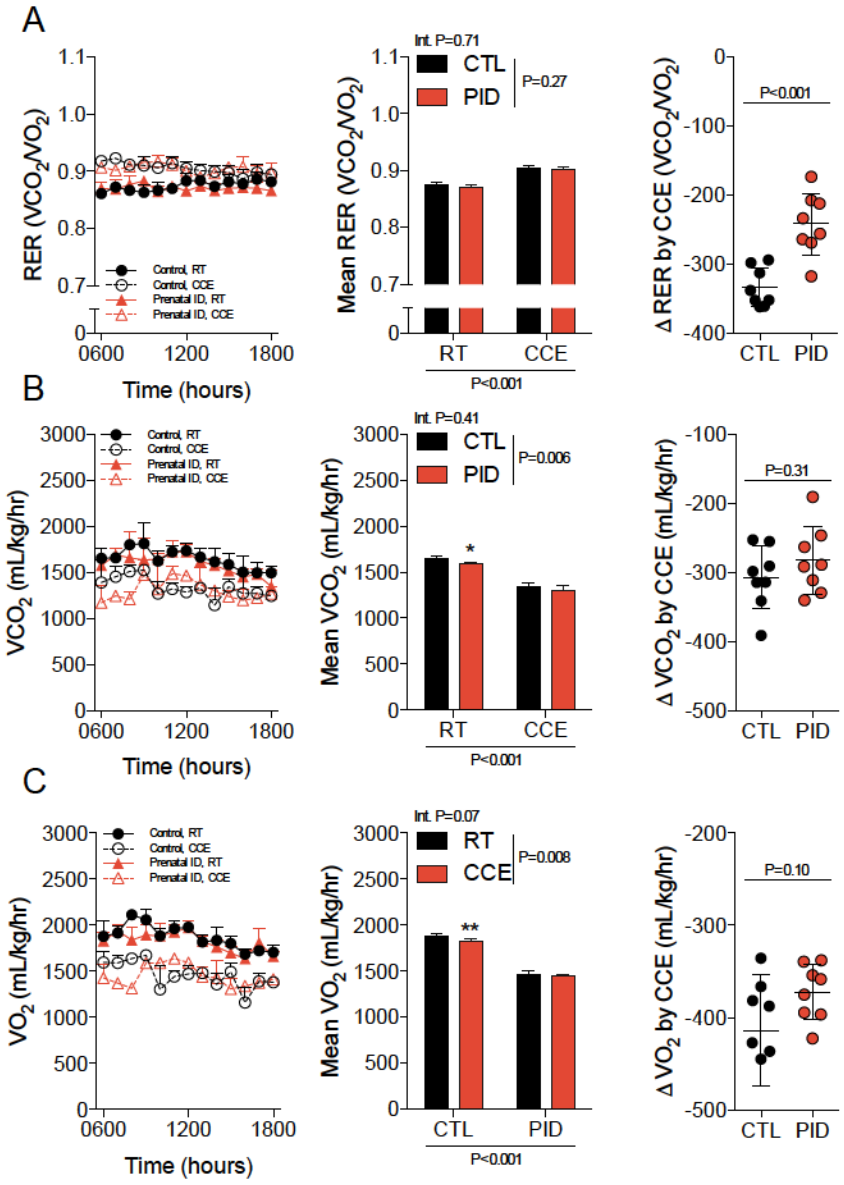

Figure 18 The immediate effect of PID and CCE on female offspring energy metabolism

Open-circuit indirect calorimetry was used to assess RER (A), VCO_2 (B), and VO_2 (C) for 12 hr uninterrupted in the light phase directly following cold exposure. CTL, control; PID, perinatal iron deficiency; RT, room temperature; CCE, chronic cold exposure. Data are presented as means ± SEM, n=8 per group. *, P<0.05; **, P<0.01 compared to control.

Neither CCE nor PID affected the proportion of lean mass (Figure 19A) or fat mass (Figure 19B) in female offspring. Furthermore, there were no alterations determined in BW (Figure 20A), despite an increase in caloric intake by the effects of both PID ($P<0.001$) and CCE ($P<0.001$) (Figure 20B). The caloric intake was also affected by PID in addition to CCE ($P=0.001$); the interaction between the two is illustrated in the Δ of food intake between PID and CTL offsprings when RT and CCE littermate are paired ($P=0.01$).

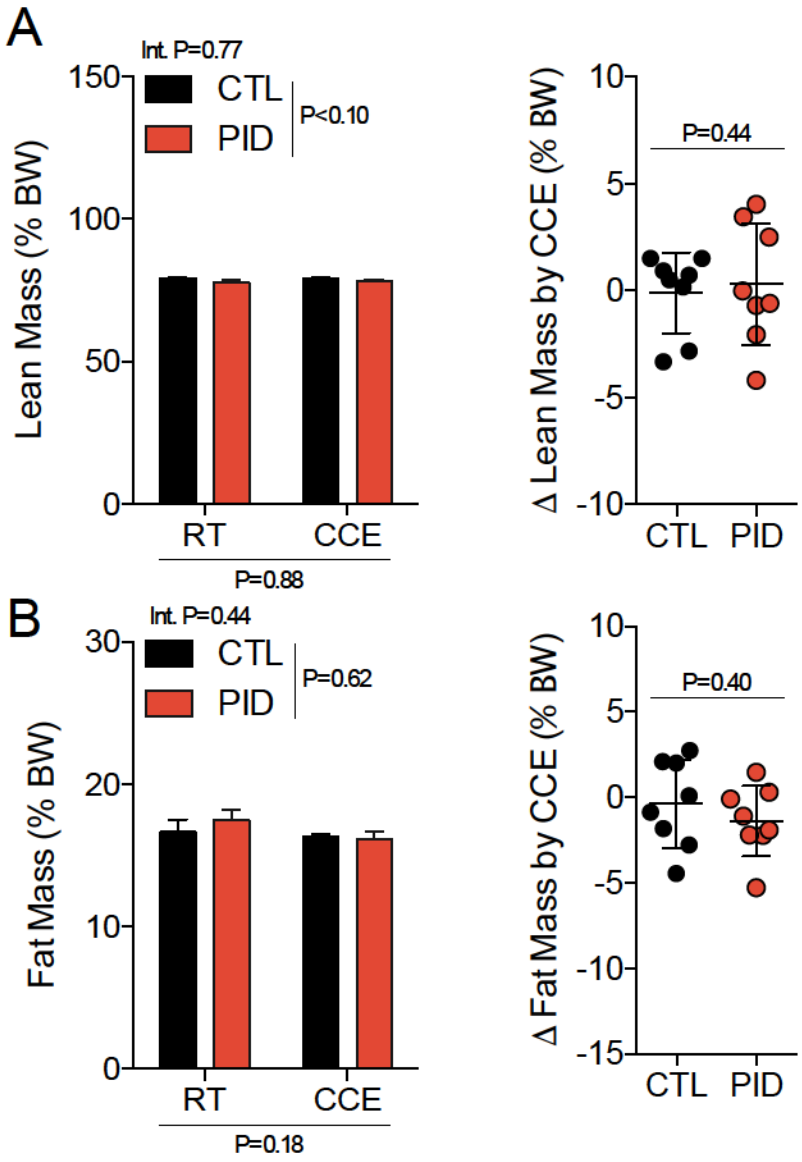

Figure 19 The immediate effect of PID and CCE on female Echo-MRI

Lean mass (A) and fat mass (B) proportionate to body weight was determined by whole-body composition analysis directly following cold exposure. CTL, control; PID, perinatal iron deficiency; RT, room temperature; CCE, chronic cold exposure. Data are presented as means ± SEM, n=8 per group.

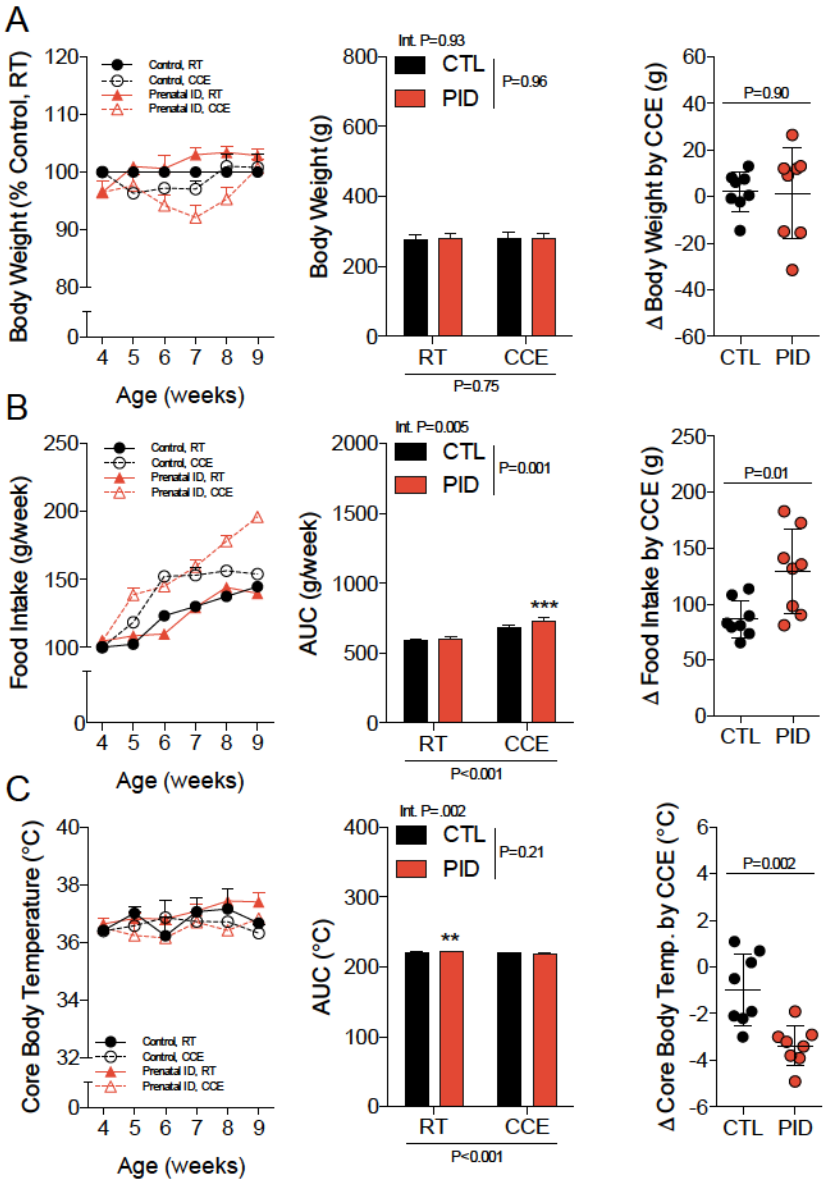

Figure 20 The immediate effect of PID and CCE on female offspring body weight, food intake, and core body temperature

Body weight (A) was assessed at 9 wk of age; food intake (B) and core body temperature (C) was assessed directly following cold exposure. CTL, control; PID, perinatal iron deficiency; RT, room temperature; CCE, chronic cold exposure. Data are presented as means ± SEM, n=8 per group. **, P<0.01; ***, P<0.001 compared to control.

Table 2 The immediate effect of PID and CCE on offspring growth characteristics

Male	**Control**		**Perinatal ID**		**P Values**		
	RT (n=8)	**CCE (n=8)**	**RT (n=8)**	**CCE (n=8)**	**Hb**	**˚C**	**Int**
Body Weight (g)	456 ± 16	436 ± 8	470 ± 14	422 ± 7*	>0.90	<0.01	0.25
Crown-Rump (cm)	18.6 ± 0.6	17.1 ± 0.3*	18.5 ± 0.4	17.3 ± 0.2	0.90	<0.01	0.71
Visceral Girth (cm)	20.7 ± 0.4	18.7 ± 0.7**	20.3 ± 0.3	23.0 ± 0.3***	<0.001	0.45	<0.001
CR:VG	0.90 ± 0.02	0.92 ± 0.04	0.91 ± 0.02	0.75 ± 0.01***	<0.01	<0.01	<0.05
Female	Control		Perinatal ID		P Values		
	RT (n=8)	CCE (n=8)	RT (n=8)	CCE (n=8)	Hb	˚C	Int
Body Weight (g)	277 ± 4	280 ± 5	278 ± 6	280 ± 5	0.92	0.62	0.92
Crown-Rump (cm)	15.6 ± 0.5	15.8 ± 0.3	15.2 ± 0.3	14.8 ± 0.4	0.08	0.80	0.44
Visceral Girth (cm)	16.7 ± 0.1	16.7 ± 0.1	16.7 ± 0.3	16.2 ± 0.5	0.41	0.41	0.41
CR:VG	0.93 ± 0.03	0.95 ± 0.02	0.91 ± 0.02	0.92 ± 0.02	0.28	0.52	0.83

Data are mean ± SEM. All data was measured directly following cold exposure at 9 wk of age. CTL, control; PID, perinatal iron deficiency; RT, room temperature; CCE, chronic cold exposure. *, P<0.05; **, P<0.01; ***, P<0.001 compared with room temperature littermates.

3.3 The Residual Effects of Chronic Cold Exposure

3.3.1 Male Offspring

Although a 5 wk CCE protocol immediately increased expression of all thermogenic proteins assessed, only PPARγ exhibited an increase at 4 wk thereafter (P=0.01) (Figure 21B). There was no effect of CCE on the expression of PGC-1α, but all PID offspring exhibited an increased expression in comparison to CTL (Figure 21C); no differences were found between PID and CTL groups within RT and CCE paired littermates.

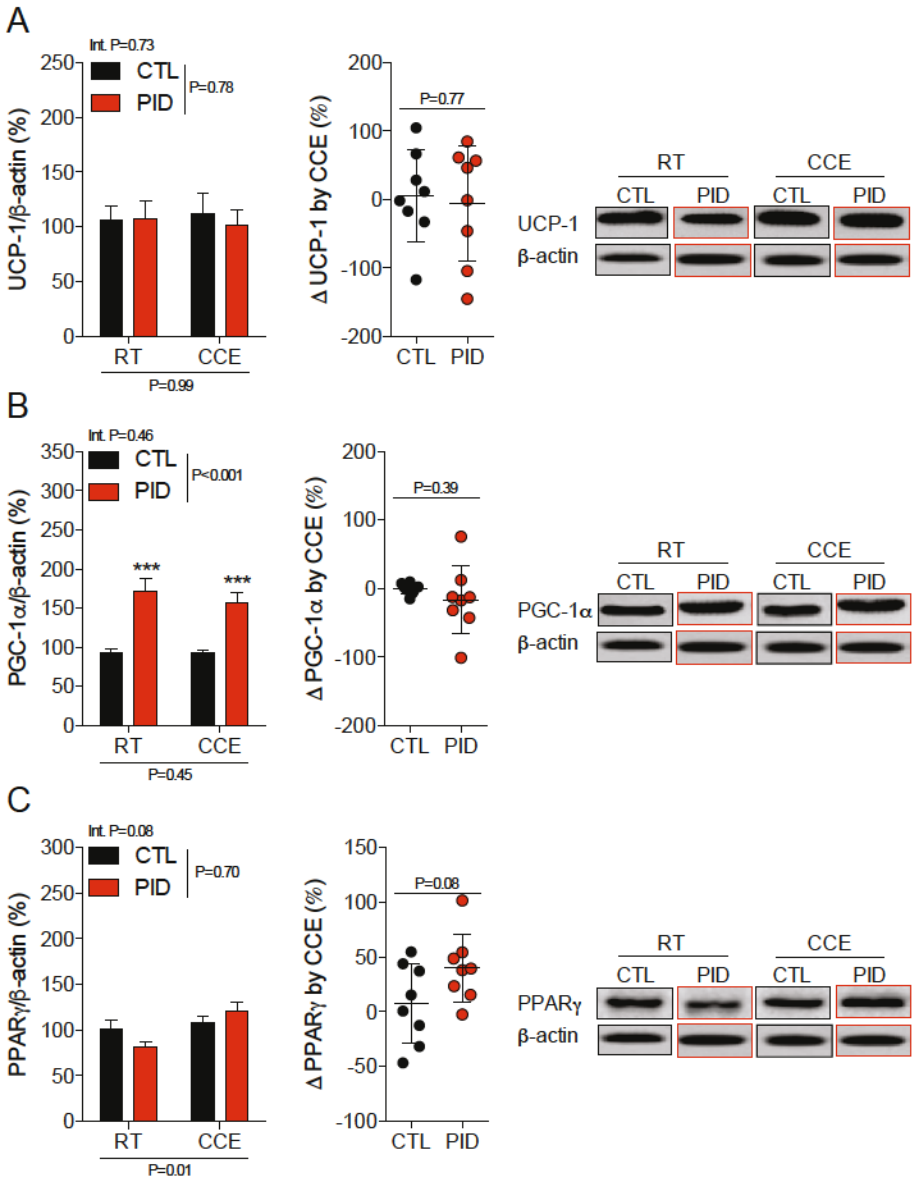

Figure 21 The residual effect of PID and CCE on male thermogenic protein expression

Expression of UCP-1 (A), PGC-1α (B), and PPARγ (C) was determined by Western blot analysis 4 wk following cold exposure. CTL, control; PID, perinatal iron deficiency; RT, room temperature; CCE, chronic cold exposure. Data are presented as means ± SEM, n=8 per group. ***, P<0.001 compared to control.

Not surprisingly, the relative mass of IBAT in CCE offspring decreased over the post-CCE period, although an effect of CCE was still evident at 4 wk after CCE ($P=0.02$) (Figure 22A). There were no differences between CTL and PID groups. In contrast, virtually no alterations in the reduced IBAT adipocyte area occurred over 4 wk. as a decrease was still observed due to CCE ($P<0.001$); here, the Δ between RT and PID paired littermates was greater in CTL offspring ($P=0.002$) compared to PID (Figure 22B). Similar results were found in the WAT adipocyte area, such that CCE offspring maintained a smaller WAT adipocyte area for 4 wk following CCE ($P=0.004$), and the Δ was greater in CTL compared to PID offspring ($P<0.001$) (Figure 22D). Conversely, the relative WAT mass did not differ between RT and CCE offspring but was increased in all PID offspring ($P=0.009$) (Figure 22A).

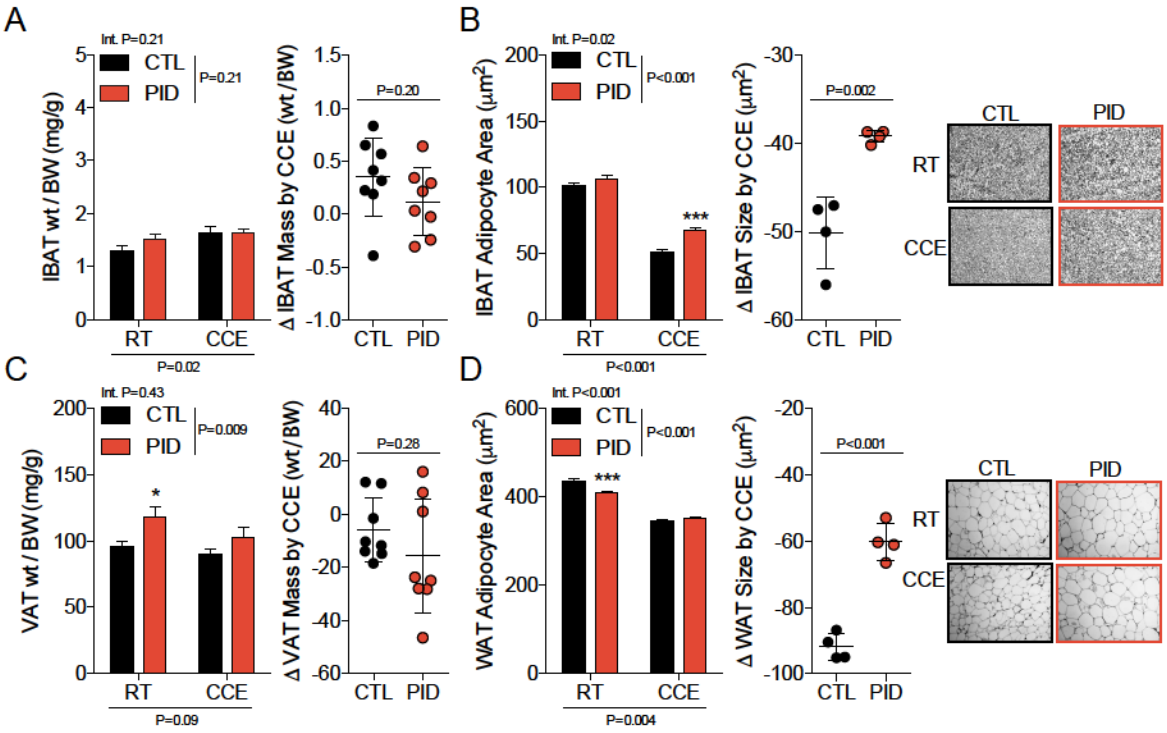

Figure 22 The residual effect of PID and CCE on male adipose tissue

IBAT mass (A) and VAT mass (C) was determined from adipose tissue samples directly following euthanasia. IBAT size (B) and WAT size (D) was determined by routine H&E staining. CTL, control; PID, perinatal iron deficiency; RT, room temperature; CCE, chronic cold exposure. Data are presented as means ± SEM, n=8 per group. *, P<0.05; ***, P<0.001 compared to control.

The effects of a 5 wk CCE protocol on basal (Figure 23A) and maximal heat production (Figure 23B) were maintained at 4 wk thereafter ($P<0.001$, for both parameters), such that the effects of CCE and PID were exhibited on both ($P<0.001$, for both effects). Accordingly, an interaction was determined ($P<0.001$, for both parameters). Interestingly, when RT and CCE offspring were paired, the Δ in basal heat production by way of CCE was greater in PID offspring ($P<0.001$), which reflects an interaction between the effects of CCE and PID ($P<0.001$). In contrast, paired PID offspring exhibited a lesser Δ in maximal heat production than CTL offspring ($P<0.001$), and again an interaction was observed ($P<0.001$).

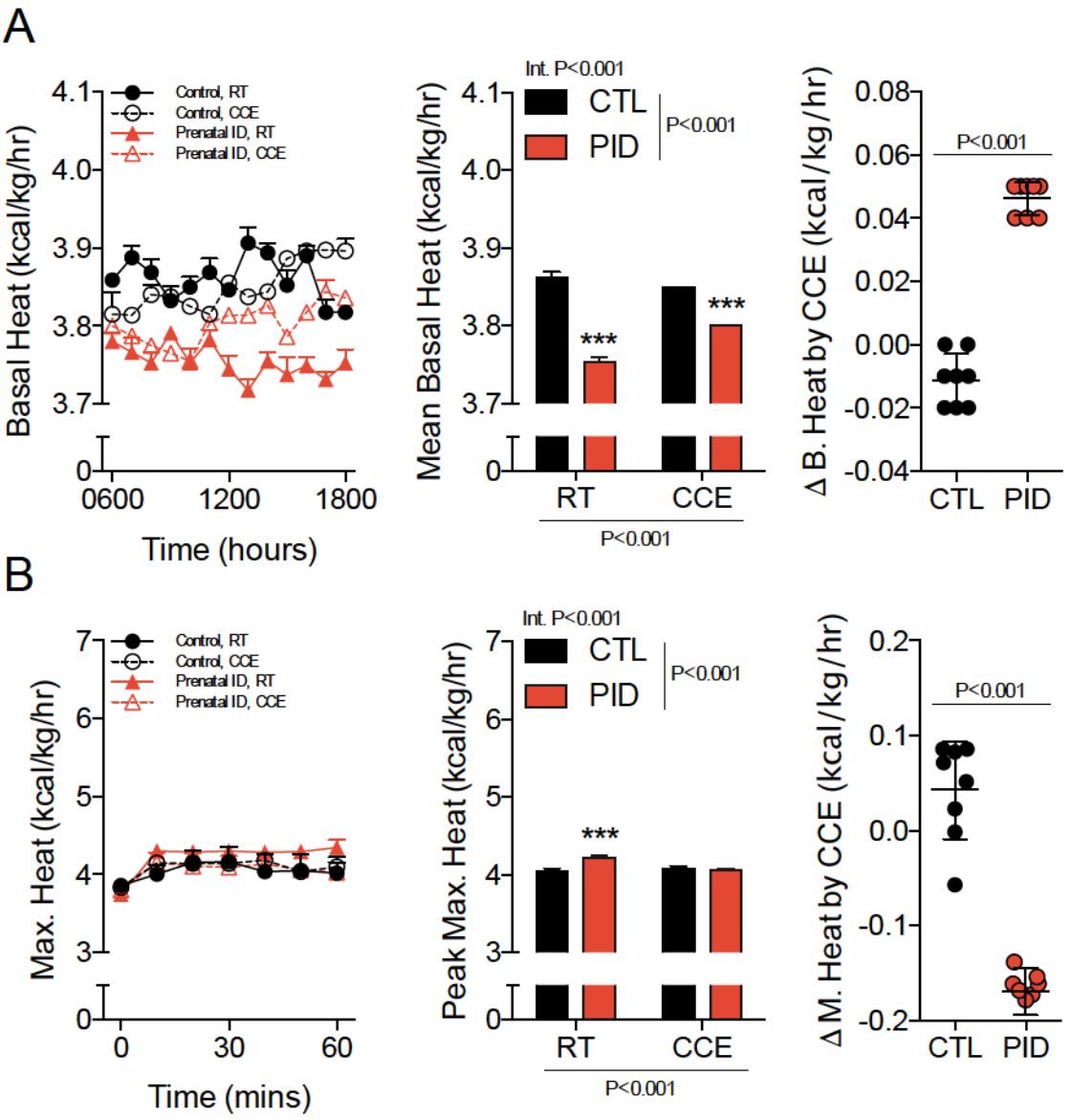

Figure 23 The residual effect of PID and CCE on male heat production

Basal heat production (A) was collected for 12 hr uninterrupted in the light phase and maximal heat production (B) was calculated from the peak maximum following a single supramaximal dose (2 mg/kg, i.p.) of CL216,243 4 wk following cold exposure. CTL, control; PID, perinatal iron deficiency; RT, room temperature; CCE, chronic cold exposure. Data are presented as means ± SEM, n=8 per group. ***, P<0.001 compared to control.

CCE had residual effects on whole-body energy metabolism of male offspring ($P<0.001$, for all parameters), and PID did as well ($P<0.001$, for all parameters). The RER (Figure 24A), VCO_2 (Figure 24B), and VO_2 (Figure 24C) of PID offspring was lesser than CTL at both RT and CCE ($P<0.001$, all). For all measurements, the Δ by way of CCE between RT and CCE littermates was increased in PID offspring ($P<0.001$); an interaction between the effects of CCE and PID was determined in all cases ($P<0.001$, for all parameters).

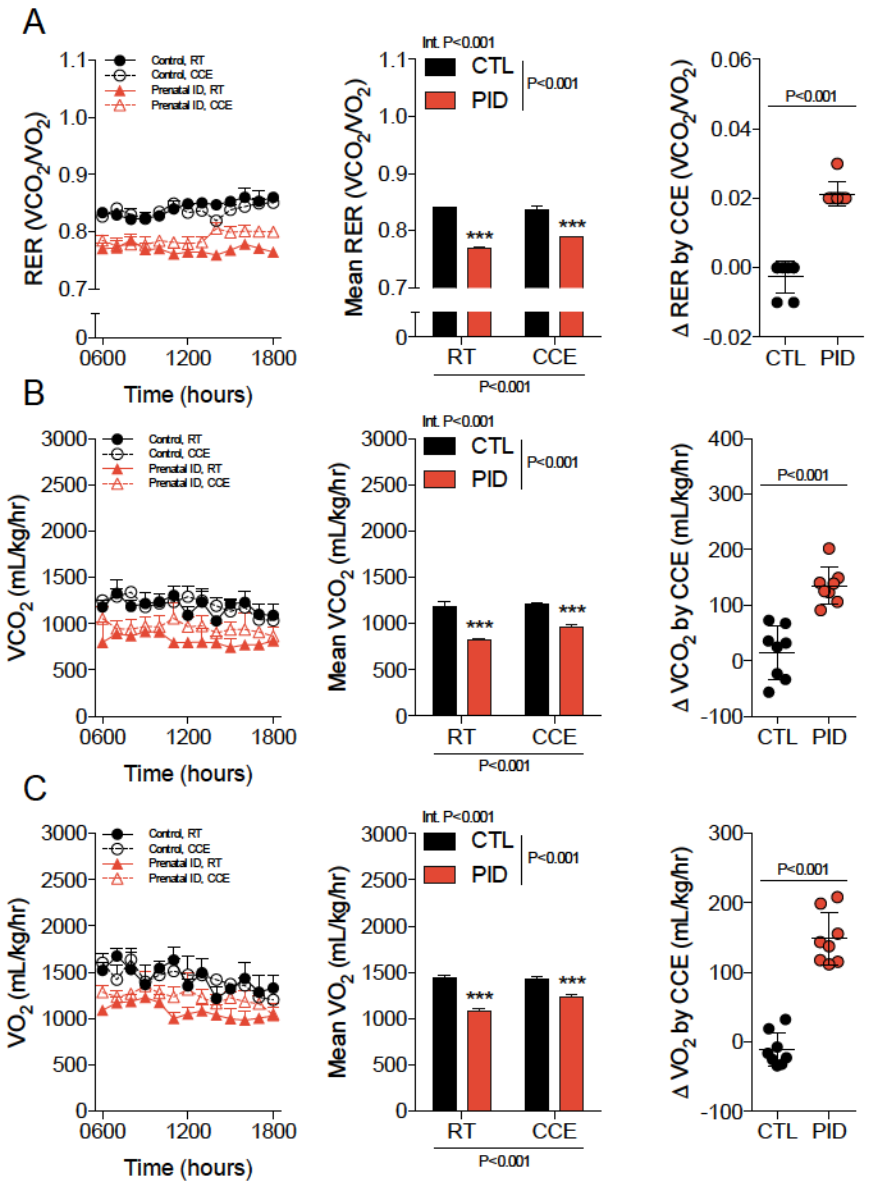

Figure 24 The residual effect of PID and CCE on male energy metabolism

Open-circuit indirect calorimetry was used to determine RER (A), VCO_2 (B), and VO_2 (C) for 12 hr uninterrupted in the light phase 4 wk following cold exposure. CTL, control; PID, perinatal iron deficiency; RT, room temperature; CCE, chronic cold exposure. Data are presented as means ± SEM, n=8 per group. ***, P<0.001 compared to control.

Residual effects of CCE were determined for the proportional lean mass (Figure 25A) and the fat mass (Figure 25B) of male offspring ($P<0.001$, for both parameters). However, it was the PID and not the CTL offspring that displayed alterations; the lean mass and the fat mass of CTL offspring at both RT and CCE did not differ. Despite an increase in PID offspring RER due to CCE, signifying a trend towards greater carbohydrate usage, measurements still indicated a greater utilization of fatty acids as the predominant fuel source. This was shown by a positive Δ in the relative lean mass between RT and CCE PID offspring, and as well by a negative Δ in the relative fat mass.

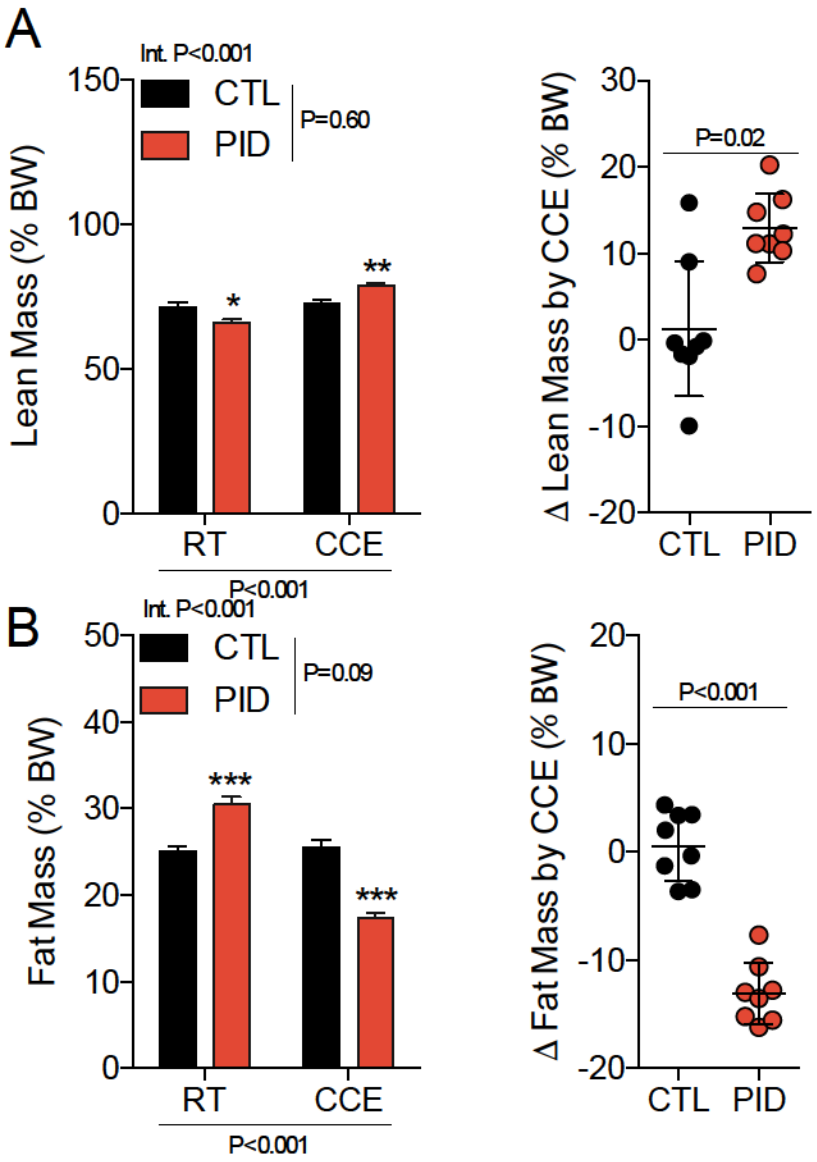

Figure 25 The residual effect of PID and CCE on male Echo-MRI

Lean mass (A) and fat mass (B) proportionate to body weight was determined by whole-body composition analysis 4 wk following cold exposure. CTL, control; PID, perinatal iron deficiency; RT, room temperature; CCE, chronic cold exposure. Data are presented as means ± SEM, n=8 per group. *, P<0.05; **, P<0.01; ***, P<0.001 compared to control.

Despite no alterations in the body composition of CTL offspring from CCE, all CTL and PID cold exposed offspring had a reduction in BW at 4 wk post-CCE; this was due to temperature (P=0.01) (Figure 26A). As there was no effect of PID nor an interaction of PID with CCE, the Δ in BW due to CCE was comparable between CTL and PID group. This result is notwithstanding an increased caloric consumption between RT and CCE CTL littermates (Figure 26B).

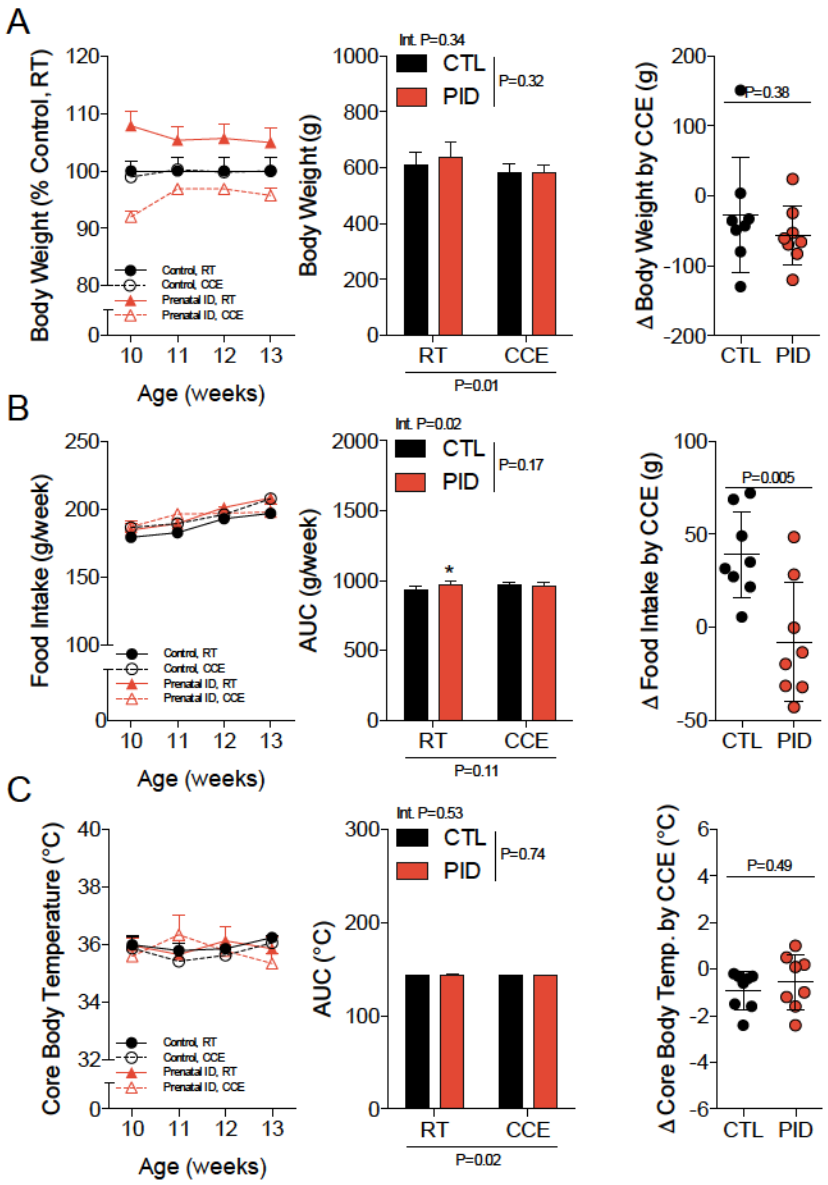

Figure 26 The residual effect of PID and CCE on male body weight, food intake, and core body temperature

Body weight (A) was assessed at 13 wk of age; food intake (B), and core body temperature (C) was assessed 4 wk following cold exposure. CTL, control; PID, perinatal iron deficiency; RT, room temperature; CCE, chronic cold exposure. Data are presented as means ± SEM, n=8 per group. *, P<0.05 compared to control.

3.3.2 Female Offspring

In female offspring at 4 wk following CCE, the expression of UCP-1 was not affected by CCE or PID (Figure 27A). Nevertheless, the key thermogenic regulatory proteins, PGC-1α (Figure 27B) and PPARγ (Figure 27C), were increased by CCE at 4 wk thereafter ($P<0.001$, for both parameters). While no differences between CTL and PID were seen in PGC-1α expression, the expression of PPARγ in PID offspring was increased in comparison to CTL ($P<0.001$). The Δ calculated between RT and CCE offspring for PPARγ expression demonstrated no difference between CTL and PID offspring.

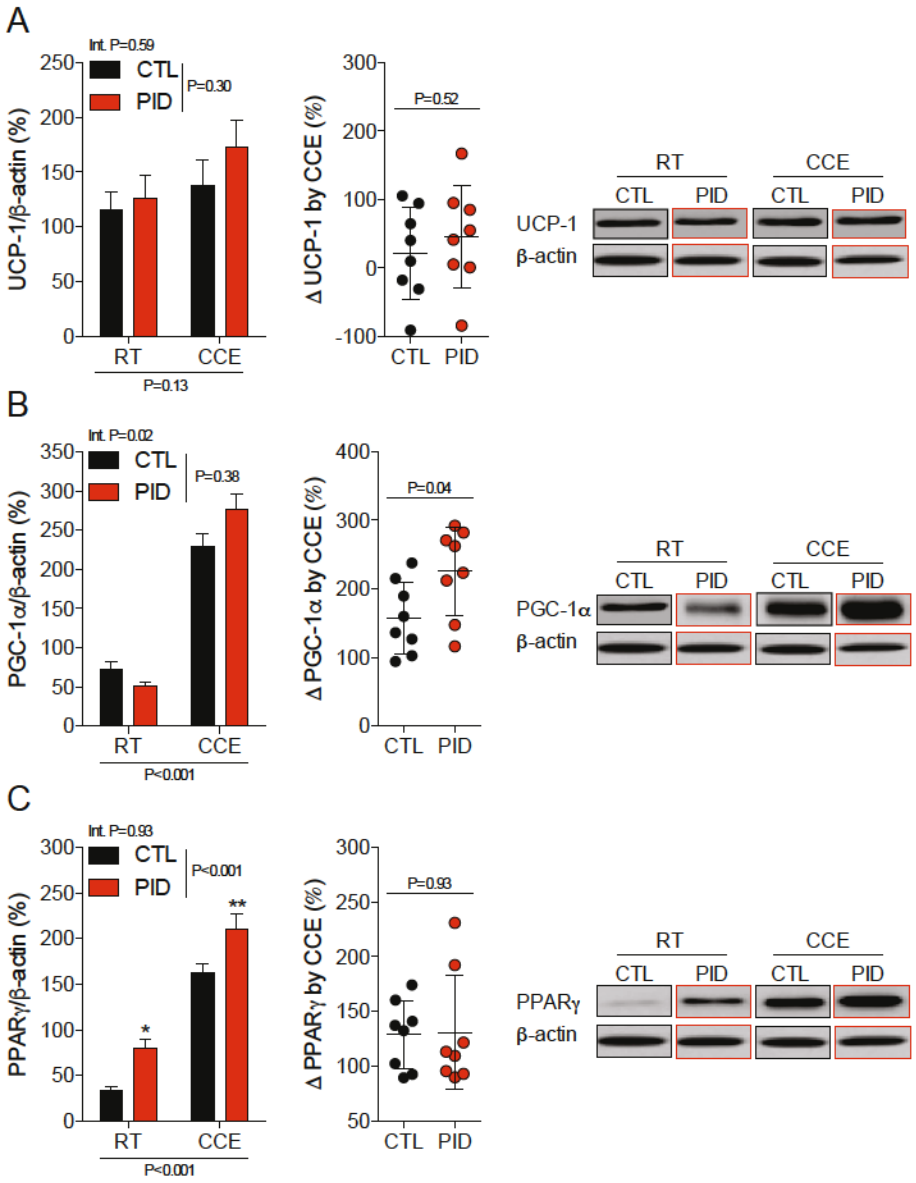

Figure 27 The residual effect of PID and CCE on female thermogenic protein expression

Expression of UCP-1 (A), PGC-1α (B), and PPARγ (C) was determined by Western blot analysis 4 wk following cold exposure. CTL, control; PID, perinatal iron deficiency; RT, room temperature; CCE, chronic cold exposure. Data are presented as means ± SEM, n=8 per group. *, P<0.05; **, P<0.01 compared to control.

The quantity of IBAT in CCE offspring was increased when compared to those at RT ($P<0.001$) (Figure 28A), and to a similar extent in the CTL and PID groups. Although IBAT adipocyte area did not exhibit residual effects of CCE (Figure 28B), an interaction between CCE and PID was determined and this is reflected in the Δ by way of CCE in the CTL and PID groups ($P<0.001$); while CTL offspring showed a decreased IBAT adipocyte area from CCE, PID offspring demonstrated an increase. Interestingly, a similar result was shown in the WAT adipocyte size (Figure 28D), which was affected by both CCE ($P=0.002$) and PID ($P<0.001$); the Δ calculated between RT and CCE offspring demonstrated a decrease in WAT adipocyte area in CTL offspring whereas PID offspring showed an increase ($P<0.001$).

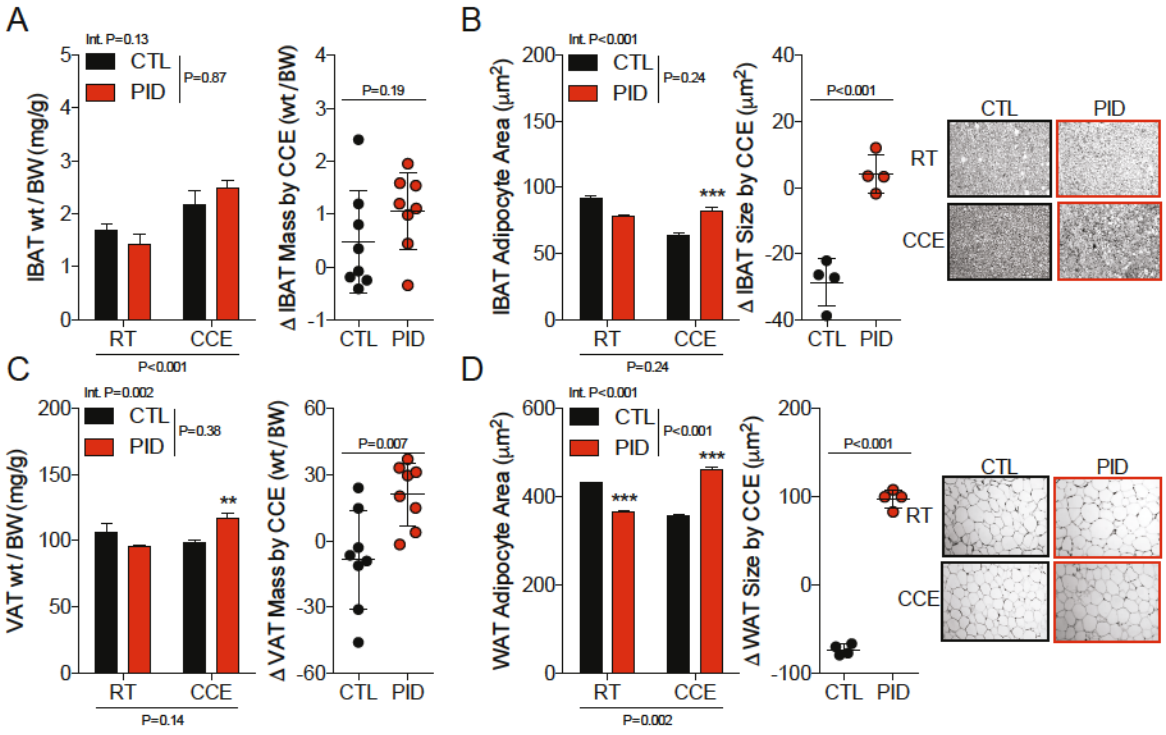

Figure 28 The residual effect of PID and CCE on female adipose tissue

IBAT mass (A) and VAT mass (C) was determined from adipose tissue samples directly following euthanization. IBAT size (B) and WAT size (D) was determined by routine H&E staining 4 wk following cold exposure. CTL, control; PID, perinatal iron deficiency; RT, room temperature; CCE, chronic cold exposure. Data are presented as means ± SEM, n=8 per group. **, P<0.01; ***, P<0.001 compared to control.

A 5 wk CCE protocol did not affect the basal heat production (Figure 29A) of female CTL offspring at 4 wk following. In contrast, PID offspring that were cold exposed showed a lower basal heat production compared to their RT littermates ($P<0.001$), and the heat production exhibited from both RT and CCE PID offspring was lesser than that exhibited from the CTL offspring ($P<0.001$). The maximal heat production (Figure 29B) of all CCE offspring indeed maintained an increased response ($P<0.001$). An interaction between the effects of CCE and PID was determined ($P<0.001$) and is reflected in the Δ by CCE; PID offspring exhibited a larger increase in maximal heat production from CCE when compared to that observed in the CTL offspring ($P<0.001$).

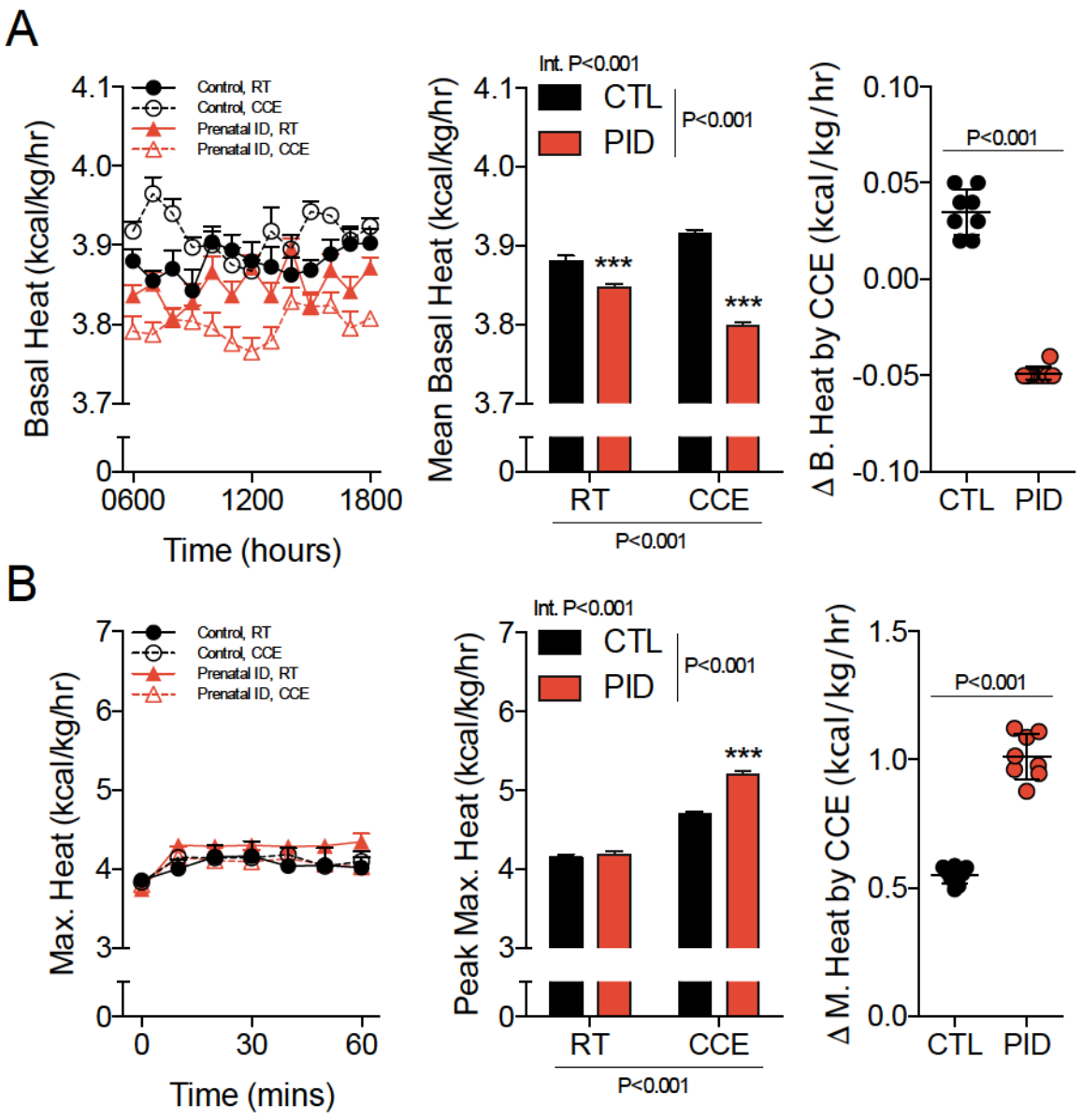

Figure 29 The residual effect of PID and CCE on female heat production

Basal heat production (A) was collected for 12 hr uninterrupted in the light phase and maximal heat production (B) was calculated from the peak maximum following a single supramaximal dose (2 mg/kg, i.p.) of CL216,243 4 wk following cold exposure. CTL, control; PID, perinatal iron deficiency; RT, room temperature; CCE, chronic cold exposure. Data are presented as means ± SEM, n=8 per group. ***, P<0.001 compared to control.

Both CCE and PID affected female whole-body energy metabolism, including RER (Figure 30A), VCO_2 (Figure 30B), and VO_2 (Figure 30C) ($P<0.001$, for all parameters). PID offspring showed a larger increase in both VCO_2 and VO_2, and a larger decrease in RER by CCE when compared to that observed in the CTL offspring ($P<0.001$, for all parameters).

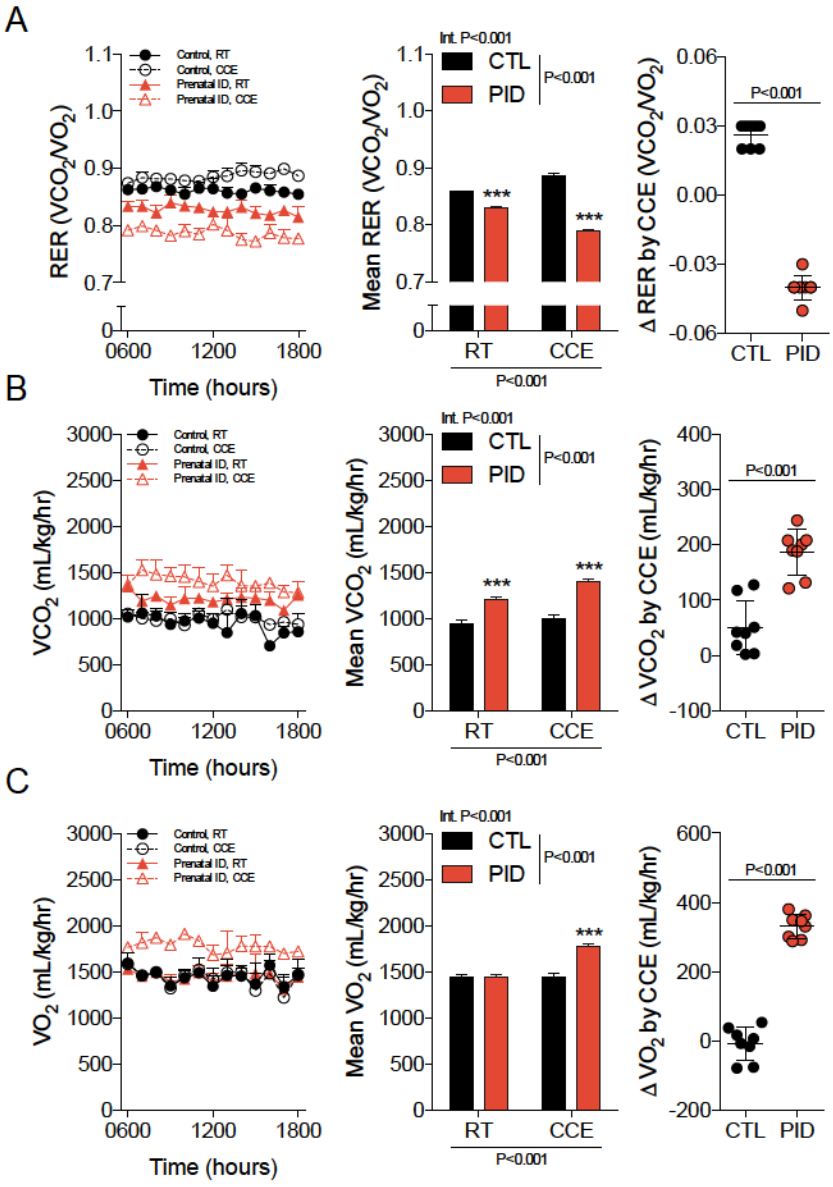

Figure 30 The residual effect of PID and CCE on female energy metabolism

Open-circuit indirect calorimetry was used to determine RER (A), VCO_2 (B), and VO_2 (C) for 12 hr uninterrupted in the light phase 4 wk following cold exposure. CTL, control; PID, perinatal iron deficiency; RT, room temperature; CCE, chronic cold exposure. Data are presented as means ± SEM, n=8 per group. ***, P<0.001 compared to control.

Despite an RER indicative of a greater fatty acid utilization, the RT and CCE PID offspring showed more fat mass (Figure 31B) compared to CTL ($P<0.001$). The Δ by CCE, however, was not different between CTL and PID groups when RT and CCE littermates were paired. In contrast, the lean mass (Figure 31A) was residually affected by CCE ($P=0.002$), and as well by PID ($P<0.001$). Although CTL offspring did not exhibit an altered lean mass due to CCE, PID offspring showed a decrease between RT and CCE paired offspring, and this difference reflects the interaction determined by the two-way ANOVA ($P=0.009$).

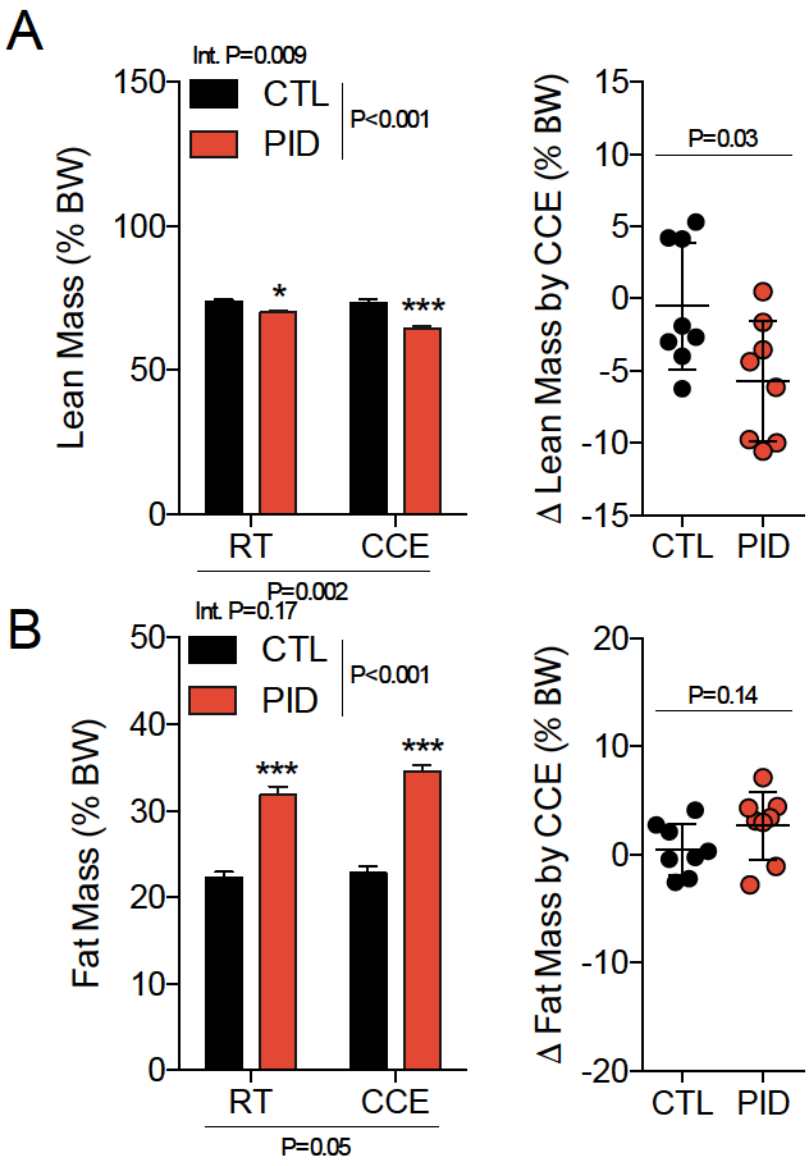

Figure 31 The residual effect of PID and CCE on female Echo-MRI

Lean mass (A) and fat mass (B) proportionate to body weight was determined by whole-body composition analysis 4 wk following cold exposure. CTL, control; PID, perinatal iron deficiency; RT, room temperature; CCE, chronic cold exposure. Data are presented as means ± SEM, n=8 per group. *, P<0.05; **, P<0.01; ***, P<0.001 compared to control.

The CCE protocol residually affected female offspring BW for 4 wk following ($P<0.001$) (Figure 32A). Whereas CTL offspring showed a decrease in BW effective of CCE, PID offspring showed an increase, which reflects the interaction between CCE and PID ($P<0.001$). When caloric intake (Figure 32B) was calculated similar results were found, such that all CCE offspring demonstrated greater food intake ($P<0.001$), and the intake as an effect of CCE was to a larger degree in the PID offspring when compared to that shown in the CTL. The difference between CTL and PID offspring caloric intake ($P<0.001$) was all well evidenced by the interaction between CCE and PID ($P<0.001$).

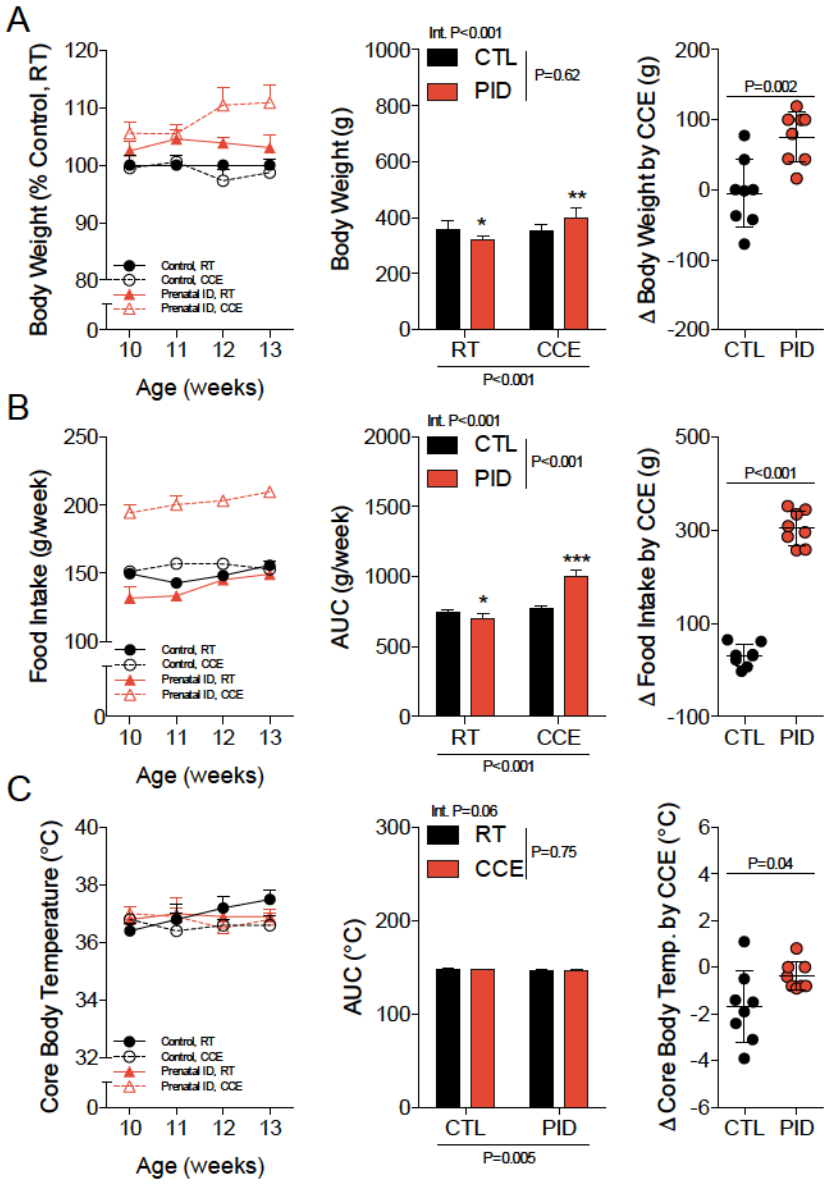

Figure 32 The residual effect of PID and CCE on female body weight, food intake, and core body temperature

Body weight (A) was assessed at 9 wk of age; food intake (B) and core body temperature (C) was assessed throughout cold exposure. CTL, control; PID, perinatal iron deficiency; RT, room temperature; CCE, chronic cold exposure. Data are presented as means ± SEM, n=8 per group. *, P<0.05; **, P<0.01; ***, P<0.001 compared to control.

Table 3 The residual effect of PID and CCE on offspring growth characteristics

	Control		Perinatal ID		P Values		
Male	**RT (n=8)**	**CCE (n=8)**	**RT (n=8)**	**CCE (n=8)**	**Hb**	**˚C**	**Int**
Body Weight (g)	607 ± 18	580 ± 12	637 ± 19	581 ± 10*	0.32	<0.05	0.35
Crown-Rump (cm)	20.6 ± 0.4	17.1 ± 0.6***	23.7 ± 0.9	19.5 ± 0.2***	<0.001	<0.001	0.57
Visceral Girth (cm)	24.1 ± 0.5	18.7 ± 0.5***	26.0 ± 0.7	23.6 ± 0.3**	<0.001	<0.001	<0.01
CR:VG	0.85 ± 0.01	0.92 ± 0.03	0.91 ± 0.02	0.83 ± 0.02**	0.14	<0.05	<0.01
Female	Control		Perinatal ID		P Values		
	RT (n=8)	CCE (n=8)	RT (n=8)	CCE (n=8)	Hb	˚C	Int
Body Weight (g)	357 ± 11	353 ± 5	322 ± 4	397 ± 14	0.64	<0.001	<0.003
Crown-Rump (cm)	16.7 ± 0.1	16.8 ± 0.4	17.0 ± 0.2	17.5 ± 0.2	0.06	0.24	0.44
Visceral Girth (cm)	18.6 ± 0.3	18.8 ± 0.4	18.4 ± 0.3	20.8 ± 0.5	<0.05	<0.01	<0.01
CR:VG	0.89 ± 0.01	0.90 ± 0.01	0.91 ± 0.01	0.84 ± 0.02	<0.001	<0.001	<0.001

Data are mean ± SEM. All data was measured 4 wk following cold exposure at 13 wk of age. CTL, control; PID, perinatal iron deficiency; RT, room temperature; CCE, chronic cold exposure. *, $P < 0.05$; **, $P < 0.01$; ***, $P < 0.001$ compared with room temperature littermates.

3.4 Using IBAT as an Indicator of Visceral Obesity and Energy Expenditure

The crude mass of IBAT was correlated with total VAT, and with maximal heat production in male (Figure 33) and female (Figure 34) offspring. The effect of PID was assessed.

3.4.1 Male Offspring

There was no relationship between IBAT and VAT in all male offspring (P=0.18) (Figure 33A). Whereas a correlation was determined in CTL offspring (P=0.05), no such relationship was seen in PID offspring (P=0.91). Moreover, PID offspring did not exhibit a correlation between IBAT and maximal heat capacity (P=0.27) (Figure 33B). Although, the trend seen by CTL offspring (P<0.001) was maintained when all offspring were pooled (P=0.004).

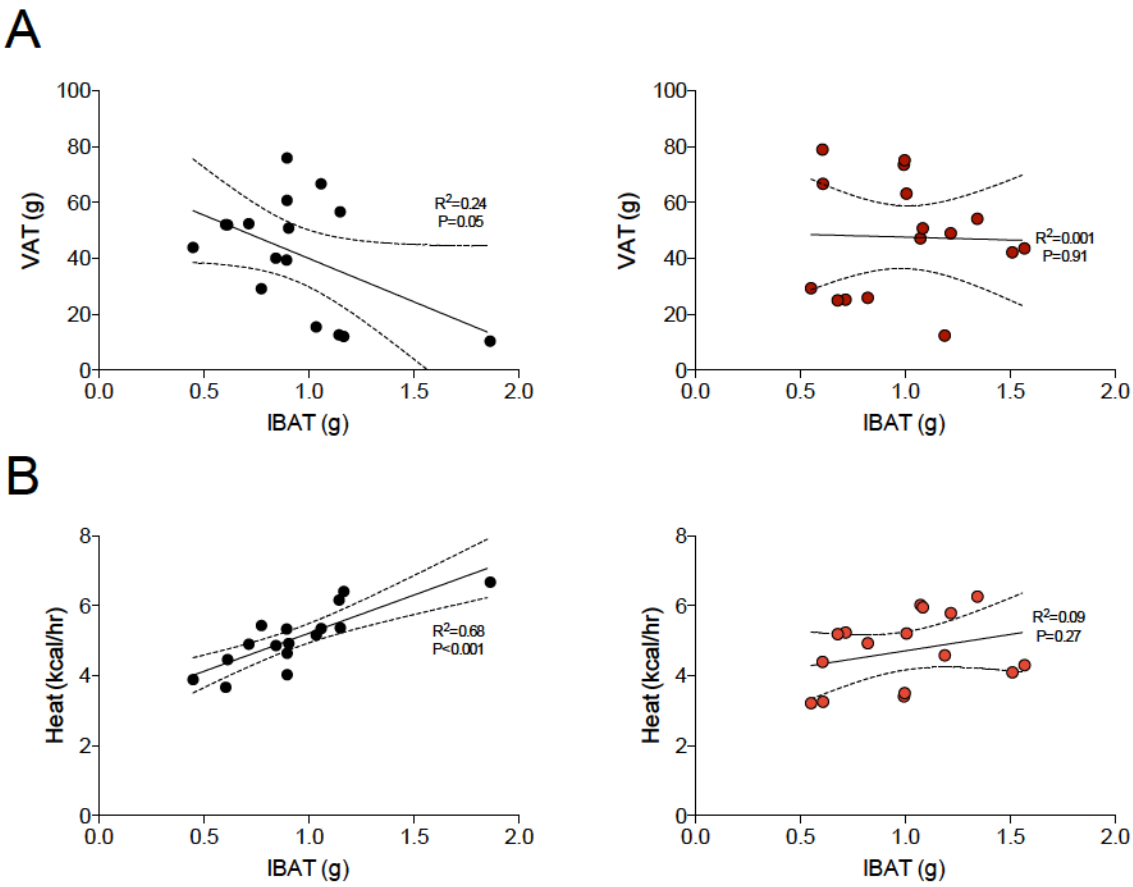

Figure 33 The relationship between IBAT and VAT with maximal heat production in male offspring

Correlation of IBAT mass with VAT mass (A) and maximal heat production (B) when assessed immediately following cold exposure. Total VAT was calculated from gastric, mesenteric and epididymal depots. Maximal heat production was calculated from the peak maximum following a single supramaximal dose (2 mg/kg, i.p.) of CL216,243. Data was assessed by linear regression. The goodness of fit (solid) and 95% confidence intervals (hashed) are indicated. CTL, control; PID, perinatal iron deficiency; RT, room temperature; CCE, chronic cold exposure. Data are presented as individual values, n=16 per group. Black, control offspring; red, perinatal iron deficient offspring. Room temperature and cold exposed offspring are pooled.

3.4.2 Female Offspring

The effect of PID did not alter the correlation between IBAT and VAT determined for all offspring ($P=0.001$); indeed, PID offspring exhibited a relationship alone ($P=0.04$) (Figure 34A). This result was as well seen when IBAT was compared to maximal heat capacity (Figure 34B), such that all offspring ($P<0.001$), CTL offspring ($P<0.001$), as well as PID offspring ($P=0.05$), showed a defined trend.

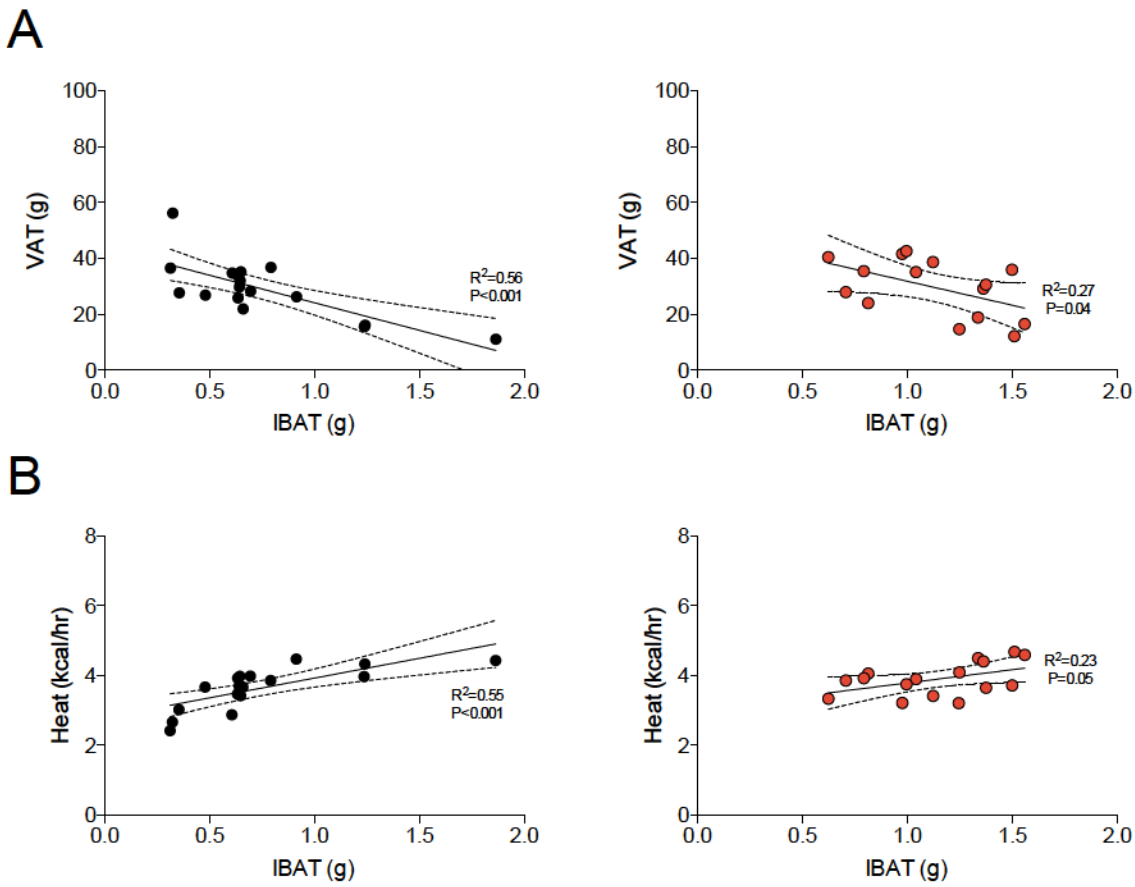

Figure 34 The relationship between IBAT and VAT with maximal heat production in female offspring

Correlation of IBAT mass with VAT mass (A) and maximal heat production (B) when assessed immediately following cold exposure. Total VAT was calculated from gastric, mesenteric and epididymal depots. Maximal heat production was calculated from the peak maximum following a single supramaximal dose (2 mg/kg, i.p.) of CL216,243. Data was assessed by linear regression. The goodness of fit (solid) and 95% confidence intervals (hashed) are indicated. CTL, control; PID, perinatal iron deficiency; RT, room temperature; CCE, chronic cold exposure. Data are presented as individual values, n=16 per group. Black, control offspring; red, perinatal iron deficient offspring. Room temperature and cold exposed offspring are pooled.

Chapter 4

Discussion and Concluding Remarks

4.1 Discussion

The experiments presented herein were intended to identify and characterize the effects of PID on BAT in adult offspring. The ultimate goal of this work was to test the hypothesis that PID offspring exhibit a reduced quantity of IBAT, and a decrease in BAT activity, thereby influencing basal metabolic rate and increasing susceptibility to obesity in adult life. To summarize, we found that PID causes immediate and residual alterations in BAT composition and function. When using a CCE activation of BAT, both male and female PID offspring had a reduced BAT quantity and activity, which propagated into long-term alterations in body composition. In male offspring, an alteration in BAT physiology did not impair cold-induced loss of fat, suggesting that alternative mechanisms may be implicated in chronic cold-stimulated weight loss. Conversely, female PID offspring showed an increase in BW but no change in body composition. Overall, the results shown herein demonstrate that PID causes persistent effects on the underlying morphological and molecular regulation of BAT thermogenesis, and these alterations implicate body growth and composition, as well as whole-body energy metabolism, in the long-term. Moreover, the results presented herein suggest a sexual dimorphism in the programming of BAT quantity and function by perinatal stressors.

Women of child bearing ages have lower tissue iron stores than men. This is due to smaller livers and muscle mass, and as well to periodic iron loss through menstruation. Specifically, menstruating women can average a 6-fold greater iron loss than non-menstruating women. Despite the knowledge that pregnant women need more iron , the median dietary iron intake for pregnant women is 15 mg/day-- a quantity that is insufficient to meet the demands of pregnancy [29]. As such, despite iron supplementation during pregnancy, more than 50% of women in Western countries exhibit signs of low iron status by the end of gestation [49,145].

The degree of PID presented in our model closely resembles a sizable cohort of pregnant women in the global population. The 2 wk iron restriction prior to pregnancy was designed to partially diminish iron stores without causing overt symptoms of anemia; a phase of negative iron balance that is common in women of child bearing ages. Furthermore, a necessary amount of minimal iron was provided throughout gestation so as to cause PID without substantially compromising offspring survival. In our experimental model that closely recapitulated the clinical features of anemia during pregnancy, we observed marked growth restriction and altered growth trajectories in the postnatal period. These data confirm our previous findings that ID during pregnancy, within clinically relevant levels, impacts growth trajectories in the fetus and can affect long-term metabolic health in the offspring.

Maternal iron restriction during pregnancy programmed alterations in offspring BW and body composition for the long-term. In the early postnatal period, male PID offspring demonstrated an increased percentage of fat mass despite similar BW. With age, male PID offspring exhibited a striking increase in BW to greater than that of CTL. In previous studies, the severity of alterations on BW and body composition in PID offspring fed a high-fat/high-sucrose Western diet was marked. Moreover, a clear programming effect of PID on caloric intake was observed [140], and PID offspring fed a high-fat/high-sucrose Western diet had an increased caloric intake when compared to CTL. Furthermore, in the present studies, an increased proportion of fat mass in male PID offspring was observed, and this is consistent with previous studies [140]. However, the same degree of VAT deposition was not shown, suggesting that the majority of fat deposition was subcutaneous. Indeed, the immediate group of offspring was assessed for body composition at only 9 wk of age; this represents a time when longitudinal growth has only recently been completed. It was therefore likely that a continued challenge of a high-fat/high-sucrose Western Diet would further exacerbate even subtle metabolic deficiencies in this group. Consistent with this hypothesis, accumulating VAT in the PID offspring was observed in the residual group, suggesting that a prolonged exposure to metabolic stressors – such as a high-fat/high sucrose Western diet – intensifies the subtle metabolic alterations in these offspring.

In accordance with male PID offspring, female PID offspring had a greater proportional fat mass in the postnatal period, as well as an increase in BW that intensified with age. Interestingly, female PID offspring did not demonstrate an increase in fat mass, now in VAT deposition, at 9 wk of age. With a continued high-fat/high-sucrose Western diet challenge, female PID offspring in the residual group demonstrated a greater proportionate fat mass, but VAT deposition did not follow accordingly. These results are inconsistent with the notion that females store fat greatly in the visceral/abdominal region. Nonetheless, the demonstrated alterations in the PID offspring suggested a strong influence by developmental stressors for the long-term [146].

An important goal of this research was to describe the phenotypes resultant from morphological and molecular alterations in BAT. By the use of an animal model, a combination of *in vivo* and *in vitro* techniques afforded a complete examination of the objectives. Our combined approach has significant advantages. Whole-body energy metabolism *in vivo* was monitored for a prolonged duration. To assess adaptive thermogenic capacity *in vivo*, energy expenditure was measured under basal conditions and maximal stimulation. This approach was established by Rothwell and Stock in their seminal study [125] and is currently considered the gold standard to explore BAT function [93]. Techniques to analyze IBAT *in vitro* showed the morphological and molecular adaptations underlying the alterations in whole-body physiology.

In the present studies, a model of a 5 wk chronic cold exposure was utilized. A CCE was chosen specifically as BAT undergoes extensive remodeling in response to cold, with this remodeling taking 3-5 wks in rodents [101,147]. BAT is not considered to be fully acclimated until between 3-5 wks after moving from a room temperature (20-24˚C) to a cold environment (4-5˚C) [91]. Moreover, electromyography traces have previously indicated that cold acclimated rodents exhibit readings similar to their thermoneutral counterparts (i.e. non-shivering thermogenesis is maintained) only after 4 wk [101,148]. In the present experiments, the CCE protocol ensured that cold acclimation had occurred, and BAT likely reached a steady state with respect to its level of thermogenic capacity. Specifically, this exposure protocol caused increased the quantity of IBAT relative to BW, and decreased brown adipocyte size. Additionally, increased expression of UCP-1 in IBAT was determined as well was an increased level of thermogenesis. As UCP-1 is considered the sole uncoupling protein responsible for adaptive non-shivering thermogenesis in BAT [101], the protocol herein cause stimulation of BAT activity. The increase in BAT quantity and thermogenic activity proved to be effective, in that core body temperature did not differ significantly between groups; even at 4˚C, BAT thermogenic activation was able to prevent changes in body temperature.

The theoretical potential for BAT to oxidize nutrients is limited by its nutrient supply and capacity for oxidative metabolism. Essentially, all aspects of BAT have evolved to maximize its capacity for thermogenesis [93,101]. Below thermoneutrality, energy

expenditure increases by 8% per 1˚C drop in environmental temperature [149]. Consistent with previous results, the experiments herein show that both basal and maximal heat production is augmented by a CCE protocol, and this was to a similar degree in both male and female offspring.

Calorimetry is a useful tool to assess BAT function *in vivo*. Indirect calorimetry by gas exchange is the most common type of calorimetry used to measure energy expenditure in rodents. The amount of energy produced per mole of oxygen consumed varies dependent on substrate by approximately 6%, with fatty acid oxidation producing less energy per mole of oxygen than carbohydrate oxidation [149]. Accordingly, as the principle product of BAT is heat due to a heightened metabolic rate, an increase in VO_2 and VCO_2 was expected. Despite an increase in both basal and maximal heat production, the results herein do not demonstrate an increase in either VO_2 or VCO_2, and there are a few potential reasons for this disparity. Firstly, several metabolic processes can impact the RER of an organism. For example, the process of *de novo* lipogenesis, by which carbohydrate is converted to lipid, has an exceptionally high RER that could conceivably alter metabolic data [150]. As well, despite the extensive remodeling that occured in BAT in response to a 5 wk CCE [149], perhaps the protocol as performed herein did not provide sufficient time for the small changes in basal metabolism to affect body metabolism.

The thermogenesis of BAT has an important role in energy balance. Activation of BAT can result in body mass loss, whereas a deficiency may lead to obesity [120,151]. Here, maximal thermogenic capacity was assessed through activation of the β3-adrenergic receptor; this method is considered the gold standard to explore BAT function. Interestingly, despite an increase in both basal and maximal heat production in CCE offspring, no alteration in either BW nor in body composition was observed. As β3-adrenergic receptor agonist administration has been shown to cause peripheral vasoconstriction [152], the alteration in BAT basal and maximal heat production could be the result of an increased thermal insulation rather than an increase in BAT activity [153].

Total body energy expenditure can be subdivided into basal energy expenditure or resting metabolic rate (RMR) required for normal cell functioning [154], energy expenditure resulting from physical activity [155], and energy expenditure attributed to adaptive thermogenesis [14,156]. The uncoupling of ATP synthesis under basal conditions constitutes a considerable part of the RMR [156]; approximately 20%-50% of total energy expenditure is due to proton leaks [120,151]. Moreover, it is well known that energy expenditure can therefore predict future weight gain, and only a slight imbalance between energy intake and energy expenditure is necessary for weight gain if it persists for extended periods of time [112,151]. Previous research has shown that small differences of just 10 kcal/day can lead to substantial differences in body fat in the long term; a difference of 10 kcal/day is equivalent to 1.1 g of body fat/day and 4 kg (~10 lbs) of body fat/10 yrs. Furthermore, the

energy expenditure from activated BAT is estimated at a remarkable 200-400 kcal/day [104,131]. Indeed, humans with non-activated BAT possess approximately 6 kg more body fat than do their activated BAT counterparts [131] as BAT is responsible for 1%-2% of basal energy expenditure, thus preventing weight gain of 1-2 kg/year [157]. In the present experiments, it may be that the subtle alterations in metabolic activity, caused by PID and driven by changes in BAT, may have a modest effect over the short term but amount to marked effects when the cumulative differences in energy dissipation are considered over a longer period of time.

The experiments herein contain the first data to demonstrate that PID causes alterations in BAT composition and function. Newborn babies require heat production through non-shivering thermogenesis [158–160]. The *in utero* environment is a critical period for the development of BAT, and inadequate maternal nutrition negatively affects BAT for the postnatal and adolescent periods. More specifically, caloric restriction in the third trimester of gestation reduces the quantity of BAT and decreases BAT thermogenic capacity [161,162]. Here, male PID offspring exhibit a reduction in both BAT mass and function when compared to CTL. Remarkably, despite male PID offspring showing lesser BAT upregulation, they demonstrated greater BW reduction. Perhaps the observed weight loss in the PID offspring exposed to CCE could be due to a heightened level of lipid content in BAT. The first physiological adaptation to cold exposure in BAT is an increase in lipid uptake [163], and the expression of genes essential for lipid uptake into BAT are induced as

early as 1 hr post-cold exposure [138], with *de novo* lipogenesis rates increasing significantly by 24 hr [163]. Such changes in gene expression suggest that BAT increases the rate of lipid restocking within adipose tissue to maintain an increased rate of lipid uptake for the long-term. Possibly, an increased level of BAT lipid content in male PID offspring could be related to an increase in BAT function and therefore heightened reductions in body mass. However, if the increased fatty-acid utilization underlies the observed changes in body composition, it is likely that this would manifest in a shit in the RER. Alternatively, it may be that the relative amount of BAT is too low to affect the whole-body RER, and a shift in substrate utilization would be undetectable using indirect calorimetry. Indeed, this may as well explain why no alterations in RER were observed between the RT and CCE groups.

Sex-based differences were not factored into the experimental design herein, and differences between male and female offspring were not directly compared. However, from a qualitative perspective, the effect of PID on CCE induced BAT in female offspring was notably different than that observed in the male offspring. While the relative mass of BAT was increased in PID females exposed to cold, the expression of UCP-1 was decreased, despite a marked increase in both basal and maximal heat production. Interestingly, despite this discrepancy in BAT upregulation, female PID offspring showed no changes in either BW or body composition. These results suggest that a deficiency in BAT thermogenesis is not involved in the physiological functions related to weight gain in PID offspring. Furthermore, it is probable that these alterations are related to an estrogen-induced

thermogenesis. In addition to the effects normally associated with estrogens, they also affect metabolic efficiency; this is routinely examined after ovariectomy as animals become spontaneously obese [164]. Mechanistically, estrogen effects could be directly mediated through estrogen receptors present in BAT [165]. Moreover, previous studies have demonstrated that female rodents exhibit a lower threshold temperature for a cold-induced thermogenic response; female rats had a greater basal heat production at 23˚C than did their male counterparts [128]. Here, such sexual dimorphisms appear to be accentuated by the programming of PID.

There have been many studies in human adults that suggest the beneficial effect of activating BAT. Numerous studies have demonstrated an inverse relationship between the amount of BAT with BMI [106–108,110], central obesity parameters (visceral adipose tissue, visceral/total adipose tissue, waist circumference) [129], and subcutaneous adipose tissue [96]. In humans, several studies have confirmed that the quantity and activity of BAT was decreased in obesity [105–107,110], diabetes [130], insulin resistance [108], and fasting [105]. These results suggest an intimate role for BAT in the regulation of energy metabolism and body composition [91,131,132]. The data herein shows that, when you look at the CTL offspring alone, this relationship holds true. But, when the PID offspring are assessed no relationship is observed. These results confirm that while alterations in BAT quantity and thermogenesis are observed for both males and females in the PID group, these alterations do not predict body composition in either case. Therefore, more sophisticated metrics are

needed to factor in related metabolically active tissues in order to make a more reflective predictive model.

Much effort is underway to develop a pharmacological means to activate BAT in human adults. A β3-adrenergic receptor agonist increased fatty acid oxidation and insulin sensitivity in lean adult males, but it failed to alter energy expenditure after 8 wks of consistent use [166]. These results were supplemented with a similar study in obese adult males, which showed an initially increased resting energy expenditure [152], but extended consistent treatment over 4 wks did not alter thermogenic capacity or BW [167]. Here, we observed similar trends in offspring exposed to CCE at 4 wks following (i.e. the residual group). While a single maximal stimulation of the β3-adrenergic receptor can markedly increase energy expenditure, it can only do so temporarily and moreover, at 4 wk following completion of a CCE protocol, no increase was observed. These results were expected as the relative quantity of IBAT decreased over the 4 wk period without a consistent exposure to cold. Furthermore, others have observed that by 7 days post cold exposure, BAT has become largely restocked in lipid content, with lipid droplets returning to almost the same size as warm acclimated rodents [163]. Therefore, it would be of interest to utilize pairwise feeding as a technique to assess differences in metabolic rate following a CCE. This is of particular interest for the animals shown herein, where differences in BW and food intake were observed post-cold exposure. Taken together, the results herein underpin the necessity to better understand how alterations in BAT function impact on a given phenotype, and

especially so for those programmed by perinatal stressors. This will allow for proper interpretation of results to fully understand BAT and its metabolic consequences for long-term translatable information.

It is important to briefly outline the limitations and translatability of this study. While several experimental design elements could be improved, there are several notable limitations that warrant brief discussion. Firstly, while it is commonplace to use body condition scores, such as body fat percentage, the term 'obese' was used in a relative context in the present studies, since a standard guide for characterization of obesity in rodents does not exist. However, when used in a context referring to humans, defined criteria are used that has direct bearing on disease outcomes.

Secondly, it is not clear which animal model has the most comparable developmental and functional profile of BAT as in humans. The human infant demonstrates the greatest quantity of BAT in the supraclavicular region that has a similar molecular and morphological profile to rodent IBAT [168]. The genetic lineage and signature of human supraclavicular BAT has been debated; some suggest it is analogous to rodent IBAT [108,109], whereas others propose it resembles a WAT-BAT hybrid exhibiting characteristics distinct from rodent IBAT [96,119]. Further, others postulate that human supraclavicular BAT may be comprised of both classical brown adipocytes and beige fat cells [96], as it exhibits a heterogeneous cell composition of both large unilocular and smaller multilocular lipid

droplets [169]. Comparatively, rodent IBAT consists of homogeneous multilocular cells [149]. Despite these differences, human supraclavicular BAT and rodent IBAT have similar mitochondrial UCP-1 function per mitochondrion [138]. UCP-1 dependent respiration per mg of adipose tissue was greater in rodent BAT compared to human BAT, which is most likely reflective of the more homogenous population of brown adipocytes and thus more mitochondria and UCP-1 protein content in rodent IBAT [96]. This revelation was important to the experiments contained herein; human and rodent BAT are qualitatively similar in terms of UCP-1 function, allowing us to extend the results contained herein to the human population.

4.2 Concluding Remarks

The DOHaD hypothesis has resulted in a paradigm shift in the way we view determinants of disease. Previously, genetic inheritance and adult lifestyle factors were deemed as the primary contributors to disease, but it is now suggested that diseases may also originate *in utero* in response to adverse maternal environments. Inadequate fetal nutrition has been associated with several unfavourable outcomes in adulthood, and the mechanisms proposed to account for these associations include factors prior to conception, during fetal life, and in postnatal and adult life.

A common theme in DOHaD is the remarkable similarity between long-term programming outcomes despite differences in perinatal stressors. It is suggested that variation in fetal nutrition could result in permanent organ damage, resetting of hormonal axes and metabolism, and epigenetic modifications. It has also been suggested that the resulting consequences interact with postnatal growth and factors in adulthood. Therefore, PID, along with a myriad of other maternal nutrient imbalances, may impact function of a limited number of systems thereby resulting in a limited number of adult life outcomes. Proof of the involvement of mutual mechanisms may be an elegant solution to the DOHaD challenge.

The identification of BAT in adult humans in 2009 was of major importance due to its immense capacity to covert chemical energy from food into heat. Pharmacological activation of BAT may provide a treatment option for some of the most widespread metabolic disease states of current time. It is estimated that a mean BAT mass of around 300 g is present in normal weight individuals, and full activation could theoretically result in a body mass loss of around 16 kg/year in the obese. Although the direct targeting of BAT seems a plausible therapeutic option, certain groups demonstrate a substantially lower propensity for BAT activation. Perhaps, intrinsic differences in the ability to activate BAT may stem from perinatal stressors. As the priorities of resource allocation during pharmacological development depend on many criteria, it is therefore crucial to better understand the predicted efficacy of BAT alteration in all patient cohorts.

The findings from the present thesis have supported the hypothesis that PID can influence the quantity and thermogenic activity of BAT, which can further impact basal metabolic rate. But, the link between these effects and body composition are not supported, in that (1) male PID CCE offspring did not show a reduced capacity to lose weight with CCE, and (2) while female PID offspring showed an increase in both basal and maximal thermogenic capacity, they did not exhibit the weight loss we would have expected to accompany.

Furthermore, it was shown that male and female PID offspring respond differently in their programming of BAT thermogenic function. This is consistent with many aspects of metabolic and cardiovascular function that are differentially programmed between males and females. By better understanding the molecular mechanisms governing the expression and activity of BAT, we can better understand the sex differences in fat accumulation, distribution, and energy metabolism in the physiology and pathophysiology. Future studies into the nature of these apparent sex-differences in obesity are warranted.

Investigating the adverse effects of prenatal stressors in the intrauterine and postnatal periods of life bring forth a myriad of ethical impediments. Thus, for future research, the value of prospective, longitudinal studies is emphasized. Importantly, recent advances in imaging techniques will likely enable the development of protocols in infants

and children for the quantification of subcutaneous and visceral fat depots [6,170], and these techniques will allow the characterization of, and differentiation between, WAT and BAT [157]. Ideally, monitoring even before conception, and extending through pregnancy and birth and into childhood, would be critical to appropriately follow the long-term programming effects of maternal stressors for obesity.

Considerable attention must be directed towards a greater awareness of the potential deleterious effects of PID. The immense impact of PID on the long-term health of the developing offspring represents a debilitating and pervasive outcome in terms of cardiovascular health. It is of great importance to establish the important programming mechanisms by which this common nutritional deficiency impacts long-term metabolic function in the offspring in order to identify modifiable targets for intervention. Prevention, rather than treatment, is undoubtedly a more strategic and cost-effective approach to treating obesity.

References

1. Barker, D. J. In utero programming of chronic disease. *Clin. Sci. (Lond).* **95,** 115–28 (1998).
2. Godfrey, K. M. & Barker, D. J. Fetal programming and adult health. *Public Health Nutr.* **4,** 611–24 (2001).
3. Barker, D. J. P. In utero programming of cardiovascular disease. *Theriogenology* **53,** 555–574 (2000).
4. Barker, D. The fetal and infant origins of adult disease. *BMJ Br. Med. J.* **301,** 1111 (1990).
5. Jones, R. H. & Ozanne, S. E. Fetal programming of glucose-insulin metabolism. *Mol. Cell. Endocrinol.* **297,** 4–9 (2009).
6. Gluckman, P. D. *et al.* A conceptual framework for the developmental origins of health and disease. *J. Dev. Orig. Health Dis.* **1,** 6–18 (2010).
7. Forsdahl, a. Living Conditions in Childhood. *Mortality* 91–95 (1977).
8. Barker, D. J. & Osmond, C. Diet and coronary heart disease in England and Wales during and after the second world war. *J. Epidemiol. Community Health* **40,** 37–44 (1986).
9. Xita, N. & Tsatsoulis, A. Fetal origins of the metabolic syndrome. *Ann. N. Y. Acad. Sci.* **1205,** 148–55 (2010).
10. Ruager-Martin, R., Hyde, M. J. & Modi, N. Maternal obesity and infant outcomes. *Early Hum. Dev.* **86,** 715–722 (2010).
11. Langley-Evans, S. C., Phillips, G. J. & Jackson, A. A. In utero exposure to maternal low protein diets induces hypertension in weanling rats, independently of maternal blood pressure changes. *Clin. Nutr.* **13,** 319–324 (1994).
12. Langley-Evans, S. C. Developmental programming of health and disease. *Proc. Nutr. Soc.* **65,** 97–105 (2006).

13. Ojeda, N. B., Grigore, D. & Alexander, B. T. Intrauterine Growth Restriction: Fetal Programming of Hypertension and Kidney Disease. *Adv. Chronic Kidney Dis.* **15,** 101–106 (2008).

14. Ng, M. *et al.* Global, regional, and national prevalence of overweight and obesity in children and adults during 1980–2013: a systematic analysis for the Global Burden of Disease Study 2013. *Lancet* **384,** 766–781 (2014).

15. Puttabyatappa, M., Cardoso, R. C. & Padmanabhan, V. Effect of maternal PCOS and PCOS-like phenotype on the offspring's health. *Mol. Cell. Endocrinol.* **435,** 29–39 (2016).

16. Wilcox, A. J. & Russell, I. T. Birthweight and perinatal mortality: I. On the frequency distribution of birthweight. *Int. J. Epidemiol.* **12,** 314–318 (1983).

17. Wilcox, A. J. On the importance--and the unimportance--of birthweight. *Int J Epidemiol* **30,** 1233–1241 (2001).

18. Neubig, R. R., Spedding, M., Kenakin, T. & Christopoulos, A. International Union of Pharmacology Committee on Receptor Nomenclature and Drug Classification. XXXVIII. Update on terms and symbols in quantitative pharmacology. *Pharmacol. Rev.* **55,** 597–606 (2003).

19. Richards, M., Hardy, R., Kuh, D. & Wadsworth, M. E. J. Birth weight and cognitive function in the British 1946 birth cohort: longitudinal population based study. *Bmj* **322,** 199–203 (2001).

20. Gluckman, P. D., Hanson, M. A., Morton, S. M. B. & Pinal, C. S. Life-Long Echoes – A Critical Analysis of the Developmental Origins of Adult Disease Model. *Neonatology* **87,** 127–139 (2005).

21. Hélène, D. Programming of chronic disease by impaired fetal nutrition Evidence and

implications for policy and intervention strategies. *Who*

22. Harding, J. E. The nutritional basis of the fetal origins of adult disease. *Int J Epidemiol* **30,** 15–23 (2001).

23. Calkins, K. & Devaskar, S. U. Fetal origins of adult disease. *Curr. Probl. Pediatr. Adolesc. Health Care* **41,** 158–176 (2011).

24. Alfaradhi, M. Z. & Ozanne, S. E. Developmental programming in response to maternal overnutrition. *Front. Genet.* **2,** 1–13 (2011).

25. Lakshmy, R. Metabolic syndrome: Role of maternal undernutrition and fetal programming. *Rev. Endocr. Metab. Disord.* **14,** 229–240 (2013).

26. Symonds, M. E. & Budge, H. Nutritional models of the developmental programming of adult health and disease. *Proc. Nutr. Soc.* **68,** 173 (2009).

27. Hanson, M. A. & Gluckman, P. D. Early Developmental Conditioning of Later Health and Disease: Physiology or Pathophysiology? *Physiol. Rev.* **94,** 1027–1076 (2014).

28. Bager, P. Acute upper gastrointestinal bleeding/chronic inflammatory bowel disease used as a model Palle. *Dan. Med. J.* **61,** 1–16 (2014).

29. Coad, J. & Pedley, K. Iron deficiency and iron deficiency anemia in women. *Scand. J. Clin. Lab. Invest. Suppl.* **244,** 82–9; discussion 89 (2014).

30. Rosenthal, A. M. WHO names top 10 health risks. *Environ. Health Perspect.* **111,** A456 (2003).

31. Halterman, J. S., Kaczorowski, J. M., Aligne, C. A., Auinger, P. & Szilagyi, P. G. Iron Deficiency and Cognitive Achievement Among School-Aged Children and Adolescents in the United States. *Pediatrics* **107,** 1381–1386 (2001).

32. Dallman, P. R. Biochemical Basis for the Manifestations of Iron Deficiency. *Annu. Rev.*

Nutr. **6,** 13–40 (1986).

33. Looker, A. C., Dallman, P. R., Carroll, M. D., Gunter, E. W. & Johnson, C. L. Prevalence of iron deficiency in the United States. *J. Am. Med. Assoc.* **277,** 973–976 (1997).

34. Development, W. H. O. D. of N. for H. and. Iron deficiency anaemia : assessment, prevention and control : a guide for programme managers. (2001).

35. Dunn, L. L., Rahmanto, Y. S. & Richardson, D. R. Iron uptake and metabolism in the new millennium. *Trends Cell Biol.* **17,** 93–100 (2007).

36. Beutler, E. & Waalen, J. The definition of anemia : what is the lower limit of normal of the blood hemoglobin concentration ? The definition of anemia : what is the lower limit of normal of the blood hemoglobin concentration ? *Blood* **107,** 1747–1750 (2006).

37. Yates, J. M., Logan, E. C. M. & Stewart, R. M. Iron deficiency anaemia in general practice: clinical outcomes over three years and factors influencing diagnostic investigations. *Postgrad. Med. J.* **80,** 405–10 (2004).

38. Koperdanova, M. & Cullis, J. O. Interpreting raised serum ferritin levels. *Bmj* h3692 (2015). doi:10.1136/bmj.h3692

39. HASKINS, D., STEVENS, A. R., FINCH, S. & FINCH, C. A. Iron metabolism; iron stores in man as measured by phlebotomy. *J. Clin. Invest.* **31,** 543–547 (1952).

40. Kling, P. J., Schmidt, R. L., Roberts, R. A. & Widness, J. A. Serum erythropoietin levels during infancy: Associations with erythropoiesis. *J. Pediatr.* **128,** 791–796 (1996).

41. Bothwell, T. H. Iron requirements in pregnancy and strategies to meet them. *American Journal of Clinical Nutrition* **72,** (2000).

42. McLean, E., Cogswell, M., Egli, I., Wojdyla, D. & de Benoist, B. Worldwide prevalence of anaemia, WHO Vitamin and Mineral Nutrition Information System, 1993–2005. *Public*

Health Nutr. **12,** 444 (2009).

43. Rao, R. & Georgieff, M. K. Iron in fetal and neonatal nutrition. *Semin. Fetal Neonatal Med.* **12,** 54–63 (2007).

44. Gogoi, M. & Prusty, R. K. Maternal Anaemia, Pregnancy Complications and Birth Outcome: Evidences from North-East India. **3,** 74–85 (2013).

45. Chang, S.-C., O'Brien, K. O., Nathanson, M. S., Mancini, J. & Witter, F. R. Hemoglobin concentrations influence birth outcomes in pregnant African-American adolescents. *The Journal of Nutrition* **133,** 2348–2355 (2003).

46. Kalaivani, K. Prevalence & consequences of anaemia in pregnancy. *Indian J. Med. Res.* **130,** 627–33 (2009).

47. Scholl, T. O. Iron status during pregnancy: setting the stage for mother and infant. *Am. J. Clin. Nutr.* **81,** 1218S–1222S (2005).

48. Walter, T., Pino, P., Pizarro, F. & Lozoff, B. Prevention of iron-deficiency anemia: Comparison of high- and low-iron formulas in term healthy infants after six months of life. *J. Pediatr.* **132,** 635–640 (1998).

49. Kelly, A. M., Macdonald, D. J. & McDougall, A. N. Observations on Maternal and Fetal Ferritin Concentrations At Term. *BJOG An Int. J. Obstet. Gynaecol.* **85,** 338–343 (1978).

50. Widness, J. A. Pathophysiology of Anemia During the Neonatal Period, Including Anemia of Prematurity. *Neoreviews* **9,** e520–e525 (2008).

51. Examina-, N. Iron Deficiency. 491–492 (2007). doi:10.1002/pbc

52. Brugnara, C. Iron deficiency and erythropoiesis: New diagnostic approaches. *Clin. Chem.* **49,** 1573–1578 (2003).

53. Nemeth, E. & Ganz, T. The role of hepcidin in iron metabolism. *Acta Haematol.* **122,** 78–

86 (2009).

54. Girelli, D., Nemeth, E. & Swinkels, D. W. Hepcidin in the diagnosis of iron disorders. *Blood* **127,** 2809–2813 (2016).

55. Neves, J. V., Caldas, C., Ramos, M. F. & Rodrigues, P. N. S. Hepcidin-dependent regulation of erythropoiesis during anemia in a teleost fish, dicentrarchus labrax. *PLoS One* **11,** 1–17 (2016).

56. Casanueva, E. & Viteri, F. E. Iron and oxidative stress in pregnancy. *J Nutr* **133,** 1700S–1708S (2003).

57. Lao, T. T. & Tam, K.-F. Gestational diabetes diagnosed in third trimester pregnancy and pregnancy outcome. *Acta Obstet. Gynecol. Scand.* **80,** 1003–1008 (2001).

58. Manoguerra, A. S. *et al.* Iron Ingestion: an Evidence-Based Consensus Guideline for Out-of-Hospital Management. *Clin. Toxicol.* **43,** 553–570 (2005).

59. McElhatton, P. R., Roberts, J. C. & Sullivan, F. M. The consequences of iron overdose and its treatment with desferrioxamine in pregnancy. *Hum. Exp. Toxicol.* **10,** 251–9 (1991).

60. Milman, N. *et al.* Iron prophylaxis during pregnancy - How much iron is needed? A randomized dose-response study of 20-80 mg ferrous iron daily in pregnant women. *Acta Obstet. Gynecol. Scand.* **84,** 238–247 (2005).

61. Sies, H. Oxidative stress: From basic research to clinical application. *Am. J. Med.* **91,** 31–38 (1991).

62. Novak, D. a, Desai, M. & Ross, M. G. Gestational programming of offspring obesity/hypertension. *J. Matern. Fetal. Neonatal Med.* **19,** 591–9 (2006).

63. McArdle, H. J., Andersen, H. S., Jones, H. & Gambling, L. Fetal Programming: Causes and Consequences as Revealed by Studies of Dietary Manipulation in Rats - A Review. *Placenta*

27, 56–60 (2006).

64. Twells, L. K., Gregory, D. M., Reddigan, J. & Midodzi, W. K. Current and predicted prevalence of obesity in Canada: a trend analysis. *CMAJ Open* **2,** E18–E26 (2014).

65. Baboota, R. K. *et al.* Functional food ingredients for the management of obesity and associated co-morbidities – A review. *J. Funct. Foods* **5,** 997–1012 (2013).

66. Olinto, M. T. A. & Moreira-Filho, D. de C. Fatores de risco e preditores para o aborto induzido: estudo de base populacional. *Cad. Saude Publica* **22,** 365–375 (2006).

67. Sandeep, S., Gokulakrishnan, K., Velmurugan, K., Deepa, M. & Mohan, V. Visceral & subcutaneous abdominal fat in relation to insulin resistance & metabolic syndrome in non-diabetic south Indians. *Indian J. Med. Res.* **131,** 629–635 (2010).

68. Taksali, S. E. *et al.* A Determinant of an Adverse Metabolic Phenotype. **57,** (2008).

69. Demerath EW, Reed D, Rogers N, Sun SS, Lee M, Choh AC, et al. Visceral adiposity and its anatomical distribution as predictors of the metabolic syndrome and cardiometabolic risk factor levels. *Am J Clin Nutr.* **88,** 1263–1271 (2008).

70. Romero-Corral, A. *et al.* Modest visceral fat gain causes endothelial dysfunction in healthy humans. *J. Am. Coll. Cardiol.* **56,** 662–666 (2010).

71. Matsuzawa, Y. Establishment of a concept of visceral fat syndrome and discovery of adiponectin. *Proc. Japan Acad. Ser. B* **86,** 131–141 (2010).

72. van der Schouw, Y. T., van der Graaf, Y., Steyerberg, E. W., Eijkemans, J. C. & Banga, J. D. Age at menopause as a risk factor for cardiovascular mortality. *Lancet* **347,** 714–8 (1996).

73. Love, T. J. *et al.* Obesity and the risk of psoriatic arthritis: a population-based study. *Ann. Rheum. Dis.* **71,** 1273–7 (2012).

74. Taylor, V. H., Forhan, M., Vigod, S. N., McIntyre, R. S. & Morrison, K. M. The impact of obesity on quality of life. *Best Pract. Res. Clin. Endocrinol. Metab.* **27,** 139–146 (2013).

75. Hill, J. O. Response to Comment on 'Obesity and the Environment: Where Do We Go from Here?' *Science (80-.).* **301,** 598c–598 (2003).

76. Alexander, B. T. Placental insufficiency leads to development of hypertension in growth-restricted offspring. *Hypertension* **41,** 457–462 (2003).

77. Loria, A. S., Pollock, D. M. & Pollock, J. S. Early life stress sensitizes rats to angiotensin II-induced hypertension and vascular inflammation in adult life. *Hypertension* **55,** 494–499 (2010).

78. Bam, N. B. *et al.* Tween protects recombinant human growth hormone against agitation-induced damage via hydrophobic interactions. *J. Pharm. Sci.* **87,** 1554–9 (1998).

79. Woods, L. L., Ingelfinger, J. R., Nyengaard, J. R. & Rasch, R. Maternal protein restriction suppresses the newborn renin-angiotensin system and programs adult hypertension in rats. *Pediatr. Res.* **49,** 460–7 (2001).

80. Komolova, M., Bourque, S. L., Nakatsu, K. & Adams, M. A. Sedentariness and increased visceral adiposity in adult perinatally iron-deficient rats. *Int. J. Obes. (Lond).* **32,** 1441–4 (2008).

81. Bourque, S. L., Komolova, M., Nakatsu, K. & Adams, M. A. Long-term circulatory consequences of perinatal iron deficiency in male Wistar rats. *Hypertens. (Dallas, Tex. 1979)* **51,** 154–9 (2008).

82. Bourque, S. L., Iqbal, U., Reynolds, J. N., Adams, M. A. & Nakatsu, K. Perinatal iron deficiency affects locomotor behavior and water maze performance in adult male and female rats. *J. Nutr.* **138,** 931–7 (2008).

83. Dunlap, W. M., James, G. W. & Hume, D. M. Anemia and neutropenia caused by copper deficiency. *Ann. Intern. Med.* **80,** 470–476 (1974).

84. Yousheng Jia, Nguyen, T., Desai, M. & Ross, M. G. Programmed alterations in hypothalamic neuronal orexigenic responses to ghrelin following gestational nutrient restriction. *Reprod. Sci.* **15,** 702–9 (2008).

85. Symonds, M. E., Pearce, S., Bispham, J., Gardner, D. S. & Stephenson, T. Timing of nutrient restriction and programming of fetal adipose tissue development. *Proc. Nutr. Soc.* **63,** 397–403 (2004).

86. Insel, B. J., Schaefer, C. A., McKeague, I. W., Susser, E. S. & Brown, A. S. Maternal Iron Deficiency and the Risk of Schizophrenia in Offspring. *Arch. Gen. Psychiatry* **65,** 1136 (2008).

87. Lozoff, B. & Georgieff, M. K. Iron Deficiency and Brain Development. *Semin. Pediatr. Neurol.* **13,** 158–165 (2006).

88. Prieto-Hontoria, P. L., Pérez-Matute, P., Fernández-Galilea, M., Martínez, J. A. & Moreno-Aliaga, M. J. Effects of lipoic acid on AMPK and adiponectin in adipose tissue of low- and high-fat-fed rats. *Eur. J. Nutr.* **52,** 779–787 (2013).

89. Smith, R. E. & Horwitz, B. a. Brown fat and thermogenesis. *Physiol. Rev.* **49,** 330–425 (1969).

90. Shechtman, O., Papanek, P. E. & Fregly, M. J. Reversibility of cold-induced hypertension after removal of rats from cold. *Can. J. Physiol. Pharmacol.* **68,** 830–835 (1990).

91. Ouellet, V. *et al.* Brown adipose tissue oxidative metabolism contributes to energy expenditure during acute cold exposure in humans. *J. Clin. Invest.* **122,** 545–52 (2012).

92. Lin, J. *et al.* Defects in adaptive energy metabolism with CNS-linked hyperactivity in PGC-

1α null mice. *Cell* **119,** 121–135 (2004).

93. Cannon, B. *et al.* Brown Adipose Tissue : Function and Physiological Significance. 277–359 (2008). doi:10.1152/physrev.00015.2003

94. Enerbäck, S. Human Brown Adipose Tissue. *Cell Metab.* **11,** 248–252 (2010).

95. Cedikova, M. *et al.* Mitochondria in White, Brown, and Beige Adipocytes. *Stem Cells Int.* **2016,** 1–11 (2016).

96. Sharp, L. Z. *et al.* Human BAT Possesses Molecular Signatures That Resemble Beige/Brite Cells. *PLoS One* **7,** (2012).

97. Cypess, A. M. *et al.* NIH Public Access. **19,** 635–639 (2013).

98. Rial, E., González-Barroso, M. M., Fleury, C. & Bouillaud, F. The structure and function of the brown fat uncoupling protein UCP1: current status. *Biofactors* **8,** 209–19 (1998).

99. HEATON, G. M., WAGENVOORD, R. J., KEMP, A. & NICHOLLS, D. G. Brown-Adipose-Tissue Mitochondria: Photoaffinity Labelling of the Regulatory Site of Energy Dissipation. *Eur. J. Biochem.* **82,** 515–521 (1978).

100. Fedorenko, A., Lishko, P. V. & Kirichok, Y. Mechanism of fatty-acid-dependent UCP1 uncoupling in brown fat mitochondria. *Cell* **151,** 400–413 (2012).

101. Nedergaard, J. *et al.* UCP1: The only protein able to mediate adaptive non-shivering thermogenesis and metabolic inefficiency. *Biochim. Biophys. Acta - Bioenerg.* **1504,** 82–106 (2001).

102. Brück, K. Temperature Regulation in the Newborn Infant. *Neonatology* **3,** 65–81 (1961).

103. Himms-Hagen, J. Nonshivering Thermogenesis. *Brain Res. Bull.* **12,** 151–160 (1984).

104. Gilsanz, V. *et al.* The depiction of brown adipose tissue is related to disease status in pediatric patients with lymphoma. *Am. J. Roentgenol.* **198,** 909–913 (2012).

105. Vijgen, G. H. E. J. *et al.* Brown adipose tissue in morbidly obese subjects. *PLoS One* **6,** 2–7 (2011).

106. Cypess, A. M. *et al.* Identification and importance of brown adipose tissue in adult humans. *N. Engl. J. Med.* **360,** 1509–17 (2009).

107. van Marken Lichtenbelt, W. D. *et al.* Cold-activated brown adipose tissue in healthy men. *N. Engl. J. Med.* **360,** 1500–8 (2009).

108. Virtanen, K. A. *et al.* Functional Brown Adipose Tissue in Healthy Adults. *N. Engl. J. Med.* **360,** 1518–1525 (2009).

109. Zingaretti, M. C. *et al.* The presence of UCP1 demonstrates that metabolically active adipose tissue in the neck of adult humans truly represents brown adipose tissue. *FASEB J.* **23,** 3113–20 (2009).

110. Saito, M. *et al.* High Incidence of Metabolically Active Brown Adipose Tissue in Healthy Adult Humans. *Diabetes* **58,** (2009).

111. Nakamura, K. & Morrison, S. F. Central efferent pathways mediating skin cooling-evoked sympathetic thermogenesis in brown adipose tissue. *Am. J. Physiol. Regul. Integr. Comp. Physiol.* **292,** R127-36 (2007).

112. Wu, Z. *et al.* Mechanisms controlling mitochondrial biogenesis and respiration through the thermogenic coactivator PGC-1. *Cell* **98,** 115–124 (1999).

113. Lafontan, M. & Berlan, M. Fat cell adrenergic receptors and the control of white and brown fat cell function. **34,** (1993).

114. Krief, S. *et al.* Rapid Publication Tissue Distribution of 8B3-adrenergic Receptor mRNA in Man. *J. Clin. Invest.* **91,** 344–349 (1993).

115. Jockers, R. *et al.* Desensitization of the beta-adrenergic response in human brown

adipocytes. *Endocrinology* **139,** 2676–2684 (1998).

116. Arch, J. R. *et al.* Atypical beta-adrenoceptor on brown adipocytes as target for anti-obesity drugs. *Nature* **309,** 163–5 (1984).

117. Arechaga, I., Ledesma, a & Rial, E. The mitochondrial uncoupling protein UCP1: a gated pore. *IUBMB Life* **52,** 165–173 (2001).

118. Matthias, A., Jacobsson, A., Cannon, B. & Nedergaard, J. The bioenergetics of brown fat mitochondria from UCP1-ablated mice. UCP1 is not involved in fatty acid-induced de-energization ('uncoupling'). *J. Biol. Chem.* **274,** 28150–28160 (1999).

119. Puigserver, P. *et al.* A cold-inducible coactivator of nuclear receptors linked to adaptive thermogenesis. *Cell* **92,** 829–839 (1998).

120. Lowell, B. B. *et al.* Development of obesity in transgenic mice after genetic ablation of brown adipose tissue. *Nature* **366,** 740–742 (1993).

121. Lehman, J. J. *et al.* Peroxisome proliferator – activated receptor γ coactivator-1 promotes cardiac mitochondrial biogenesis. *J. Clin. Invest.* **106,** 847–856 (2000).

122. Puigserver, P. & Spiegelman, B. M. Peroxisome proliferator-activated receptor-γ coactivator 1α (PGC-1α): Transcriptional coactivator and metabolic regulator. *Endocr. Rev.* **24,** 78–90 (2003).

123. Czubryt, M. P., McAnally, J., Fishman, G. I. & Olson, E. N. Regulation of peroxisome proliferator-activated receptor gamma coactivator 1 alpha (PGC-1 alpha) and mitochondrial function by MEF2 and HDAC5. *Proc. Natl. Acad. Sci. U. S. A.* **100,** 1711–6 (2003).

124. Puigserver, P. Tissue-specific regulation of metabolic pathways through the transcriptional coactivator PGC1-α. *Int. J. Obes.* **29,** S5–S9 (2005).

125. Rothwell, N. & Stock, M. Luxuskonsumption, dietinduced thermogenesis and brown fat:

the case in favour. *Clin. Sci.* **64,** 19–23 (1983).

126. Norrbom, J. PGC-1 mRNA expression is influenced by metabolic perturbation in exercising human skeletal muscle. *J. Appl. Physiol.* **96,** 189–194 (2003).

127. Lin, J. Transcriptional co-activator PGC-1[alpha] drives the formation of slow- twitch muscle fibres . *Nat.* **418,** 797–801 (2002).

128. Valle, A., García-palmer, F. J. & Oliver, J. Cellular Physiology Biochemistry and Biochemistr y Sex Differences in Brown Adipose Tissue Thermogenic Features During Caloric Restriction. *Cell. Physiol. Biochem.* 195–204 (2007).

129. Wang, Q. *et al.* Brown Adipose Tissue in humans is activated by elevated plasma catecholamines levels and is inversely related to central obesity. *PLoS One* **6,** (2011).

130. Fenzl, A. & Kiefer, F. W. Brown adipose tissue and thermogenesis. *Horm. Mol. Biol. Clin. Investig.* **19,** 25–37 (2014).

131. Yoneshiro, T. *et al.* Recruited brown adipose tissue as an antiobesity agent in humans. *J. Clin. Invest.* **123,** 3404–3408 (2013).

132. Sutherland, J. S. *et al.* Differential gene expression of activating Fcγ receptor classifies active tuberculosis regardless of human immunodeficiency virus status or ethnicity. *Clin. Microbiol. Infect.* **20,** O230-8 (2014).

133. Kozak, L. P. & Koza, R. A. The genetics of brown adipose tissue. *Prog. Mol. Biol. Transl. Sci.* **94,** 75–123 (2010).

134. Kortelainen, M. L., Pelletier, G., Ricquier, D. & Bukowiecki, L. J. Immunohistochemical detection of human brown adipose tissue uncoupling protein in an autopsy series. *J. Histochem. Cytochem.* **41,** 759–764 (1993).

135. Kajimura, S. *et al.* Initiation of myoblast/brown fat switch through a PRDM16-C/EBP-b

transcriptional complex. *Nature* **460,** 1154–1158 (2009).

136. 'USA-Fat': Prevalence Is Related to Ambient Outdoor Temperature—Evaluation with. 1–4 (2003).

137. Ghorbani, M. & Himms-Hagen, J. Appearance of brown adipocytes in white adipose tissue during CL 316,243-induced reversal of obesity and diabetes in Zucker fa/fa rats. *Int. J. Obes. Relat. Metab. Disord.* **21,** 465–475 (1997).

138. Chondronikola, M. *et al.* Brown Adipose Tissue Activation Is Linked to Distinct Systemic Effects on Lipid Metabolism in Humans. *Cell Metab.* **23,** 1200–1206 (2016).

139. Desai, M., Gayle, D., Babu, J. & Ross, M. G. Programmed obesity in intrauterine growth-restricted newborns: modulation by newborn nutrition. *Am. J. Physiol. Regul. Integr. Comp. Physiol.* **288,** R91-6 (2005).

140. Bourque, S. L., Komolova, M., McCabe, K., Adams, M. A. & Nakatsu, K. Perinatal iron deficiency combined with a high-fat diet causes obesity and cardiovascular dysregulation. *Endocrinology* **153,** 1174–82 (2012).

141. Lim, S. *et al.* Cold-induced activation of brown adipose tissue and adipose angiogenesis in mice. *Nat. Protoc.* **7,** 606–615 (2012).

142. Gribskov, C. L., Henningfield, M. F., Swick, A. G. & Swick, R. W. Evidence for unmasking of rat brown-adipose-tissue mitochondrial GDP-binding sites in response to acute cold exposure. Effects of washing with albumin on GDP binding. *Biochem. J.* **233,** 743–747 (1986).

143. Johnson, P. R. & Hirsch, J. Cellularity of adipose depots in six strains of genetically obese mice. *J. Lipid Res.* **13,** 1–10 (1972).

144. Puigserver, P. *et al.* Induction and degradation of the uncoupling protein thermogenin in

brown adipocytes in vitro and in vivo. *Biochem. J.* **284,** 393–398 (1992).

145. Jp, P., Lm, D., Dowswell, T. & Fe, V. Daily oral iron supplementation during pregnancy (Review) SUMMARY OF FINDINGS FOR THE MAIN COMPARISON. (2012).

146. Gardner, D. S. & Rhodes, P. Early Nutrition Programming and Health Outcomes in Later Life. **646,** 1–10 (2009).

147. Nedergaard, J. & Cannon, B. UCP1 mRNA does not produce heat. *Biochim. Biophys. Acta - Mol. Cell Biol. Lipids* **1831,** 943–949 (2013).

148. Feldmann, H. M., Golozoubova, V., Cannon, B. & Nedergaard, J. UCP1 Ablation Induces Obesity and Abolishes Diet-Induced Thermogenesis in Mice Exempt from Thermal Stress by Living at Thermoneutrality. *Cell Metab.* **9,** 203–209 (2009).

149. Virtue, S. & Vidal-Puig, A. Assessment of brown adipose tissue function. *Front. Physiol.* **4,** 1–18 (2013).

150. Rogge, M. M. The Role of Impaired Mitochondrial Lipid Oxidation in Obesity. *Biol. Res. Nurs.* **10,** 356–373 (2009).

151. Lowell, B. B. & Spiegelman, B. M. Towards a molecular understanding of adaptive thermogenesis. *Nature* **404,** 652–660 (2000).

152. Van Baak, M. A. *et al.* Acute effect of L-796568, a novel β3-adrenergic receptor agonist, on energy expenditure in obese men. *Clin. Pharmacol. Ther.* **71,** 272–279 (2002).

153. Hardman, M. J. & Hull, D. Fat metabolism in brown adipose tissue in vivo. *J. Physiol.* **206,** 263–273 (1970).

154. Vimaleswaran, K. S. & Loos, R. J. F. Progress in the genetics of common obesity and type 2 diabetes. *Expert Rev. Mol. Med.* **12,** e7 (2010).

155. McAllister, E. J. *et al.* Ten Putative Contributors to the Obesity Epidemic. *Crit. Rev. Food*

Sci. Nutr. **49,** 868–913 (2009).

156. Dalgaard, L. T. & Pedersen, O. Uncoupling proteins: Functional characteristics and role in the pathogenesis of obesity and Type II diabetes. *Diabetologia* **44,** 946–965 (2001).

157. Hamann, A. *et al.* Analysis of the uncoupling protein-1 (UCP1) gene in obese and lean subjects: identification of four amino acid variants. *Int.J.Obes.Relat Metab Disord.* **22,** 939–941 (1998).

158. Clarke, L., Bryant, M. J., Lomax, M. a & Symonds, M. E. Maternal manipulation of brown adipose tissue and liver development in the ovine fetus during late gestation. *Br. J. Nutr.* **77,** 871–83 (1997).

159. Symonds, M. E., Bryant, M. J., Clarke, L., Darby, C. J. & Lomax, M. A. Effect of maternal cold exposure on brown adipose tissue and thermogenesis in the neonatal lamb. *J. Physiol.* **455,** 487–502 (1992).

160. Sellayah, D., Bharaj, P. & Sikder, D. Orexin is required for brown adipose tissue development, differentiation, and function. *Cell Metab.* **14,** 478–490 (2011).

161. Burdge, G. C., Hanson, M. A., Slater-Jefferies, J. L. & Lillycrop, K. A. Epigenetic regulation of transcription: a mechanism for inducing variations in phenotype (fetal programming) by differences in nutrition during early life? *Br. J. Nutr.* **97,** 1036 (2007).

162. Watkins, A. J., Lucas, E. S., Wilkins, A., Cagampang, F. R. A. & Fleming, T. P. Maternal periconceptional and gestational low protein diet affects mouse offspring growth, cardiovascular and adipose phenotype at 1 year of age. *PLoS One* **6,** (2011).

163. Christoffolete, M. a, Linardi, C. C. G., Jesus, L. De & Ebi, K. N. Mice with Targeted Disruption of the Dio2 Gene Have Cold-Induced Overexpression of thre Uncoupling Protein 1 Gene but Fail to Increase Brown Adipose Tissue Lipogenesis and Adaptative

Thermogenesis. *Diabetes* **53,** 577–584 (2004).

164. Wadef, G. N. & Gray, J. M. Cytoplasmic 17 /? - [3 H] Estradiol Binding in Rat Adipose Tissues *. **103,** (1978).

165. Sambasivarao, D. *et al.* Investigation of Escherichia coli Dimethyl Sulfoxide Reductase Assembly and Processing in Strains Defective for the sec-Independent Protein Translocation System Membrane Targeting and Translocation. *J. Biol. Chem.* **276,** 20167–20174 (2001).

166. Grasso, G., Satriano, C. & Milardi, D. A neglected modulator of insulin-degrading enzyme activity and conformation: The pH. *Biophys. Chem.* **203–204,** 33–40

167. De Jesus, L. A. *et al.* The type 2 iodothyronine deiodinase is essential for adaptive thermogenesis in brown adipose tissue. *J. Clin. Invest.* **108,** 1379–1385 (2001).

168. Cypess, A. M. *et al.* Identification and importance of brown adipose tissue in adult humans. *N. Engl. J. Med.* **360,** 1509–17 (2009).

169. Tiraby, C. *et al.* Acquirement of brown fat cell features by human white adipocytes. *J. Biol. Chem.* **278,** 33370–33376 (2003).

170. Knittle, J. L., Timmers, K., Ginsberg-Fellner, F., Brown, R. E. & Katz, D. P. The growth of adipose tissue in children and adolescents: Cross-sectional and longitudinal studies of adipose cell number and size. *J. Clin. Invest.* **63,** 239–246 (1979).

Appendix A

Nutritional Information of Diets Employed

Control Diet *Product # D10012G*

Ingredient	gm%	kcal%	mg Fe added
Protein	20.0	20.3	
Carbohydrate	64.0	63.9	
Fat	7.0	15.8	
Total		**100.0**	
kcal/gm	**3.9**		
Casein, 20 Mesh	200	800	1.7
L-Cystine	3	12	0.0048
Corn Starch	397	1590	0.397486
Maltodextrin	132	528	0.1056
Sucrose	100	400	0.08
Cellulose	50	0	5
Soybean Oil	70	630	0
t-Butylhydroquinone	0.014	0	0.00014
Mineral Mix S10022G	35	0	45.0
Mineral Mix S18706	0	0	0
Vitamin Mix V10037	10	40	0.009
Choline Bitartrate	2.5	0	0.0005
Ferric Citrate	0	0	0
Total	**1000**	**4000**	**52.3**

Ingredient	gm%	kcal%	mg Fe added
Protein	20.0	20.3	
Carbohydrate	64.0	63.9	
Fat	7.0	15.8	
Total		**100.0**	
kcal/gm	**3.9**		
Casein, 20 Mesh	200	800	1.7
L-Cystine	3	12	0.0048
Corn Starch	397	1590	0.397486
Maltodextrin	132	528	0.1056
Sucrose	100	400	0.08
Cellulose	0	0	0
Soybean Oil	70	630	0
t-Butylhydroquinone	0.014	0	0.00014
Mineral Mix S10022G	0	0	0
Mineral Mix S18706	35	0	0.56
Vitamin Mix V10037	10	40	0.009
Choline Bitartrate	2.5	0	0.0005
Ferric Citrate	0	0	0
Total	**1000**	**4000**	**2.9**

Ingredient	gm%	kcal%	mg Fe added
Protein	20.0	20.3	
Carbohydrate	64.0	63.9	
Fat	7.0	15.8	
Total		**100.0**	
kcal/gm	**3.9**		
Casein, 20 Mesh	200	800	1.7
L-Cystine	3	12	0.0048
Corn Starch	397	1590	0.397486
Maltodextrin	132	528	0.1056
Sucrose	100	400	0.08
Cellulose	50	0	5
Soybean Oil	70	630	0
t-Butylhydroquinone	0.014	0	0.00014
Mineral Mix S10022G	0	0	0
Mineral Mix S18706	35	0	0.56
Vitamin Mix V10037	10	40	0.009
Choline Bitartrate	2.5	0	0.0005
Ferric Citrate	0.01	0	2.12
Total	**1000**	**4000**	**10.0**

Ingredient	**gm%**	**kcal%**
Protein	24	20
Carbohydrate	41	35
Fat	34	45
Total		**100.0**
kcal/gm	**4.73**	
Casein, 20 Mesh	200	800
L-Cystine	3	12
Corn Starch	72.8	291
Maltodextrin	100	400
Sucrose	172.8	691
Cellulose	50	0
Soybean Oil	25	225
Lard	177.5	1598
Mineral Mix S10026	10	0
Vitamin Mix V10001	10	40
Choline Bitartrate	2	0
Total	**1000**	**4000**